T.R.

GEBZE TECHNICAL UNIVERSITY

GRADUATE SCHOOL OF NATURAL AND APPLIED SCIENCES

HUMIC SUBSTANCES AND NOM REMOVAL FROM AQUEOUS SOLUTIONS AND LAKE WATERS (TERKOS-TURKEY AND SAIMAA-FINLAND) BY ELECTROCOAGULATION

FERİDE ULU KAÇ

A THESIS SUBMITTED FOR THE DEGREE OF

DOCTOR OF PHILOSOPHY

DEPARTMENT OF ENVIRONMENTAL ENGINEERING

GEBZE

2016

T. R.

GEBZE TECHNICAL UNIVERSITY

GRADUATE SCHOOL OF NATURAL AND APPLIED SCIENCES

HUMIC SUBSTANCES AND NOM REMOVAL FROM AQUEOUS SOLUTIONS AND LAKE WATERS (TERKOS-TURKEY AND SAIMAA-FINLAND) BY ELECTROCOAGULATION

FERİDE ULU KAÇ
A THESIS SUBMITTED FOR THE DEGREE OF
DOCTOR OF PHILOSOPHY
DEPARTMENT OF ENVIRONMENTAL ENGINEERING

THESIS SUPERVISOR
PROF. DR. MEHMET KOBYA

GEBZE

2016

T.C.

GEBZE TEKNİK ÜNİVERSİTESİ

FEN BİLİMLERİ ENSTİTÜSÜ

SULU ÇÖZELTİLERDEN VE GÖL SULARINDAN (TERKOS-TÜRKİYE VE SAIMAA-FİNLANDİYA) HÜMİK MADDELERİN VE DOĞAL ORGANİK MADDENİN ELEKTROKOAGÜLASYON YÖNTEMİ İLE GİDERİMİ

FERİDE ULU KAÇ

DOKTORA TEZİ

ÇEVRE MÜHENDİSLİĞİ ANABİLİM DALI

DANIŞMANI

PROF. DR. MEHMET KOBYA

GEBZE

2016

| | **DOKTORA JÜRİ ONAY FORMU** |

GTÜ Fen Bilimleri Enstitüsü Yönetim Kurulu'nun 14/01/2016 tarih ve 2016/04 sayılı kararıyla oluşturulan jüri tarafından 04/02/2016 tarihinde tez savunma sınavı yapılan Feride ULU KAÇ' ın tez çalışması Çevre Mühendisliği Anabilim Dalında DOKTORA tezi olarak kabul edilmiştir.

JÜRİ

ÜYE
(TEZ DANIŞMANI)   :   PROF. DR. MEHMET KOBYA
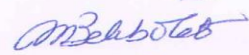
ÜYE   :   DOÇ. DR. M. SALİM ÖNCEL

ÜYE   :   PROF. DR. MİRAY BEKBÖLET

ÜYE   :   PROF. DR. İDİL ARSLAN-ALATON

ÜYE   :   PROF. DR. SEVİL VELİ

ONAY

Gebze Teknik Üniversitesi Fen Bilimleri Enstitüsü Yönetim Kurulu'nun

......./......./....... tarih ve ..../........ sayılı kararı.

İMZA/MÜHÜR

SUMMARY

The main aim of this study was to evaluate the removal of natural organic matter (NOM) from surface water by electrocoagulation (EC) process which is a promising technology. Synthetically prepared humic substance solutions and natural surface water samples were used in this investigation. EC process parameters as the pH, current density, and operating time were optimized. Aluminum, iron and hybrid electrodes were used in this study. Removal efficiency of EC process was determined with respect to DOC, UV_{254} and color removal. The best removal efficiency of DOC was obtained with 87.5% by Al electrode at initial pH (pH_i) 4, at current density of 1.2 mA/cm^2, for commercial humic acid. Soil humic acid was treated 90% DOC removal efficiency with Al electrode. The DOC reduction was 60.5% and 52.4%, Fe and hybrid, at current density of 6 mA/cm^2 and 3 mA/cm^2, respectively, for Lake Terkos Water. The Lake Saimaa Water was treated 66% DOC by hybrid electrode at original pH of raw water at current density of 3 mA/cm^2. The maximum DOC removal efficiency was 71.1% at pH_i 4 by Al electrodes, at current density 3 mA/cm^2 for Lake Saimaa Water.

Zeta potential, particle size measurements and high performance size exclusive chromatography (HPSEC) analysis were done. When the zeta potential reached isoelectric point, the removal of DOC and UV_{254} was increased for all samples. The dominat removal mechanism is charge neutralization and double layer compression at acidic conditions. The adsorption capacity of formed metal flocs is not so enough at alkaline conditions. The floc size evolution depends on solution chemistry and specific flocculation conditions. The HPSEC' results show EC process successfully removes the hydrophobic fraction of organic matter. The formation of disinfection by-products can decrease due to removal of hydrophobic moiety by EC process.

Still, more work is required to elucidating the character and removal mechanism of NOM. The results are important due to highlight for further studies.

Key Words: Electrocoagulation, Natural Organic Matter, Humic Substance, Zeta Potential, HPSEC.

ÖZET

Bu çalışmanın temel amacı, gelecek vaadeden bir proses olan elektrokoagulasyon (EC) ile yüzeysel sudan doğal organik maddenin gideriminin değerlendirilmesidir. Bu araştırmada, sentetik olarak hazırlanan hümik madde çözeltileri ve doğal yüzeysel su örnekleri kullanıldı. EC proses parametreleri olan pH, akım yoğunluğu, işletme süresi optimize edildi. Bu çalışmada alüminyum, demir ve hibrid elektrodlar kullanıldı. EC prosesinin giderim verimi, çözünmüş organik karbon (DOC), UV_{254} ve renk (VIS_{436}) giderimi açısından belirlendi. Ticari hümik asit için, en yüksek DOC giderim verimi Al elektrotlar ile başlangıç pH'ı (pH_i) 4 ve akım yoğunluğu 1.2 mA/cm^2 şartlarında %87.5 olarak elde edildi. Toprak hümik madde %90 DOC giderim verimi ile arıtıldı. Terkos göl suyu için, DOC azalımı, Fe ve hibrid elektrotlar ile akım yoğunluğu 6 mA/cm^2 ve 3 mA/cm^2'de ile sırasıyla % 60.5 ve 52.4% oldu. Saimma göl suyu, hibrid elektrod ile ham suyun orjinal pH değerinde ve 3 mA/cm^2'de DOC %66 arıtıldı. Maksimum DOC giderim verimi 3 mA/cm^2 akım yoğunluğunda Al elektrod ile pH_i 4'de %71.1 oldu.

Zeta potansiyeli, partikül boyut ölçümü ve Yüksek Performans Boyut Eleme Kromatoğrafisi (HPSEC) analizleri yapıldı. Bütün örneklerde, zeta potansiyeli izoelektrik noktaya ulaştığında DOC ve UV_{254} gideriminin arttığı tespit edildi. Asidik şartlarda baskın giderim mekanizması yük nötralizasyonu ve çift tabaka sıkışmasıdır. Alkali şartlarda, oluşan metal floklarının adsopsiyon kapasitesi çok yeterli değildir. Flok boyutu değişimi solüsyon kimyasına ve spesifik flokülasyon şartlarına bağlıdır. HPSEC sonuçları, EC prosesinin organik maddenin hidrofobik fraksiyonunu başarı ile giderdiğini göstermektedir. Dezenfeksiyon yan ürünlerinin oluşumu EC prosesi ile hydrofobik türün gideriminden dolayı azalabilir.

Doğal organik maddenin, karakter ve giderim mekanizmasının aydınlatılması için daha fazla araştırmaya ihtiyaç vardır. Bu çalışmadaki sonuçlar, ileride yapılacak olan çalışmalara ışık tutacağı için önemlidir.

Anahtar Kelimeler: Electrokoagulasyon, Doğal Organik Madde, Hümik Madde, Zeta Potansiyeli, HPSEC.

ACKNOWLEDGEMENTS

TABLE of CONTENTS

LIST of ABBREVIATIONS and ACRONYMS

Abbreviations and Acronyms		Explanations
ABS	:	Absorbance
CHA	:	Commercial Humic Acid
CC	:	Chemical Coagulation
DAD	:	Diod Array Dedector
DBPs	:	Disinfection By Products
DOC	:	Dissolved Organic Carbon
DOM	:	Dissolved Organic Matter
EC	:	Electrocoagulation
EF	:	Electroflotatiopn
EO	:	Electro-oxidation
HMM	:	High Molar Mass
HPSEC	:	High-Performance Size Exclusive Chromatography
HPLC	:	High-Performance Liquid Chromatography
HS	:	Humic Substances
IHSS	:	International Humic Substance Society
IMM	:	Intermediate Molar Mass
LMM	:	Lower Molar Mass
LSW	:	Lake Saimaa Water
LTW	:	Lake Terkos Water
MW	:	Molecular Weight
NOM	:	Natural Organic Matter
NOMs	:	Natural Organic Matters
RID	:	Refractive Index Dedector
SHA	:	Soil Humic Acid
SUVA	:	Specific UV absorbance
TOC	:	Total Organic Carbon
UV/VIS	:	Ultraviolet Visible Spectroscopy
ZP	:	Zeta Potential

LIST of FIGURES

xiv

the EC process with Al electrode (LTW,pH_i=7.76).

LISTE of TABLES

1. INTRODUCTION

Natural organic matters (NOMs) are a major topic in drinking water. The treatability and characterization of natural organic matter (NOM) are investigated in worldwide. Natural organic matters that present in surface and ground waters, soil, and sediments consist of a range of different compounds having a wide variety of chemical compositions and molecular sizes, from largely aliphatic to colored aromatics. A significant fraction of NOM present in surface and ground waters is composed of humic substances (HS). Thurman identified approximately 50 percent of NOM as HS which occur decaying of plant and animal residual in soil, water and sediment ecosystem [Thurman, 1985]. Aqueous humic substances are defined as NOM or dissolve organic carbon (DOC). The other fractions of NOM are non-humic substances. The quantity and chemical and physical character of NOM shows diversity in surface water and soil in the world due to some reason such as climate factor, the thickness of soil layer. It is typically 0.5-50 mg C/L as DOC or TOC in surface waters [Mulholland, 1990]. The Northern hemisphere usually includes a high amount of DOC and colored water, while the some region such as Turkey has low concentration (3-6 mg/L) of DOC and water is less color. Humic matter concentration increase with almost parallel rise of DOC in colored surface water that is organic matter-enriched. Its concentration constitutes of 60-80% of DOC [Malcolm, 1991].

The presence of NOMs in the environment-terrestrial and aquatic ecosystem-has important effects on quality of water in natural and engineered systems. NOMs lead to the binding and transport of organic and inorganic contaminants. These effects are due to their properties as they are proton acceptor and/or donor, and they have high pH buffering capacity. They cause precipitation reactions, and the dissolution of minerals. In addition, the knowing essential problem about NOM, it gives the color to the water. Before the 1970s, researches focused NOM removal for achieve to remove colour from drinking water [Jacangelo et al., 1995]. NOMs provide carbon source for bacterial growth in the water distribution systems, causing color, taste and odor problems [Eikebrokk, 1999], [Hem et al., 2001], [Aiken et al., 1995]. NOMs influence the permeability of light and the biological usability of nutrients in surface waters. They cause problems in drinking water purification

systems. NOMs may result in increased chlorine demand, fouling of membranes. It has been demonstrated the reaction of NOMs with chloride oxidants/disinfectants might cause formation of hazardous disinfection by-products (DBPs), some of which are mutagenic and carcinogenic [Bellar et al., 1974], [Uyak et al., 2008], [Oxenford, 1996].

NOM can be removed from water by a number of treatment processes. The most common and economically feasible method is coagulation and flocculation followed by sedimentation/flotation and filtration. Apart from conventional treatment process, activated carbon filtration, ion exchange, membrane filtration techniques and advanced oxidation processes are placed in literature for removal of NOM from water [Metsamuuronen et al., 2014], [Matilainen and Sillanpaa, 2010a], [Singer and Bilyk, 2002], [Matilainen et al., 2006], [Toor and Mohseni, 2007]. Electrocoagulation (EC) has been suggested to be a promising alternative to chemical coagulation (CC) and current technologies for removing various pollutants from freshwaters and wastewater [Kobya et al., 2011a], [Kobya et al., 2011b], [Meas et al., 2010], [Kabdaşlı et al., 2009]. Due to water quality problems mentioned above and strict regulations (USEPA, 1998) for drinking water quality, the studies have focused on developing new, economically feasible, environment friendly processes to increase the removal efficiency of NOM and improving current treatment process.

EC process has proved to be efficient with regard to the removal of aquatic humus and including high NOM concentration water [Yildiz et al., 2007], [Bagga et al., 2008], [Dubrawski and Mohseni, 2013], [Ulu et al., 2015]. However, there are limited studies in literature about treatment of NOM from aquagenic and pedogenic water by EC process. Also, the knowledge about characterization of removal mechanism of NOM during treatment by EC remains limited. In this study, EC process was applied waters that containing different sources of NOM due to provide deeply an understanding about removal of NOM by EC process.

1.1. Aim and Scope of the Thesis

The main aim of this study was to evaluate the treatability of natural organic matter from surface water by electrocoagulation process. Within this framework, synthetic humic acid solution, extracted soil humic substance and natural surface waters were used, representing natural organic matter. Synthetic humic acid solution was prepared as given in literature. EC process parameters were explored as initial pH (pH_i), current density, operating time, different electrode types –aluminium and iron- by using synthetic humic acid solution. At obtained optimum pH_i and current density, treatment of extracted soil humic substance was investigated by using aluminium, iron and hybrid by EC process. Natural surface waters were treated by EC process using three electrode types-aluminium, iron and hybrid-. The effect of pH_i, current density, operating time on removal of NOM was investigated for real water samples. Eventually, the optimum conditions were determined for each NOM sources. At the optimum conditions, the treatability of humic substance and NOM sources that have different properties was compared by EC.

Another purpose of this investigation was to elucidate the removal mechanism and the structure of NOM in order to optimize of NOM removal by EC process. In this manner, characterization of NOM was investigated before and after EC treatment process. Specific UV absorbance (SUVA) value was determined of samples. The effect of pH_i and EC operating time on zeta potential (ζ) was done by zeta meter. Particle size measurements and chromatography analyses were done.

2. THEORITICAL BACKGROUND

2.1. Structure of Humic Substance

Rivers and lakes have plenty of living organisms (such as plants and animals) that reside in them. However, once these organisms die, their remains will be broken down by fungus and bacteria. Brown and black biopolymers associated with soil, sediment and particulates in water consist of material derived from the degradation of animals and plants and are called humic substance.

HS are present water supplies and comprises a significant portion of NOM. NOM is present all over ecosystems-in soil and sediment as well as floating in water. NOM plays a few important roles in the ecosystem. First of all, it can provide nutrients to different organisms. For example, some micro-organisms rely on NOM as a source of food, whereas some plants gain a nutrient boost from the presence of NOM. It can also help reduce harmful changes in water acidity. It is really the complexity and diversity of the chemical make-up of NOM that make it such an important yet complicated player in the fate of chemicals in the environment. Living organisms are made up predominantly of organic (carbon-containing) compounds. Therefore, their breakdown products are also made predominately of carbon. While this may make it seem like NOM should be quite simple, NOM is actually very complex. In fact, NOM is so complex that no one actually knows for sure exactly what its atom-by-atom chemical structure is! This diversity and complexity stems from the variety in the "starting" structures of the NOM-the different plant and animal breakdown products such as cellulose , tannin, cutin, lignin, proteins, lipids, and carbohydrates. While these components on their own may seem simple, as the compounds break down they can polymerize, or join together, forming more complex species. As a result NOM is made up of complicated structures that loosely resemble the starting material structures; the only thing we know for sure is that it contains carbon, oxygen, and hydrogen. The chemical compounds that make up different living materials (plants, trees, organisms, etc.) can decompose and join together to form the complex mixture of chemical compounds that makes up natural organic matter (Figure 2.1). Different parts of the molecule have differing affinities for water, and the structure has groups that will be neutral at an environmentally

relevant pH and others that will be charged. The environment in which NOM is formed plays a critical role in determining the specific properties of any given sample of NOM. For example, a NOM sample from Alaska will have quite different properties than one coming from the swamps of Georgia; these areas have different plant and animal life, which leads to different breakdown products and different compositions of the NOM present in these areas.
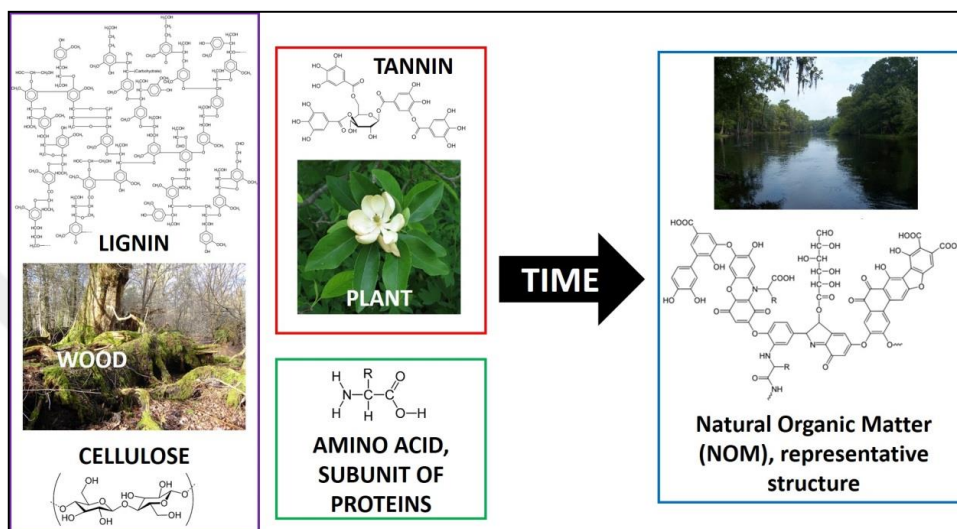
Figure 2.1: Diagram for formation of NOM.

Humic acids (HAs) are one of the main components of HS in water [Ghernaout et al., 2009]; they are soluble in dilute alkaline solution but precipitate from an acidified solution (pH <2). The acidic nature of humic acid (HA) is usually attributed to the ionization behaviour of –COOH and phenolic –OH groups [Rebhun and Lurie, 1993]. As it mentioned above, HS are present water supplies and comprise a significant portion of NOM. HS are not well defined chemically and have variable composition. HS do not have certain or general structure, hence the phrase "humic substances" is used as a general term to express colored material or its fraction is attained on the basis of solubility characteristics depending on the pH functions as follows [Suffet et al., 1989], [Gaffney et al., 1996a]:

- Fulvic acid is soluble at all pH conditions.
- Humic acid fraction is alkali-dissolving (soluble at higher pH values) and insoluble in water under acidic conditions (pH< 2).

5

- Humin is the fraction of humic substances that is insoluble in any pH and cannot be done extracted by acid or base.

The characteristic structure of humic substance (humic and fulvic acid) is proposed in literature as shown in Figure 2.2 and 2.3. Percent by weight elemental composition of HS are C: 45-55%, O: 30-45%, H: 3-6%, N: 1-5%, and S: 0-1%. The exact chemical structure depends on the source and the history of biodegradation.
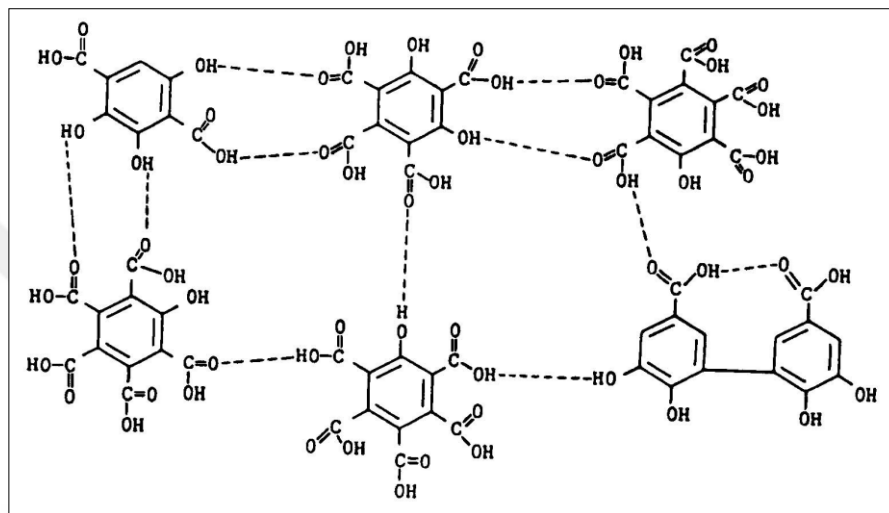
Figure 2.2: Structure of humic substances.
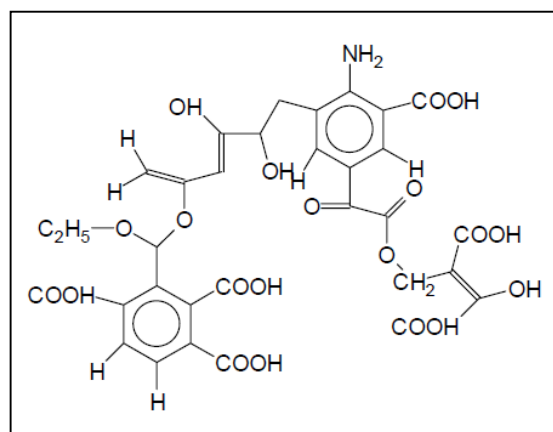
Figure 2.3: Hypothetical structure of aquatic fulvic acid.

Also, another method for identify humic substance is basis of compositional, structural and functional data [Schnitzer and Khan, 1972], [Stevenson, 1982], [Buffle et al., 1977]. In this manner, humic and fulvic acids differ from each other by the

6

variations in molecular weight, the number of functional groups (carboxyl and phenolic OH) and the extent of polymerization. Generally, fulvic acids have lower molecular weights than HA, and the structure of fulvic acid is more aliphatic and less aromatic than HA. It is also known that the soil derived HS are larger than aquatic substances [Gaffney et al., 1996b]. The hypothetical relationships between species of HS were shown in Figure 2.4 [Gamble and Schnitzer, 1974]. Hypotetical structure of Bersbo aquatic fulvic acid based on elemental analysis and potentiometric titrations in aqueous and non-aqueous media was shown in Figure 2.3 [Gamble and Schnitzer, 1973].
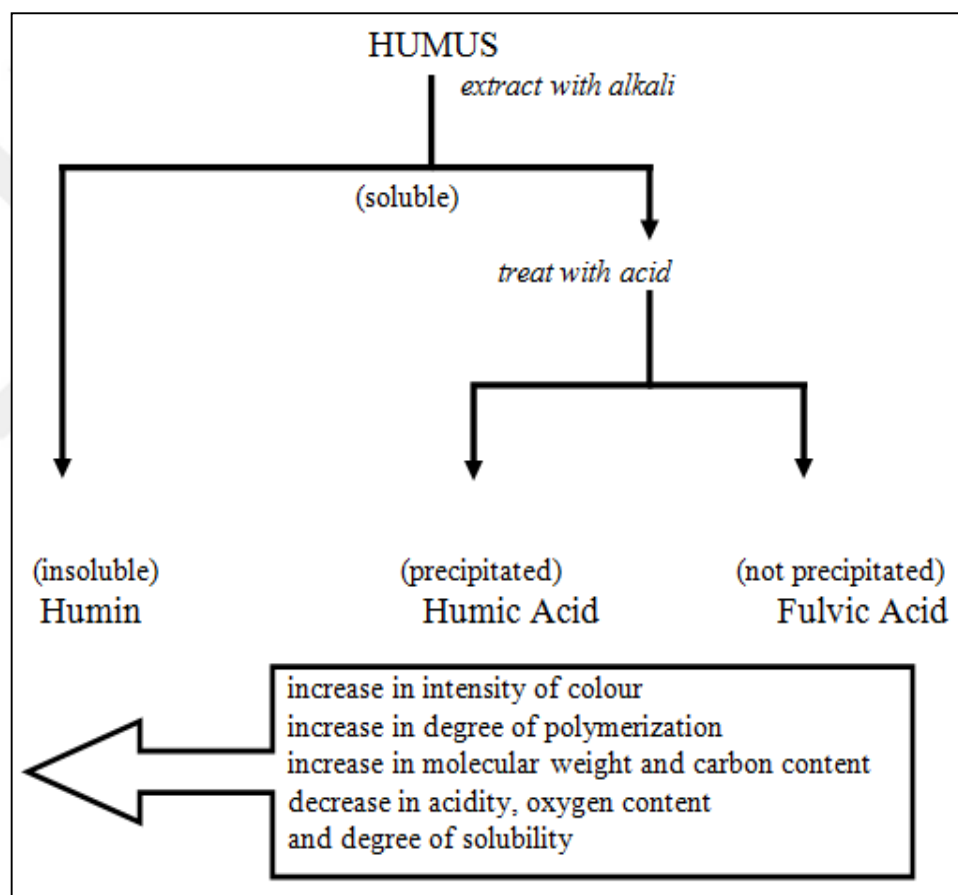
Figure 2.4: The hypothetical relationships between humic substances.

Organic substances are soluble containing many –COOH, -OH, and NH_3^+ functional groups that partially ionize in water, releasing H^+ ions and providing negative charge centers on the macromolecule to which cations are strongly attracted. Ionization can be as shown in equation 2.1, 2.2, and 2.3. Dissociation and protonation of functional group in humic molecule depends on the pH of solution.

Electrostatic repulsions between negatively charged sites cause stretching of the molecule. Moreover, ionic strength of the compounds with the nearby ionized functional groups also affects the electrostatic forces [Ghosh and Schitzer, 1980], [Rehbun and Luire, 1993], [Ghernaout et al., 2011] as shown in the following reactions:

$$R - NH_3^+ \rightarrow R - NH_2 + H^+ \qquad (2.1)$$

$$R - OH \rightarrow R - O^- + H^+ \qquad (2.2)$$

$$R - COOH \rightarrow R - COO^- + H^+ \qquad (2.3)$$
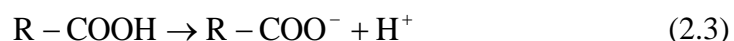
2.2. NOM and Characterization of NOM

NOM ubiquitously present in terrestrial and aquatic ecosystems. NOMs that are complex macromolecular are developed products of the chemical and biological degradation of plant and animal residual. They occur by the metabolism of wastes and soil organism in soil. Also, NOMs can be originated from anthropogenic activities, as well as. The most amount of NOM is derived from soil. The elemental composition, physicochemical structure, reactivity and amount of natural organic matters depend on their origin, such as peat soil, mineral soil. Also, the specific characteristics of NOM that presents in surface waters variety due to climatic factors, such as precipitation and temperature, environment's geology, and topography [Fabris et al., 2008], [Wei et al., 2008]. For example, the transportation of NOM in the residual of plant and animal by surface runoff, diffusion through sediment can be effect on NOM concentration in the water. Uyak found that increase of DOC concentration was observed at fall and spring season in general. Also, it was determined that the fraction of NOM was changed following precipitation and suggests that runoff leached humic substances from the upper soil layer [Uyak et al., 2008]. Dissolved organic materials (DOM) are present in almost all aquatic ecosystems at concentrations typically ranging from 0.1 to 10 mg/L and depending on biogeochemical conditions and climate [Philippe and Schaumann, 2014]. Three categories represent together the most important part of DOM in surface waters: humic substances, polysaccharides, and proteins, with highly different molecular properties (Table 2.1). Humic and fulvic acids can be regarded as supramolecular

assemblies of several thousands of different molecules. The high diversity and complexity of these assemblies constitute a challenge for the DOM characterization.

Table 2.1: Indicative molecular parameters of different types of natural DOM.

DOM-type	Molecular Weight [kDa]	most common functional groups	Charge (4<pH< 10)	solubility in water
humic acids	2−5	aliphatic and aromatic COOH, OH, and OCH$_3$ aliphatic CO	negative	well soluble at high pH
fulvic acids	0.5-2	aliphatic and aromatic COOH, OH, and OCH$_3$ aliphatic CO	negative	well soluble
carbohydrates	0.18-3000	OH, CO, COOH	side-group dependent	side groups dependent
proteins	10−a few 1000	NH$_2$, COOH, OH, SH	side-group dependent	side groups dependent
fatty acids	0.25-0.85	COOH	negative	chain length dependent
amino acids	<0.2	CNH$_2$, COOH	side-group dependent	Well soluble

Chemical composition and structure of NOM are certainly unidentified. It comprises of different compounds that have a wide variety functional groups and molecular size, from aliphatic to highly colored aromatics [Swietlik et al., 2004], [Thurman, 1985]. Humic substances as the dominate fraction of aquatic NOM constitute 40-60 percent of dissolved organic matter (DOM) in natural fresh surface waters [Rehbun and Luire, 1993], [Vik et al., 1984]. Dissolved organic matter (DOM) consists of a heterogeneous mixture of aliphatic and aromatic polymers containing oxygen, nitrogen and sulfur functional groups, which is widespread in engineered systems. Dissolved organic carbon (DOC), a substantial part of DOM, is frequently indicative of DOM [Herzsprung et al., 2012]. Humic substance has more hydrophobic character and divides two fraction, such as humic and fulvic acid. Humic substances are regarded as natural anionic polyelectrolytes of aromatic and aliphatic hydrocarbon structures having various functional groups, including carboxylic and phenolic groups [Metsamuuronen et al., 2014]. The rest amount of the DOM consists of non-humic substances that are less hydrophobic in character and

comprise about 60% of the hydrophilic acids. In the remaining 40% of the non-humic substances, 20% are carbohydrates, 14% carboxylic acids, 6% amino acids, and less than 1 % is hydrocarbon as shown in Figure 2.5 [Owen et al. 1995].
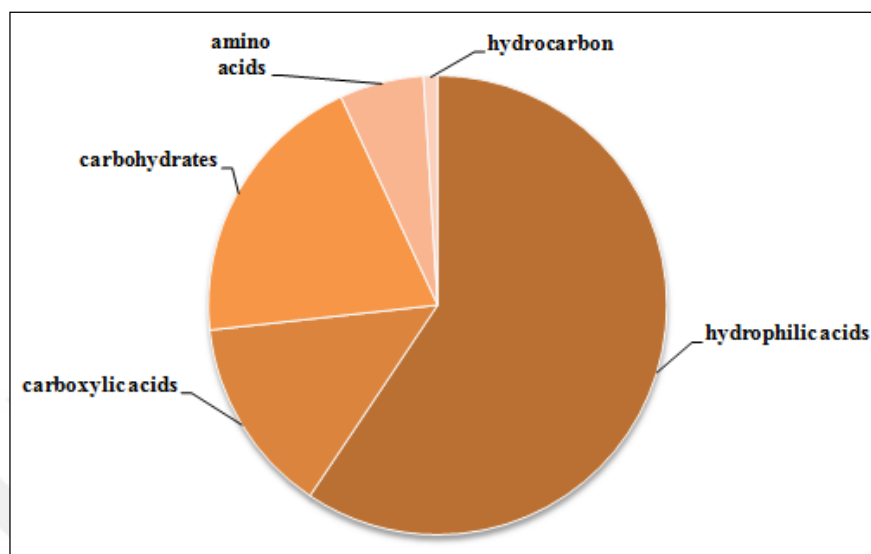
Figure 2.5: Species of non-humic substances.

There are different methods for classifications of NOM. Because, NOMs are characterized as a heterogeneous complex structure, which consists of aromatic and aliphatic organic compounds that have different size, weight, and surface charges. It mentioned above, NOM has humic and non-humic fraction. Another approach that the dissolved fraction of NOM consists of approximately 90 percent of TOC, the particular fraction consists of 10-20 percent [Malcolm et al., 1991], [Gaffeny et al., 1996]. The concentrations of humic substances in surface and ground waters depend on the concentration of total organic carbon (TOC) which may be divided into particulate form and dissolved organic carbon (DOC). The separation of particulates from the dissolved organic carbon has normally been effected using filters with an arbitrary cut-off of 0.45 micron. The DOC in surface waters in the USA has an average of 5 mgC/L rang from 1.5 mgC/L to 10 mgC/L with approximately 50% of humic substances. The DOC in groundwaters has concentrations rang from 2 to 4 mgC/L. A generalization of these data is that the concentration of humic substances in aquatic environments range from 20 µg/L in groundwaters to 30 mg/L in surface waters [Grenthe and Puigdomenech, 1997].

NOMs constitute a severe subject in engineering systems due to having specialties, such as proton acceptor and/or donor. They have high pH buffering capacity and cause precipitation reactions, the dissolution of minerals. NOMs are effective in transporting of the metals from water by sorption to negative charge sites. Humic materials also bind organic pollutants, especially like less- soluble DDT and atrazine. In this manner, the character of water supplies that used for obtain drinking water would be affected by NOM. The advance treatment process can be required for purification of more complex contaminated water supplies by NOM. Also the effluent concentration of NOM from treatment plant should be reduced with integrated systems for response to the various problems which result from NOM.

HS in waters have a number of characteristics that influence on how they may be removed from water. The essential driving forces for investigation of NOMs are the human health risks and optimization of treatment technologies. At the present time, for further understanding of organics' role in natural environments and drinking water treatment the structure of humic matters are highlighted. A range of analytical techniques and chromatographic methods have been developed for identified heterogeneous nature of NOM [Vuorio et al., 1998], [Labanowski et al., 2010], [Velten et al., 2011], [Derenne et al., 2014]. Natural organic matter exists in surface and ground water at concentrations between 2-10 mg/L, although much higher levels are sometimes found depending mainly on the watershed state. Ground water generally has a lower concentration of NOM than surface water. Organic matter in natural waters is often arbitrarily divided into dissolved (DOC) and particulate organic carbon (POC), based on filtration through a 0.45 μm filter. Generally, DOC is more abundant than POC, accounting for approximately 90% of the total organic carbon in most waters. The concentration of NOM is usually measured as total organic carbon (TOC) (mg L^{-1}) or DOC (mg L^{-1}) by catalytically combustion oxidation non-dispersive infrared detector, and UV absorbance and chemical oxygen demand (COD). TOC and DOC are the most used parameters to evaluate performance of the treatment process in all studies. A widely accepted operational definition of DOC is the organic carbon in the water sample filtered through 0.45 μm pore size membrane filter. They only measure the quantity of NOM present, except UV absorbance.

A number of spectroscopic methods offer information on NOM structure. Available methods in this technique are ultraviolet and visible (UV/Vis)

spectroscopy, fluorescence spectroscopy, fourier transform infrared (FTIR) spectroscopy, ^{1}H NMR, ^{13}C NMR, ^{15}N NMR, 2-D NMR in literature [Minor et al., 2014], [Rodríguez et al., 2014], [Nerger et al., 2015]. UV/Vis spectroscopy that is one of the mostly used methods is used to evaluate the chemical structure of organic matter [Chin et al., 1994], [Croue et al., 1999], [Baker et al., 2008], [Matilainen et al., 2011], [Ulu et al., 2014], [ElBishlawi et al., 2015], [Assaad et al., 2015]. UV-Vis absorption spectroscopy is the measurement of the attenuation of a beam of light after it passes through a sample or after reflection from a sample surface [Matilainen et al., 2011]. The concentration of an analyte in a solution can be determined by measuring the absorbance at a certain wavelength applying the Beer-Lambert Law. The different absorption wavelengths also have been used in literature for the spectral differentiation of humic substances. For instance, absorbance at 220 nm is associated with both carboxylic and aromatic chromophores, whereas, absorbance at 254 nm (UV_{254}) represents generally the aromatic groups with varying degrees of activation [Korshin et al. 2009]. Although the molar absorptivities vary due to the range of chromopheres in NOM structure [Matilainen et al., 2011], the wavelength at 436 nm (VIS_{436}) is commonly used for yellow color representing absorbance [Uyguner et al., 2005]. Conjugated C-C multiple bonds, aromatic carbon, -COOH and –OH result in increase of adsorption. UV/Vis spectroscopy is simple and fast method for molecular characterization. It does not only represent the aromatic character, can be used also as a potential surrogate measure for DOC.

SUVA is defined as the UV_{254} value of a water sample divided by DOC (mg L$^-$^{1}) concentration of a water sample. The SUVA value of a sample describes the nature of NOM as follows, <2 mostly low hydrophobicity, and low molecular weight; 2-4 mixture of aquatic humics and other NOM, mixture of molecular weights; >4 mostly aquatic humics, high hydrophobicity, high molecular weight [Edzwald et al., 1985], [Wei et al., 2008].

FTIR is used widely for characterization of NOM in applications [Kim and Yu, 2007], [Hay and Myneni, 2007], [Her et al., 2008]. Absorption spectrums are obtained by emitted energy of infrared absorption light as a result of vibration energy of atomic bonds in samples. These spectrums detect aliphatic and aromatic hydrocarbon, different bonds and functional groups, e.g. OH in carboxylic and alcoholic groups, and nitrogen. Explanation of the structure may be difficult due to the complexity and polyfunctionality of NOM. Samples can be analysed both in

liquid and solid phases. Initial operation procedure may be required depending on sample conditions such as dilution, drying.

Chromatographic methods also obtain knowledge about chemical structure of NOM. High Performance Size Exclusive Chromatography (HPSEC) is rapid, sensitive, and no pre-extraction needed method for characterizing molecules on basis of molecular sizes of organic compounds in water [Fabris et al., 2008], [Korshin et al. 2009]. It uses a small amount of sample. The bigger molecules have shorter retention time [Nobili et al., 1989], [Hongve et al., 1996]. SEC gel column applications were poor for separation of NOM, as well as had some disadvantages. Hence, high performance liquid chromatography (HPLC) method was developed and called HPSEC. HPSEC is a useful tool for characterization of NOM in different stage of drinking water treatment [Matilainen et al., 2006], [Allpike et al., 2007], [Chow et al., 2009a], [Slavik et al., 2012], [Kent et al., 2014]. Columns, mobile phase, the used standards for calibration of molecule size are major variables.

Silica-based and polymer-based gel columns have been used [Sarathy and Mohseni, 2007], [Chow et al., 2009b], [Zhao et al., 2009]. These include column like TSK [Hongve et al., 1996], [Yeow et al., 2008], [Huber et al., 2011], Shodex [Hongve et al., 1996], Waters-Protein-Pak [Kawasaki et al., 2011], [Dubrawski et al., 2013]. The choice of eluent as the mobile phase is important because of effect of its ionic strength and pH on the results. Eluent impacts the charge repulsion effects of the gel, charged sites and structure of NOM, and NOM-gel interaction. Phosphate buffer, sodium acetate, and water have been used as mobile phase. Different eluents might be tried for obtain a good resolution of solutes. Size and molecular weight of NOM can be determined with known molecular weight standards. In this meaning, poly-styrene sulphonate, polyethylene glycols and proteins usually are used [Liu et al., 2008], [Zhao et al., 2009]. HPSEC term is used if the used column is convenient for analysis of MW of matter and the mobile phase is water in HPLC. Otherwise the mobile phase is a solvent such as THF it is called GPC.

HPSEC systems have different detectors, including refractive index (RI) [Wagner and Christman, 1999], multi-angle light scattering, on-line DOC analyser [Huber et al., 2011], and excitations emission fluorescence detection [Matilainen et al., 2011]. The most commonly used detectors are UV/vis or diod-array detector (DAD) for fractionation in HPSEC analytical method [Matilainen et al., 2011]. DADs are variable wavelength UV/vis detectors. UV/vis detectors are simple and

fast to use. HPSEC with UV/vis absorbance detection has been used to calculate NOM molecular size [Hoque et al., 2003]. However, NOM structures include a range of chromophores with varying molar absorptivities, the MW calculated may not involve all of NOM compounds present [Soh et al., 2008], [Espinoza et al., 2009]. Generally, the NOM measurements are done between wavelength 230 and 280 nm. The most useful wavelength is 254 nm for NOM measurements. Therefore, it is widely used [Zhou et al., 2000].

HPSEC is used to derive weight and number average molecular weight (M_W and M_n, respectively) and hence polydispersity (ρ) a ratio of M_W and M_n, which is a measure of the homogeneity or heterogeneity of the NOM in a sample. Mw and Mn value obtain the following equations (2.1., 2.2) [Mori and Barth, 1999]:

$$M_w = \frac{\sum_i n_i M_i^2}{\sum_i n_i M_i} \tag{2.1}$$

$$M_n = \frac{\sum_i n_i M_i}{\sum n_i} \tag{2.2}$$

M_i and n_i represents molecular weight and per fraction' height of i-th fraction at the i-th elution volume.

In this study, refractive index dedector (RID) and DAD are major in terms of interpreting the results. Thus, the knowledge about these two detectors was given in the below.

RID is a detector that measures the refractive index of an analyte relative to the solvent. They are often used as detectors for high-performance liquid chromatography and size exclusion chromatography. RID is considered to be universal detector. The detection principle of RID depends on measuring of the change in refractive index of the column effluent passing through the flow-cell. The flow cell has two parts: one for the sample and one for the reference solvent. The detector measures the RI of both components. The greater the RI difference between sample and mobile phase, the larger the imbalance will become. Besides, the deflection of light beam will be high. The difference appears as a peak in the chromatogram.

Thus, the sensitivity will be higher for the higher difference in RI between sample and mobile phase. On the other hand, in complex mixtures, sample components may cover a wide range of refractive index values and some may closely match that of the mobile phase, becoming invisible to the detector. RI detector is a pure differential instrument, and any changes in the eluent composition require the rebalansing of the detector. This factor is severely limiting RI detector application in the analyses requiring the gradient elution, where mobile phase composition is changed during the analysis to effect the separation.

DAD allows the measurement of absorbance value of eluent at multi-wavelength or specific wavelength sensitively when eluent is passing through the flow-cell. These detectors, because they allow a wide range of wavelengths of 0.01 seconds or the whole wavelength of the absorbance of the elution liquid to continuous measurement of the analyte according to the elution time as well, they also provide qualitative information obtaining the analyte.

On-line excitation emission fluorescence detection used in the characterization of NOM structure gains limited information and less separation resolution compared to UV/vis absorbance detection [Wu et al., 2007]. However, compared to UV/Vis, on-line 3D excitation-emission matrix fluorescence detection gives more the chemical and structural information about the NOM, as well as molecular size, compared to UV absorbance [Shirshova et al., 2006], [Wu et al., 2007]. The HPSEC with on-line organic carbon detectors that is a recent and powerful analytical method give information on the amount of NOM, in addition to compound information [Penru et al., 2013]. Huber and Frimmel (1991), improved a HPSEC system with UV absorbance (HPSEC-UVA) and sensitive OCD. Because this system allows detection of all organic carbon, the size of NOM can be estimated both qualitatively and quantitatively [Kawasaki et al., 2011]. But, this integrated model cannot economic for most laboratories.

Resin fractionation (Affinity Chromatography) method developed by Leenher (1981), has recently become a common method for NOM. Different resin pore size, surface area and chemical composition result in various capacity factors per resin in same solution. Hydrophobic and hydrophilic fraction of NOM is determined generally by using XAD-8 and XAD-4 resins. Hydrophobic NOM primarily consists of humic and fulvic acids (humic substances) and is rich in aromatic carbon, phenolic structures and conjugated double bonds. The hydrophilic fraction of NOM consists

mostly of aliphatic carbon and nitrogenous compounds, such as carboxylic acids, carbohydrates and proteins [Matilainen et al., 2010b]. Natural organic matter can be divided into six fractions as more detailed information: hydrophobic acids, bases and neutrals; and hydrophilic acids, bases and neutrals [Leenher, 1981]. Table 2.2 represents different fractions and the chemical groups of NOM that determined using resin fractionation method. In this method the sequential use of non-ionic and ionic resins resulted in four fractions, consisting of very hydrophobic acid (VHA), slightly hydrophobic acids (SHA), charged hydrophilics (CHA) and neutral hydrophilics (NEU) [Soh et al, 2008]. In literature, Chow also determined these four fractions in the organic carbon concentration [Chow et al., 2004].

Table 2.2: Fractions and the chemical groups of NOM.

Fractions	Chemical groups
Hydrophobic *strong acids*	humic and fulvic acids
	High molar mass (HMM) alkyl monocarboxylic and dicarboxylic acids, aromatic acids
Hydrophobic *weak acids*	phenols, tannins
	Intermediate molar mass (IMM) alkyl monocarboxylic and dicarboxylic acids
Hydrophobic *bases*	proteins, aromatic amines, HMM alkyl amines
Hydrophobic *neutrals*	hydrocarbons, aldehydes, HMM methyl ketones and alkyl alcohols, ethers, furans, pyrrole
Hydrophilic *acids*	hydroxyl acids, sugars, sulfonics, Low molar mass (LMM) alkyl monocarboxylic and dicarboxylic acids
Hydrophilic *bases*	amino acids, purines, pyridines, LMM alkyl amines
Hydrophilic *neutrals*	polysaccharides, LMM alkyl alcohols, aldehydes and ketones

The NOM in environment, aquatic and terrestrial regions, should be observed with available methods and techniques in order to gain more information about extraction and fractionation of NOM. But, there are so gaps in the literature certain methods and processes..

2.3. Conventional Treatment Methods of NOM

2.3.1. Coagulation Process

Coagulation treatment that is the main part of conventional water treatment facility has been employed to decrease colour, turbidity, and to remove various impurities. Natural surface waters include a range variety of contaminates as NOM, as suspended matters, like clay, silica, microbial cells or algae and pathogens. These typical impurities can be removed by coagulation process. After coagulation process, the following processes are flocculation, settling, and filtration in a conventional treatment plant.

NOM is one of the major pollutants in surface waters. It mentioned in section 2.2, NOM includes a mixture of organic substance, such as humic acid, fulvic acid, bacteria, and proteins. These substances that have a range of particle size present a major challenge in water treatment technology. They include suspended and colloid particles. Suspended particles are generally larger than 1 μm can be removed by gravity sedimentation. Some researchers have classified the size range for colloidal particles as varying from 0.01-0.1 μm, whereas the size of colloids are defined 0.001 − 1 μm by many researchers. Colloidal particles cannot be removed by sedimentation in a reasonable period of time. Chemical process such as coagulation can be used to remove of these particles. To understand the removal mechanism of colloid impurities by coagulation process, well understanding of character of colloids are important.

2.3.1.1. Structure and Stability Mechanisms of Colloids

The colloidal have a large surface area due to their in a range of small size therefore surface properties play an important role in their characteristic. Stabilization and destabilization of colloids in solution is the results of their surface charge, their electrokinetic property. A colloidal system as a whole does not have a net charge. They include ionisable fuctional groups, such as –OH, -COOH, NH$_2$, which provide surface charge to colloids. Organic matters and bacteria acquire their surface charge as a result of the ionization of these groups.

Aquatic particles are often stable particles and resistant to aggregation and settlement because of their surface charge (electrostatic stabilization and steric stabilization). Also, the result of smallness and tremendous surface area is that in colloidal suspensions [Sawyer et al., 1994]:

i) Gravitational effects are negligible, and

ii) Surface phenomena predominate.

Figure 2.6 shows that electrostatic and steric stabilization. Electrostatic stabilization operates via the electrostatic repulsion between net surface charges caused by ionization of surface atoms, binding of solution ions, and ion exchange between surface and solution. Steric stabilization involves polymers added to the system adsorbing onto the particle surface and causing repulsion. Consequently, the stability of colloid depends on electrical characteristic, the size and chemical structure of solid matter.

Electrostatic stabilization   Steric stabilization
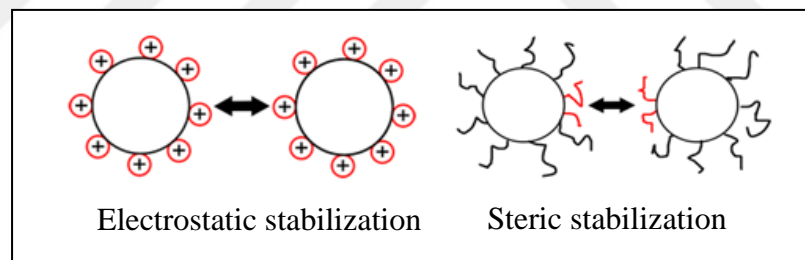
Figure 2.6: Electrostatic and steric stabilization on a colloidal in a solution.

The primary electrical charge could be negative or positive. However, the colloidal organic matters are mostly negative charged in aquous systems [Gibbs, 1983], [Elimelech et al., 1998]. When a charge forms on the surface it also affects the ions in the surrounding solution. The charged colloidal particles have the tendency to adsorb the ions of opposite charge, whereas the ions of the same charge are repelled from surface [Reynolds, 1977]. Negatively charged particles attract positive ions from the solution and on the positive charged particles attract negative ions from the solution. This separation of between charged particle and surrounding counter-ions called electrical double-layer is illustrated in Figure 2.7. The dense layer of counter-

ions fixed on the surface of the primary particle- a charged particle suspended in a liquid- is termed *Stern* layer. Stern layer is the first layer around the primary particle consists of tightly bound ions. The total potential at the surface of the primary particle is the *Nerst* potential. Ions further away from the solution (the outer ions of *Stern* layer) are more loosely bound and the layer of these loosely attached ions is called a d*iffuse* layer. Inside this layer there is an imaginary boundary called the *Slipping* layer or the surface of shear. The slipping layer separates the mobile portion of the colloid from the surrounding mixture of diffuse. When the primary particle surrounded by attached ions is moving in the liquid, all ions within the slipping plane boundary are moving with the particle and all ions outside this boundary will not move with the particle ions. The concentrated counter-ions within the surface of shear reduce the net charge on the particle by an amount that is generally referred to as the *Stern* potential. There is an electrical potential between the net overall charge on the colloids at the surface of shear (slipping plane) and the bulk solution called *Zeta* potential (ZP). Consequently, the potential (Nernst potential) that is maximum at the surface of the primary particle decrease rapidly through the Stern layer resulting in a net overall charge on the particle at the surface of shear means that the *Zeta* potential (Figure 2.7) [Sawyer et al., 2002].
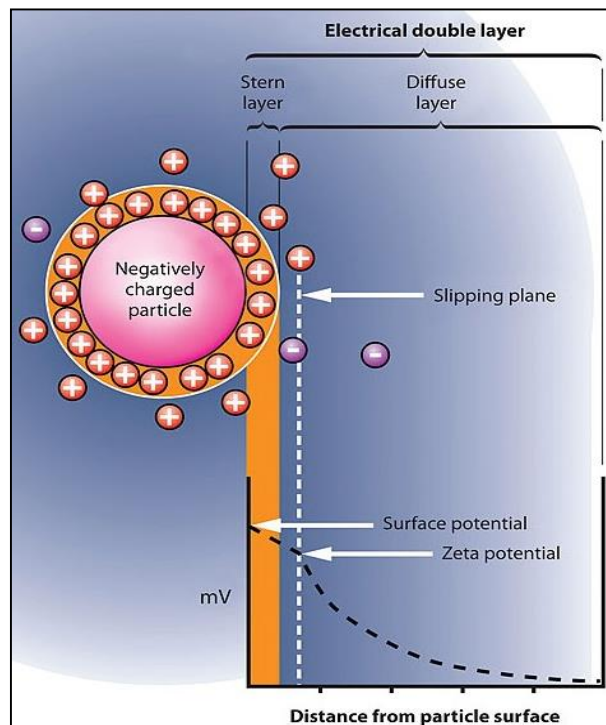
Figure 2.7: Representation of the electrical double layer.

The stability of a colloidal system depends on extent of repulsive forces between similarly charged colloid. ZP measures the extent of repulsive forces and is commonly considered to be the important cause of the stability of colloidal system. Further away from the surface of shear both the concentration and potential gradients continue decreasing, until the potential approaches the point of electrical neutrality in the surrounding solution [Shammas, 2005]. The electrical potential shows zero value after a distance from colloid.

When two similar primary charge particles drift toward each other, their diffuse layers start to interact leading to the production of a repulsive electrostatic force. The forces of attraction are because of van der Waals' force. All colloidal particles, irrespective of their composition, sign or magnitude of charge, or the composition of the dispersion medium, have such attractive forces. They arise from various features of atoms [Shammas, 2005]. The Brownian movement tends to destabilize a colloidal system in addition to van der Waals' attractive force. This is due to random motion of colloids. This movement results in kinetic energy that impart to colloid particles. Ultimately, higher energy particles moving in a random fashion tend to collide. When the energy of net resultant force that is the summation of the respective electrostatic repulsive force and van der Waals' attractive force exceeds the kinetic energy, the colloidal particles will not coagulate and the dispersion is stable. In contract with, if kinetic energy is larger than the repulsive energy, the dispersion is unstable and particles will coagulate. When the stabile colloidal particle is required to destabilize and coagulate a stable dispersion, the electrostatic repulsion energy between the particles must be lowered and/or the kinetic energy of the particles must be increased [Shammas, 2005].

The stable solid matters and fine suspended solid matters that do not effectively settle can be removed by coagulation/flocculation process with addition of inorganic and organic chemicals that are called coagulant such as inorganic salts, natural and synthetic polyelectrolytes. Because coagulants can achieve destabilization of colloidal in different ways. Depending upon the condition under which they are used by more selection. Main destabilization mechanisms are given here as following:

Double layer compression (compression of the diffuse layer): When the concentration of counter-ions- especially with higher charges- are increased by added simple electrolytes in a stabile colloid system, the high concentration of ions penetrate into the diffuse double layer surrounding the particles. The high of

concentration of the ions in the bulk solution compress it and hence double layer is thinner and smaller in volume. The net repulsive energy would be reduced and allowing approach of particles each other and agglomerate depend on the length of the double layer decreases. A mathematical model that is known as Schultze-Hardly states that the destabilization capability of the ions rises sharply with ion charge. This model is explained in detail in [Vermey et al., 1999]. Excess amount of coagulant, salts, does not lead to restabilization of particles.

Adsorption to produce charge neutralization: Charge neutralization occurs interaction between negatively charged colloids and cationic ions or metal hydrolysis products (positively charged metallic hydroxyoxide complexes) by adding metal salts [Cornelissen et al., 1997]. These products are adsorbed on the surface of negatively charged colloids. The result is decrease in the repulsive energy, and destabilization of colloid. Destabilization occurs typically at ZP values close to 0 mV. Very high concentration of coagulant dose can result in the restabilisation of the colloidal charge due to the charge is reversed. The most used coagulant, alumimiun and iron, produce numerous species which tend to polymerise to give polynuclear metallic hydroxides [Shammas, 2005], [Dennett et al., 1996].

Enmeshment in a precipitate (sweep coagulation): Hydrolysis reaction of metal salts is complex and product of reaction don not well understood. In near neutral pH, metal salts, such as alum and ferric that are the most used, form insoluble hydrolysis products and polymerise. If a sufficient quantity of metal salt is added, large amounts of metal hydroxide floc would occur. This metal hydroxide floc goes towards macroflocculation that result in large floc particles which is settleable. When floc particles settle, they sweep the colloidal particles. At higher coagulant doses, the colloidal particles can be enmeshment into sweep flocs.

Adsorption to permit interparticle bridging: Polymeric coagulants form bridge between the particles. They have reactive groups that bind to on the surface of colloidal particles. The remained long-chain molecule attached to another colloid particle. Bridged particles interlace with other bridged particles during the flocculation process. Destabilization arises from the sedimentation of tied together high molecular weight particles regardless of ZP value close to 0 mV. When polymer add excess amount, an overdose of polymer, restabilization occurs. Because the colloid completely covered by polymer. Also the rate of mixing can break the bridging and afterward restabilization is shown [Walter and Weber, 1972].

2.3.1.2. Generally Used Coagulants

Inorganic metal salts -aluminium and iron salt- are used in drinking water treatment plant. Aluminium and iron sulphates and chlorides have long been used for removal of turbidity and colour. When they added to the water, they are hydrolyzed through a series of reaction depending on the pH of solution and form soluble mononuclear [Duan and Gregory, 2003] and polynuclear complexes. Coagulation process efficiency depends on some factors such as coagulant dose, pH, mixing rate and time. This factors that effect on coagulation process have been investigated in detail by O'Melia [O'Melia, 1990], [McGhee, 1991].

The main function of coagulation is to destabilize suspended particles by neutralizing the negative charge and to aggregate destabilized particles into flocs, which are removed by sedimentation and/or filtration. Coagulation can reduce the NOM level by different patways. Gregor et al. [1997] found four patways which were responsible for coagulation (Figure 2.8) [Pernitsky and Edzwald, 2003]. First, NOM can combine with coagulants, the aluminium or ferric ions, to form a complex and precipitate in regions of pH where aluminium hydroxide precipitation is minimal (Patway C). Cationic alumminium species (monomeric and polymeric Al species) electrotastatically interacts with anionic NOM to form insoluble charge-neutral products. Second, at high coagulant doses, the insoluble metal hydroxyl can be removed by enmeshment or surface adsorption (patways A and B). The concentration of coagulant has to be high to ensure rapid precipitation of $Al(OH)_{3(s)}$. Colloidal NOM can act as nuclei for precipitate formation, or can become entrapped during floc aggregation.
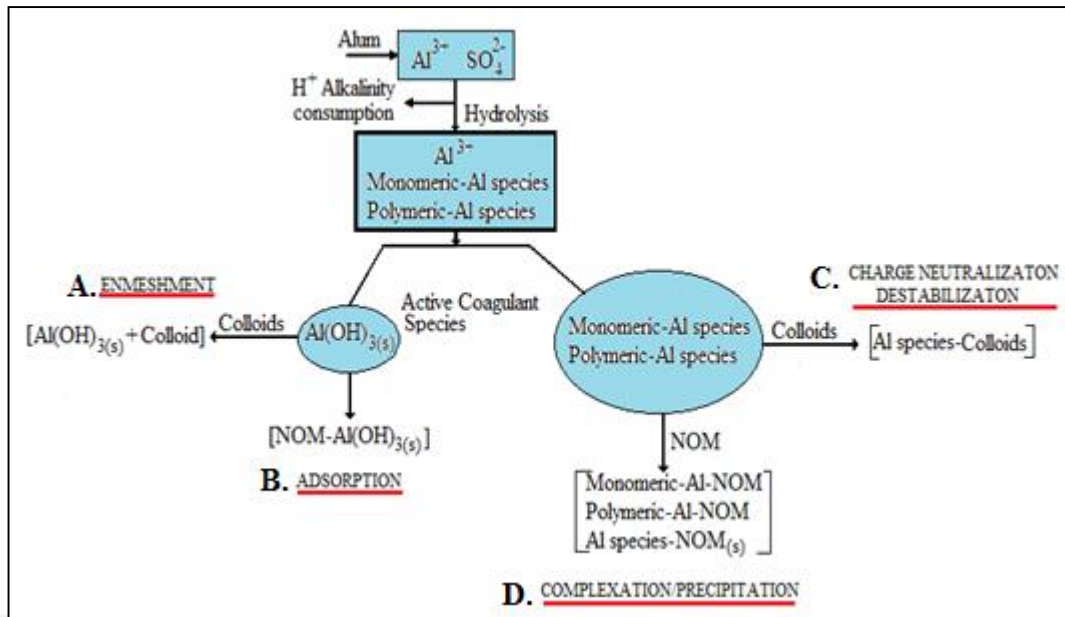
Figure 2.8: Pathway for NOM removal by alum coagulation reactions.

These mechanisms apply mainly to the removal of colloidal NOM, typically the higher molecular weight humic acids. These acids generally have low charge densities and they therefore need low coagulant doses to induce destabilization. The sweep coagulation (enmeshment) mechanism (pathway A), which operates most effectively on colloidal NOM, does not seem to be effective for these soluble fulvic acids. Charge neutralization (pathway C) may remove soluble fulvic acids, but high doses of coagulants are necessary to neutralise the high anionic charge. The high coagulant dose required by soluble fulvic acids seems to correspond to an overdosing of humic acid colloids which leads to a restabilisation of the colloids. A mechanism that is seldom mentioned is the chemical interaction of soluble NOM with soluble coagulant metal ions such as aluminium (pathway D). The metal cation and the complexed NOM remain in solution until either the binding capacity of the NOM has been satisfied, or the solubility of the metal–NOM complex is exceeded. The complex does not need to be charge-neutral to precipitate. A considerable amount of NOM can thus be removed by coagulation, sedimentation and filtration, especially at low pH (5.5 for alum) and/or higher coagulant doses. Omelia et al. (1999) indicate that the doses of coagulants required are determined by the content of NOM rather than by the turbidity. Primarily due to the negative charge carried by NOM, there is a stoichiometric relationship between the required dose of coagulant and the TOC

23

concentration in the water to be treated. After coagulation, the dominance of lower molecular weight materials increases considerably.

The pH value of medium mostly represents the removal mechanism of NOM by result in different metal hydroxide species. HMM polymer species (e.g. $AlO_4Al_{12}(OH)^{7+}_{24}$), efficiently remove particles through bridging or sweep flocculation, while medium polymer or monomer species have been suggested to have a high ability to remove DOC by complexation, adsorption, charge neutralization or co-precipitation [Yan et al., 2008], [Gregory, 1996]. The concentration of dissolved organic matter is reduced a limited amount even at the optimum doses of metal salts, using of various composite coagulants and advanced coagulants [Edwards, 1997], [van Leeuwen et al., 2002]. Especially, the removal yield of hydrophilic fraction of NOM is insufficient. The removal efficiency of hydrophobic fraction of NOM is better than hydrophilic fraction by coagulation process [Kim et al., 2005], [Sharp et al., 2006a and 2006b]

The removal efficiency of NOM generally is determined respect to DOC and UV absorbance measurements. According to many research ferric salts obtain better DOC removal efficiency than aluminium based coagulants [Budd et al., 2004], [Sharp et al., 2006c], [Rizzo et al., 2008]. However, some investigations showed that the aluminium based coagulants generally provide higher color [Yan et al., 2008], [Smith et al., 2009].

Advanced coagulants have been developed for increase removal of NOM. Enhanced coagulants can be defined as the process of improving the removal efficiency by using excess amount of coagulant. Enhance or optimized coagulation is considered the major treatment option for high alkalinity waters [Yan et al., 2008]. The important points about enhanced process are given in the following review [Matilainen et al., 2010b]. Removal of NOM for controlling DBP formation by enhanced caogulations has been studied [Liu et al., 2012]. The removal of dissolved organic matter using four typical coagulant combined with enhanced coagulation was investigated [Xie et al. 2012].

Recently, the uses of pre-hydrolyzed coagulants such as poly-ferric sulfate (PFS), poly-aluminium chloride (PACI) have been increased [Staaks et al., 2011]. These coagulants have been generated and used. They have high efficiency, wider working pH range, low cost, reduced amounts of coagulants and lower residual iron concentration convenient usage in water treatment [Zhang et al., 2008], [Shi et al.,

2007]. In many studies have been reported that PFS has improved the treatment efficiency of humic acid [Jiang and Graham, 1998], [Cheng and Chi, 2002], [Moussas P.A. and Zouboulis, 2012] and DOC [Jian et al., 1996]. Also the character of PFS has been well identified [Cheng, 2002]. Fabris and Volk compared removal efficiency of NOM using ferric and alum and PACl. Mao et al. were investigated the role of increasing dosage and composite coagulants in removal efficiency of DOC [Mao et al., 2013]. There are also polymeric coagulants combined with polysilicate such as polyferric silicate sulphate (PFSiS) [Yan et al., 2008], [Zouboulis et al., 2009], polyaluminium ferric silicate chloride (PAFSiC) [Niu et al., 2011].

Natural or synthetic polyelectrolytes have been used both primary coagulants and coagulant or flocculant aids. Polyelectrolytes can separate cationic, anionic depend on ionisable groups (e.g. carboxyl, amino or sulfonic), while polymers without ionisable groups are defined non-ionic. The role of organic polyelectrolytes in water treatment is given by Bolto and Gregory in their review [Bolto and Gregory, 2007]. The different type of polyelectrolytes has different NOM removal capacity change by case. Polyelectrolytes, especially cationic type of these coagulants have a quite toxic effect on aquatic organisms and some countries have restricted their use in water purification [Rizzo et al., 2008]. Thus the usages of these coagulants are not considered to be suitable coagulants.

2.4. Electrochemical Processes in Water Treatment

Electrochemical technologies such as electroflotation (EF), electrooxidation (EOx), and electrocoagulation (EC) for wastewater and drinking water treatment have been the subject of growing interest in recent years because of their several advantages over a typical water and wastewater treatment plant [Rajeshwar et al., 1994]. The electrochemical based treatment processes allow rapid and controlled reactions with robust and compact instrumentation, which provide ease of automation [Chen, 2004]. Instead of using chemicals and micro-organisms, the electrochemical treatment processes only employ electrons to facilitate water treatment, which offer better environmental compatibility [Mollah et al., 2004]. Electrochemical treatments generally have lower temperature requirements and require less space, and produce fewer by-products or sludge [Mollah et al., 2001].

The promising performance of electrochemical treatment has been proved in the diverse types of wastewater treatments including heavy metals [Kobya et al., 2015], [Thaveemaitree et al. 2003], agro industries [Gengec et al., 2012]; foodstuff [Chen et al. 2000], textile dyes [Martinez-Huitle and Brillas, 2009], [Naumczyk et al. 1996], oily wastes [Gotsi et al. 2005], suspended particles [Bukhari 2008], flüoride [Mameri et al. 1998], arsenic [Kobya et.al., 2015], phenolic wastes [Kobya et al., 2012], [Korbahti and Tanyolac, 2003], ultra-fine particles [Matteson et al. 1995], mine wastes [Kobya et al., 2014], [Jenke and Diebold 1984] and water disinfection [Feng et al. 2004].

The electrical circuit in an electrochemical cell may be conveniently divided into two parts. In the external electrical circuit, the current (i), flows in one direction, from anode to cathode as an electron flow. Within the cell, current flows electronically within the electrode structure and ionically in the electrolyte between them. In the electrolyte, the current flows via the two-way migration of ions, anions moving towards the anode and cations towards the cathode. The cathode is the electrode at which reduction of species occurs by electron gain from the electrode. The anode is the electrode at which oxidation of species occurs by electron loss to the electrode [Scott, 1995]. A schematic diagram of a typical electrochemical cell is shown in Figure 2.9.
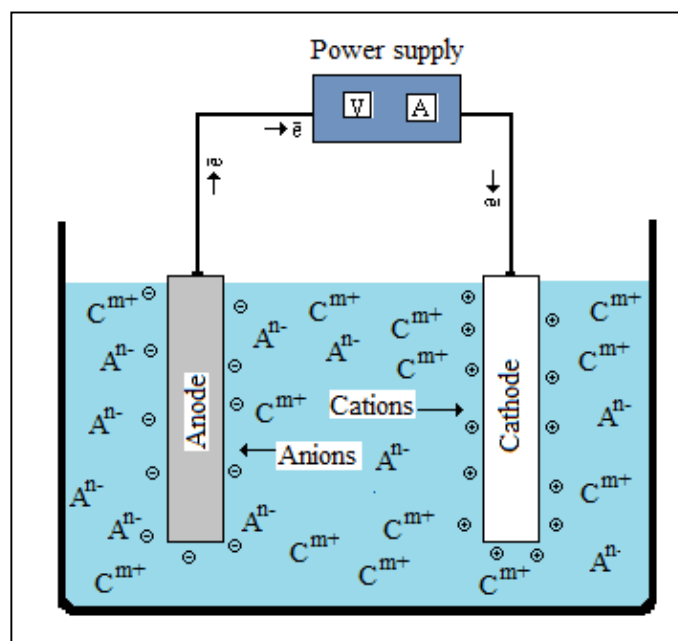
Figure 2.9: Schematic of typical electrolytic cell.

The electrocoagulation or electrochemical process is known to have two major oxidations on the wastewater: direct and indirect oxidation [Lin and Chang, 2000], [Pletcher and Walsh, 1990]. Direct oxidation occurs on the anodic surface and is due to surface adsorption and decomposition of pollutants. Indirect oxidation occurs in the bulk liquid phase and is caused by the strong oxidants such as Cl_2. In general, the indirect oxidation, which is highly dependent of the wastewater conductivity, plays a much more important role in the electrochemical oxidation process.

2.4.1. Electroflotation Process

Electroflotation or (perhaps, better) electrolytic flotation (EF) is an unconventional separation process owing its name to the bubbles generation method it uses, i.e., electrolysis of the aqueous medium (Figure 2.10). EF techniques are highly versatile and competitive to settling tank techniques which requires large land space [Matis and Peleka, 2010]. It is also competitive to other flotation techniques such as dissolved air flotation and dispersed air flotation. The EF reactors are small and compact and require less maintenance and running cost than other flotation units.
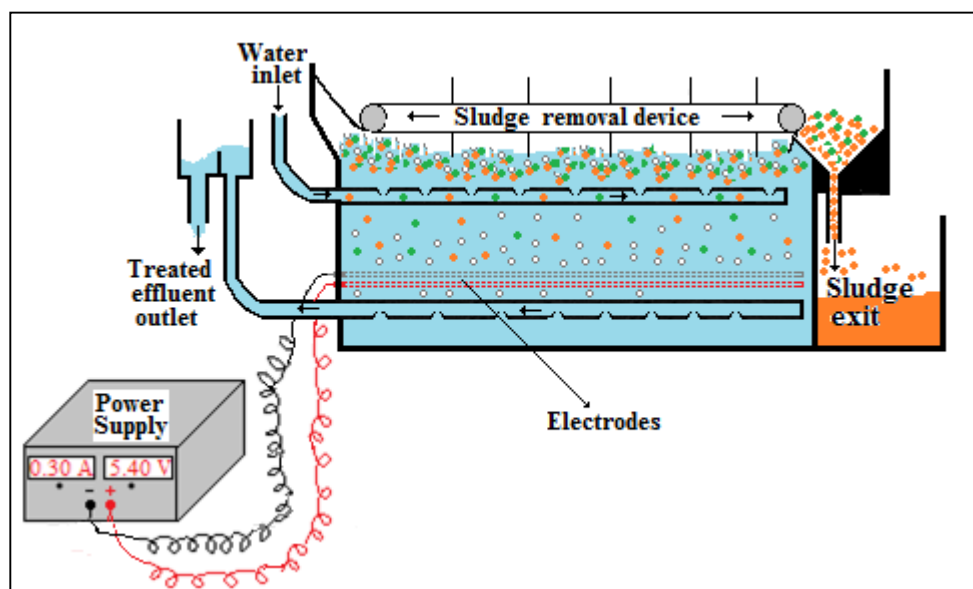
Figure 2.10: Schematic diagram of electroflocculation process.

The electroflotation process depends upon generation of hydrogen and oxygen gases during electrolysis of water. EF technique has three principal advantages. First,

dispersed gas bubbles formed from electrolysis are extremely fine and uniform, (with average bubble diameter around >20 µm. Second, varying current density gives the possibility of varying any gas bubble concentrations 'in the flotation medium, thereby increasing the probabilities of pollutants such as bubble-oil drop collision. Third, selection of appropriate electrode surface and solution conditions permit one to obtain optimum results for a specified separation process. EF method has been gaining importance in the treatment of several types of sewage and suspensions. When an effluent is brought between two electrodes, of which one is the positive anode and the other is the negative cathode, and electricity is supplied to the electrodes, an electric field is built up between them through the use of the suspension conductivity. Even without any other addition of chemical reagents, a preliminary coagulation occurs within the particulate matter of the effluent, which results in the grouping of the negative and positive particles together. EF is a simple process that floats pollutants (or other substances) by their adhesion onto tiny bubbles of hydrogen and oxygen generated from electrolysis of aqueous solutions [Chen, 2004], [Romanov, 1998]. Therefore, the electrochemical reactions at the cathode and anode are hydrogen evolution and oxygen evolution reactions, respectively. Anode and a cathode reactions produces fine oxygen and hydrogen bubbles in the EF process is as shown in the following:

$$\text{Anode reaction: } 2H_2O \rightarrow O_{2(g)} + 4H^+ + 4e^- \tag{2.4}$$

$$\text{Cathode reaction: } 4H^+ + 4e^- \rightarrow 2H_{2(g)} \tag{2.5}$$

$$\text{The total reaction is: } 2H_2O \rightarrow 2H_{2(g)} + O_{2(g)} \tag{2.6}$$
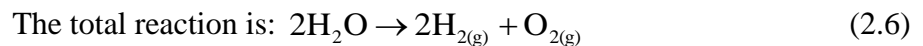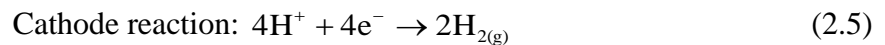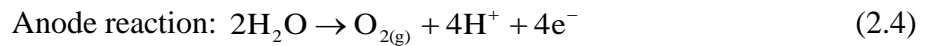
Equation (2.3) demostrates that the amount of hydrogen gas generated is twice that of oxygen gas. The gas generating rate can be calculated according to the Faraday's law:

$$Q_{H_{2(g)}} = \frac{i \times V_o}{n_{H_2} \times F} \text{ and } Q_{O_{2(g)}} = \frac{i \times V_o}{n_{O_2} \times F} \tag{2.3}$$

where $Q_{H_{2(g)}}$ and $Q_{O_{2(g)}}$ are the hydrogen and oxygen gases generating rates (L/s) at the normal state, respectively. V_o the molar volume of gases at the normal state (22.4

L/mol), F the Faraday's constant (96487 C/mol electrons), n_{H_2} the electron transfer number of H_2 (2 mol electrons per mole of H_2), and n_{O_2} is the electrons transfer number of O_2 (4 mol electrons per mole of O_2). The total gases generating rate ($Q_g = Q_{H_{2(g)}} + Q_{O_{2(g)}}$) is calculated as $1.74 \times 10^{-4} \times i$.

EF was first proposed by Elmore in 1904 for flotation of valuable minerals from ores. Since the hydrogen and oxygen gases produced by electrolysis are in their atomic state at the time of liberation, they can produce significant changes on the surface of the particles. Though these forms remain in existence only for an extremely brief period, within this duration, electrochemical changes are imparted on the minerals. Glembotskii et al. [1975] have suggested collectorless flotation of minerals by electrochemical treatment. In general, collectors (surfactants) are added to impart hydrophobic character on mineral particles that are to be floated and separated from a other gangue minerals. However, some sulfide minerals like PbS, $CuFeS_2$ and FeS_2 were made fully hydrophobic by converting sulfide ions at the surface to elemental sulfur by electrolytic oxygen. The performance of an electroflotation system is reflected by the pollutant removal efficiency and the power and/or chemical consumptions. The pollutant removal efficiency is largely dependent on the size of the bubbles formed. For the power consumption, it relates to the cell design, electrode materials as well as the operating conditions such as current density, water conductivity, etc. If the solid particles are charged, the opposite zeta-potential for the bubbles are recommended. The bubble size distribution depends on the solution pH as well as the electrode material, showed in Table 2.11 [Chen, 2004].

Table 2.3: The range of gas bubbles at different pH and electrode materials.

pH	Hydrogen (μm)			Oxygen (μm)
	Pt	Fe	C	Pt
2	45-90	20-80	18-60	15-30
7	5-30	5-45	5-80	17-50
12	17-45	17-60	17-60	30-70

The hydrogen bubbles are smallest at neutral pH. For oxygen bubbles, their sizes increase with pH. It should be noted, however, the cathode materials affect the

size of the hydrogen bubbles, so do the anode materials. The bubble sizes obey a log-normal distribution [Fukui and Yuu, 1985]. Using buffer solution, [Llerena et al. 1996] found that the recovery of sphalerite fines is optimal at pH between 3 and 4. They also documented that during this pH range, the hydrogen bubbles are the smallest, about $16\pm2\,\mu m$. Decrease or increase pH from 3 to 4 results in the increase of hydrogen bubbles. At pH of 6, the mean hydrogen bubbles is $27\,\mu m$. At pH of 2, the hydrogen bubbles are about $23\,\mu m$ when the current density was all fixed at 500 A/m^2 using a 304 SS wire mesh. Oxygen and hydrogen were separated in their research and it was found that the increase of pH in the cathode chamber and pH decrease in the anode chamber are very quick when no buffer solutions were used. The recovery efficiency of oxygen is about half of that of hydrogen proportional to the amount of gas generated at a given current. This was also confirmed by O_2 and H_2 gas sparging. The gas bubbles depends also on the current density [Ketkar et al., 1991]. The surface condition affects the particle size, too. The polished mirror surface of the stainless steel plate obtained the finest bubbles. Besides size of bubble, the bubble flux, defined as the number of gas bubbles available per second per unit cross-section area of the flotation cell, also plays a role in mineral flotation, recovery of different sized particles [Ketkar et al., 1991]. A decrease from 39 to 28 μm hidrogen and from 50 to 38 μm oxygen for 200 mesh electrodes of gas bubble sizes was found with the increase from 125 A/m^2 to 375 A/m^2 of current intensity. At the low current densities was found decrease of bubble size with increase in current density [Burns et al., 1997]. When the current density is higher than 200 A/m^2, at different conditions for graphite electrodes can be observed with gas bubbles ranging from 20 to 38 μm. A decrease of gas bubble size distribution was achieved with increase in current intensity, as also observed by Shen et al. [Shen et al., 2003]. The key to floatability of chemical species in liquid streams is hydrophobicity, the ratio of collector to metal ion being an important factor. The amount of collector used in ion flotation should be at least stoichiometric if it has frother properties [Casqueira et al., 2006]. Usually a small excess of collector is added to guarantee maximum removal of the metallic ions in solution. There have been a number of studies that have used electroflotation involving mineral flotation. Raju and Khangaonkar (1984) reported a 74-81% recovery of 4 μm chalcopyrite with electrolytically generated hydrogen bubbles using a current density in the range of 490-1470 A/m^2. Ketkar et

al. (1991) reported more than 60% recovery of +4-10 μm quartz with hydrogen bubbles of 22 μm diameter. Han et al. (2006) used electroflotation to generate very fine bubbles with 27 μm mean diameter to obtain 98% recovery of 28 μm flocculated kaolin particles. EF has mainly been used in mineral processing.

Examples from the literature given in the present review include heavy metals, textile dyes, food, paper industry, oily effluents, laundry wastewaters, sludge etc. and are accompanied by typical laboratory results [Matis and Peleka, 2010]. However, in water and wastewater treatment, flotation is often the most effective process for the separation of oil and low-density suspended solids. EF is a promising technique especially in oily wastewater treatment [Hosny, 1996]. The increase in SS and COD removal due to electroflotation from restaurant wastewater is significant. As the charge loading increased from zero to 0.50 Faradays/m^3 of charge loading, the removal efficiencies increased rapidly from 65 to >90% for SS and from 62 to 71% for COD [Chen et al., 2000]. Turbidity, total solids, oils and greases, COD and methanol from biodisel wastewater (pH 7.5, TS = 745 mg/L, Oil-grease = 1900 mg/L, COD = 121768 mg/L, turbidity = 84.4 NTU, methanol = 12.52 mol/L) by EF using aluminum electrodes at process conditions (current density of 8 mA/cm^2 and reaction time of 60 min were effectively removed as 92%, 98%, 100%, 57%, and 23%, respectively [Romero et al., 2013]. The separation of finely dispersed oil from oil-water emulsions was carried out in an electroflotation cell which has a set of electrodes, a lead anode and stainless steel screen cathode [Hosny, 1996]. The oil separation reached 65% at optimum conditions; 75% in the presence of NaCl (3.5% by wt. of solution); and 92% with the presence of NaCl and at optimum concentration of flocculant agent. Electrical energy consumption varied from 0.5 to 10.6 KWh/m^3 according to experimental conditions. Belkacem et al. [2008] experimentally studied the clarification of textile wastewater using EF process with aluminum electrodes. The application of the optimized parameters as applied voltage = 20 V, distance between electrodes = 1 cm, and period of time = 20 min on an industrial wastewater derived from an Algerian velvet manufacture showed a high removal of 93.5% BOD$_5$, 90.3% COD, 78.7%, turbidity, SS = 93.3%) and color (>93%).

2.4.2 Electrooxidation Process

In recent years, electrochemical technologies have caused great interest because they offer effective means to solve environmental problems related to industrial processes. such as wastewater contamination. The highest advantage of these methods is their environmental compatibility. Their principal reagent is the electron, which is an inherently clean species whose energy can be carefully controlled by means of an applied potential, thus avoiding parallel reactions. In traditional chemistry, secondary reactions often result in subproducts which sometimes increase removal costs. The principal electrochemical methods are the following:

(i). *direct electrochemical oxidation*, where the organic compound degradation occurs directly over the anode trough the adsorbed $^{\bullet}$OH, or chemisorbed active oxygen in the anode surface (often called "anodic oxidation, direct oxidation or electrochemical incineration"), by means of the following general reaction 2.7 and Figure 2.12 and 2.13, [Peralta-Hernandez et al., 2012], [Vlyssides et al., 2004], [Panizza and Cerisola, 2004]:

$$M + H_2O \rightarrow M(^{\bullet}OH) + H^+ + e^- \qquad (2.7)$$
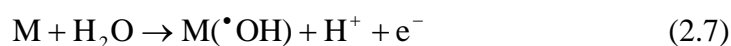
where the pollutants are first adsorbed on the anode surface (M) and then destroyed by the anodic electron transfer reaction,

(ii) *indirect electrochemical oxidation,* where the organic compounds are treated in the bulk solution by means of species generated in the electrode, such as $^{\bullet}$OH (by means of the Fenton reaction), Cl_2, hypochlorite, peroxodisulfate, and ozone, as the most common electrochemically generated oxidants (Figure 2.11 and 2.12).
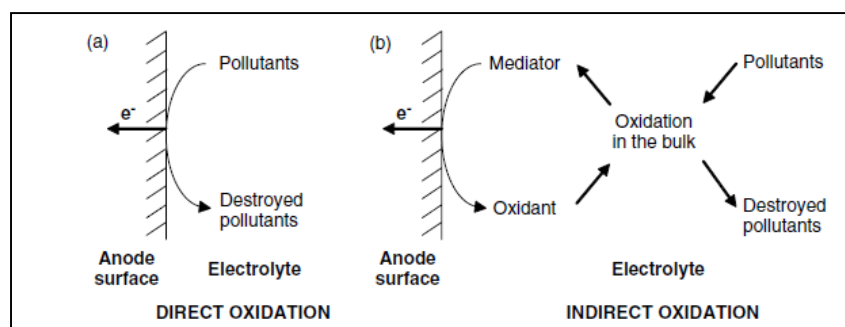
Figure 2.11: Schemes for a) direct and b) indirect electrolytic treatment of pollutants.
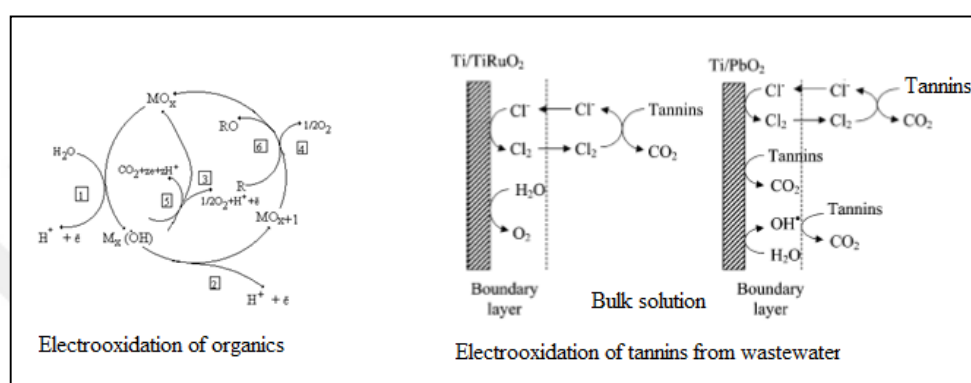
Figure 2.12: Scheme of the reactions involved in electrooxidation.

The choice of electrode material is of paramount importance as it affects the selectivity and the efficiency of the process. The electrode material must have the following properties: high physical and chemical stability, resistance to erosion, corrosion and formation of passivation layers, high electrical conductivity, catalytic activity and selectivity, low cost/life ratio. The use of electrode materials that are inexpensive and durable must be favoured.

In order to assess the selectivity of an anodematerial, competition between the oxidation of organics at the anode and the side reaction of oxygen evolution must be considered:

$$2H_2O \rightarrow O_2 + 4H^+ + 4e^- \tag{2.8}$$

The oxidation of water to oxygen occurs at approximately 1.2 V vs. NHE (normal hydrogen electrode). However, in fact, a higher voltage has to be applied for electrochemical oxidation of water to occur at the anode. The difference between the

value of the voltage at which the oxidation of water actually begins to take place, and the thermodynamic value is the oxygen evolution overpotential [Anglada et al., 2009]. Low O_2 overvoltage anodes are characterized by a high electrochemical activity toward oxygen evolution and low chemical reactivity toward oxidation of organics. Effective oxidation of pollutants at these anodes may occur at low current densities; at high current densities, significant decrease of the current efficiency is expected due to the production of oxygen. In contrast, at high O_2 overvoltage anodes, higher current densities may be applied with minimal contribution from the oxygen evolution side reaction. In view of the afore mentioned facts, high O_2 overvoltage anodes are usually preferred. In particular, boron-doped diamond (BDD) anodes have been reported to yield higher organic oxidation rates and greater current efficiencies than other commonly used metal oxides such as PbO_2, and Ti/SnO_2-Sb_2O_5.

Among the variables that are usually modified in electrochemical oxidation processes, the current density (intensity per unit area of electrode) may be the term most frequently referred to because it controls the reaction rate. It should be highlighted that an increase in current density does not necessarily result in an increase in the oxidation efficiency or oxidation rate and that for a given anode material, the effect of current density on the treatment efficiency depends on the characteristics of the effluent to be treated [Anglada et al., 2009]. However, the use of higher current densities usually results in higher operating costs due to the increase in energy consumption. In contrast to current density, the effect of temperature on the overall efficiency of the electro-oxidation process has not been widely studied. It is generally acknowledged that direct oxidation processes remain almost unaffected by temperature whereasmediated oxidation processes do not. An improvement with increasing temperature of the mediated oxidation processes by inorganic electrogenerated reagents (active chlorine, peroxodisulfate) has been reported. Nevertheless, operation at ambient temperature is usually preferred as it provides electrochemical processes with lower temperature requirements than those of the equivalent non-electrochemical counterparts (i.e. incineration, supercritical oxidation).

The physico-chemical characteristics of the waste-water (natüre and concentration of electrolyte, pH value and concentration of target pollutants) also affect the electrochemical oxidation process. Although no agreement has been

reached on the effect of the nature and concentration of electrolyte on the overall oxidation efficiency, it has to be kept in mind that the higher the concentration of electrolyte, the higher the conductivity and consequently the lower the cell voltage for a given current density. For this reason, electrochemical oxidation treatment is more convenient and cost effective when the waste-waters to be treated already have high salinity. The pH value, like temperature, affectsmostly indirect oxidation processes. However, a review of previous publications does not allow a conclusion to be reached on whether increasing or decreasing pH favours pollutant removal in electrochemical oxidation of waste-waters. In chloride mediated reactions, the pH value may affect the oxidation rate because it determines the primary active chloro species that is present in the effluent.

$$Cl^- \rightarrow \frac{1}{2} Cl_2 + e^- \tag{2.9}$$

$$Cl_2 + H_2O \rightarrow HOCl + H^+ + Cl^- \tag{2.10}$$

$$HOCl \rightarrow OCl^- + H^+ \tag{2.11}$$

During indirect oxidation, chlorine evolution occurs at the anode (reaction 2.9). At pH values lower than 3.3, the primary active chloro species is Cl_2 while at higher pH values its diffusion away from the anode is coupled to its disproportionation reaction to form HClO at pH<7.5 (Reaction 2.10) and ClO^- at pH>7.5 (Reaction 2.11). In principle, operation at strongly acidic conditions would be considered to be the best option as chlorine is the strongest oxidant followed by HClO. However, the system setup usually employed in electrochemical oxidation of waste-waters promotes its desorption, hindering its action as an oxidizing agent. Consequently, higher pH values would theoretically enhance the electro-oxidation of pollutants, as HClO and ClO^- are almost unaffected by desorption of gases and they can act as oxidizing reagents in the total volume of wastewater.

Electrooxidation (EO) is another electrochemical technique used to successfully treat different types of wastewater such as olive mill wastewater, distillery industry wastewater, landfill leachates, pesticides, and tannery saline wastewater [Chen, 2004], [Mollah et al., 2001]. In EO, anodic oxidation does not require added chemicals or oxygen and does not produce secondary pollutants or

require complicated accessories. The most important component in EO process is the anode. In recent decades, several electrodes have been evaluated to rank anode material in terms of high stability, high activity toward organic oxidation, and cost. The types of electrodes tested included graphite, platinum, IrO_2, RuO_2, SnO_2, PbO_2, Ti/Pt, Ti/RuO_2, Ti/Pt–Ir, Ti/RuO_2-TiO_2, Ti/PbO_2, Ti/Pt–Ir, $Ti/PbO2$, Ti/PdO–Co_3O_4, and $Ti/RhOx$–TiO_2, Ti coated with oxides of Ru/Ir/Ta, boron-doped diamond (BDD) thin films, and others. An electrochemical oxidation mechanism involves the production of ˙OH-radicals that result in electrochemical mineralization of organic compounds at the active sites of the anode. Efficient degradation of paper mill wastewater has been achieved using three-dimensional electrodes ($Ti/Co/SnO_2$–Sb_2O_5) combined with activated carbon treatment [Wang et al., 2007]. "Non-active" electrodes, such as SnO_2, form hydroxyl radicals on their surface more easily, which can result in the complete oxidation of the organic molecules to CO_2 [Miwa et al., 2006]. Electro-oxidation was effective in removing humic acid and algae from pondwater Liao et al. [Liao et al., 2008]. Motheo and Pinhedo [Motheo et al., 200] investigated natural peat humic acid electro-oxidation by DSA electrodes, demonstrating that electrolysis efficiency was highly dependent on electrode composition. Landfill leachated color removal was 84% at 18 mA/cm^2 by BDDm100. Cooking water and synthetic waste water treatment efficiency almost 100% by BDD, and BDD and Pt at different current density, respectively [Zhu et al., 2009], [Murugananthan et al., 2010]. BDD electrodes are highly efficient for the removal of different organic pollutants and refractory organic pollutants. Considerable ˙OH amounts may be electrogenerated on BDD anodes. These radicals, due to their weak interaction with the BDD film, present high reactivity towards organics (Reaction 2.12-2.14); these processes have been efficiently used in wastewater treatment as follows:

$$BDD + H_2O \rightarrow BDD(^{\bullet}OH) + H^+ + e^- \qquad (2.12)$$

$$BDD(^{\bullet}OH) + R \rightarrow BDD + mCO_2 + nH_2O \qquad (2.13)$$
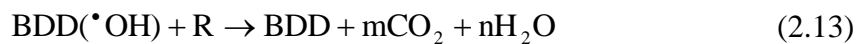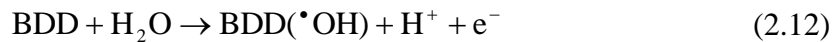
According to the literature, reaction (3) is in competition with the side reaction of free ˙OH discharge to O_2 without any participation of BDD surface, following the next reaction:

$$BDD(^{\bullet}OH) \rightarrow BDD + \frac{1}{2}O_2 + H^+ + e^- \qquad (2.14)$$
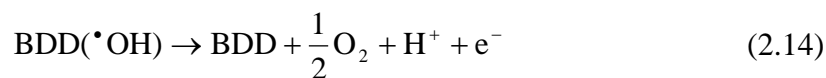
However, many authors have reported that during incineration process of BDD anodes at high potentials, a great number of organic pollutants are completely mineralized by the reaction with electrogenerated free $^{\bullet}OH$ species [Peralta-Hernandez et al., 2012].

Degradation current efficiencies can vary significantly, however, and it is important to achieve the required removal efficiency by adjusting current density together with the removal time and energy consumption of the process. In EO technology, electrolysis efficiency is strongly linked to electrode composition. The discovery of an effective and stable yet economical electrode material would speed up the use of EO techniques for NOM removal.

2.4.3. Electrocoagulation Process

EC treatment is a complicated process involving many chemical and physical phenomena that use the in situ generation of coagulants by electrolytic oxidation of the sacrificial electrode materials. Through the connection to the external DC source, the electrode materials such as Fe or Al are dissolved from the anode generating corresponding metal ions, which almost immediately hydrolyze to polymeric iron or aluminium hydroxides. These polymeric hydroxides are excellent coagulating agents which can combine with charged particles or colloidal contaminants in the wastewater. The coagulated contaminants are then removed by electroflotation, sedimentation, or filtration to provide clean water in the end.

The first EC plant has been first proposed in London towards the end of nineteenth century. First time, the large scale EC plant performed for treatment of drinking water in 1946, ABD. The river water was treated by same EC process in 1956, England [Mollah et al., 2001]. Color and turbidity removed efficiently with both of these two investigations. At that time, the applications and studies about EC has been interested in limited due to some reason such as high operational cost compared to chemical dosage. The alternative technologies have been needed due to

increase in pollution in environment, the restricted regulation on water quality. Recently, EC has been again high interested in purification of water with developed scientific and economic world. It seems that EC process is a promising, innovative electrochemical technology in water and waste water treatment.

EC is one of the alternative treatment processes to the conventional processes and advanced technologies. There are advantages for EC compared to current processes, which are as follows [Martinez-Huitle and Brillas, 2009], [Mollah et al., 2004]:

- EC needs simple equipments, designable for virtually any size, and easily operable. It requires low maintenance cost with no moving parts. The start-up and operating costs are relatively low.
- Environmental compatibility, versatility, energy efficiency, safety, selectivity, amenability to automation, and cost effectiveness.
- More effective and rapid organic matter separation than in coagulation. The treating water is odorless, low turbidity.
- EC is an efficient technique since adsorption of hydroxide on mineral surfaces are a 100 times greater on 'in situ' rather than on preprecipitated hydroxides when metal hydroxides are used as coagulant. EC.
- pH control is not necessary, except for extreme values.
- Flocs formed by EC are similar to chemical floc, except that EC floc tends to be much larger, contains less bound water, is acid-resistant and more stable, and therefore, can be separated faster by filtration.
- EC is a low-sludge producing process. The formed sludge tends to be easily settable and de-water, because it is composed of essentially metallic oxides/hydroxides.
- The EC process has the advantage of removing the smallest colloidal particles, because the applied electric field sets them in faster motion, thereby facilitating the coagulation.
- The gas bubbles produced during electrolysis can carry the pollutant to the top of the solution where it can be more easily concentrated, collected and removed.

- EC produces effluent with less total dissolved solids (TDS) content as compared with chemical treatments. If this water is reused, the low TDS level contributes to a lower water recovery cost.

- The EC process avoids uses of chemicals and so there is no problem of neutralizing excess chemicals and no possibility of secondary pollution (i.e. sulfate and chloride) caused by chemical substances added at high concentration as when chemical coagulation of wastewater is used.

- Operating costs are much lower than in most conventional technologies.

- The electrolytic processes in the EC cell are controlled electrically and with no moving parts, thus requiring less maintenance.

- It needs low current, and it can be run even by green processes, such as, solar, wind mills and fuel cells.

However, this method presents as major disadvantages [Martinez-Huitle and Brillas, 2009], [Mollah et al., 2004]:

- The cost of operating EC may be high in those are as where the cost of electricity is high.

- The sacrificial electrodes are dissolved into wastewater streams as a result of oxidation, and need to be regularly replaced.

- In some EC systems an impermeable oxide film (anode passivation) can form on the cathode, leading to loss of efficiency of the EC unit. However, changing polarity may help reduce this interference.

- It requires a minimum conductivity depending on reactor design, limiting its use with water containing low dissolved solids.

- In case of the removal of organic compounds, some toxic chlorinated organic compound may be formed in situ if chlorides are also present.

- High concentrations of iron and aluminium ions in the effluent that have to be removed

2.4.3.1. The Theory of EC

Electrocoagulation theory and fundamentals are well described in bibliography [Mollah et al., 2001], [Chen, 2004], and [Kuokkanen et al., 2013]. The chemical coagulation remove the organic pollutant from water various mechanisms that are double layer compression, adsorption-charge neutralization, sweep coagulation, and interparticle bridging. They are explained in the section 2.3.1. The CC occurs when the various chemicals are added to the solution. However, in electrocoagulation, coagulants are produced in-situ by dissolution of electrode material. The EC process shows similarly removal mechanisms with CC. On the other hand, EC has side reaction as different from CC. In anode and cathode electrodes a serious of reaction occurs simultaneously, as EC, EO and EF. The main processes that result in removal of impurities in EC process can be summarized in Figure 2.13.
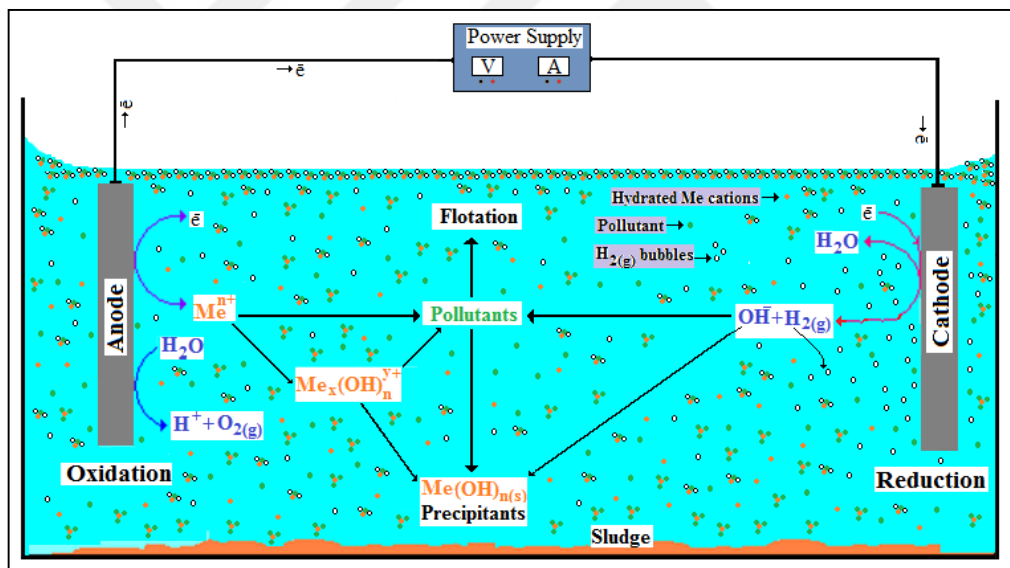
Figure 2.13: Schematic representation of the EC process.

In the EC process, the destabilization mechanisms of the pollutants, particulate suspensions, and breaking of emulsions may be summarized as follows. (1) compression of the diffuse layer around the charged species by the interactions of ions generated by oxidation of the sacrificial anode due to application of current through solution. (2) Charge neutralization of the ionic species present in water by counter ions produced by electrochemical dissolution of the sacrificial electrode. The electrostatic inter-particle repulsion is reduced by these counter ions to the extent that

the van der Waals attraction predominates, thus causing coagulation. (3) Floc formation: the floc formed as a result of coagulation creates a sludge blanket that entraps and bridges colloidal particles that are still remaining in the aqueous medium.

EC process depends on a current that is applied from an external power pass through the electrodes. The simple EC reactor comprises one anode and one cathode electrodes. Anode electrode undergoes oxidation, and dissolves and produces charged species in solution while the cathode electrode that is inert electrodes will be subjected to reduction of metals. These ions (Fe^{2+}, Fe^{3+}, Al^{3+}) are gradually hydrolyzed and form metal hydroxides such as $Al(OH)_2$, $Fe(OH)_2$ and $Fe(OH)_3$ that are of very low solubility depend on pH of the solution. They cause coagulation and the generated gas cause flotation of the coagulated materials in EC process (Figure 2.14). Holt [2004] showed the clay pollutant flocs formed after 12 minute of electrocoagulation operation at 1 A (Figure 2.15). In the electrocoagulation process, highly charged cations destabilize any colloidal particles by the formation of polyvalent poly hydroxide complexes. These complexes have high adsorption properties, forming aggregates with pollutants. Evolution of hydrogen gas aids in mixing and hence (flocculation). Once the floc is generated, the electrostatic gas creates a flotation effect removing the pollutants to the floc-foam layer at the liquid surface.
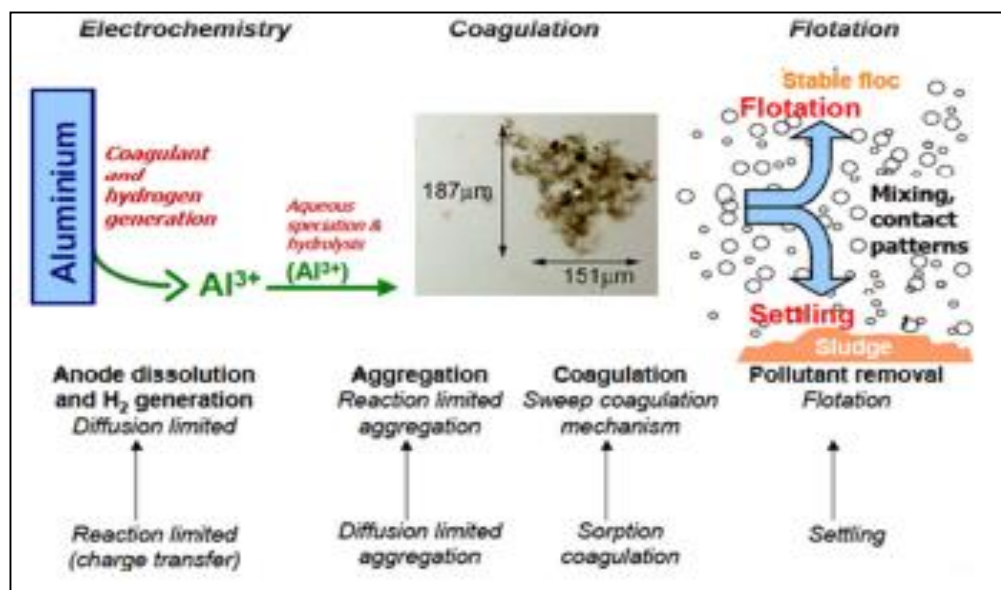
Figure 2.14: Mechanistic summary of electrocoagulation.
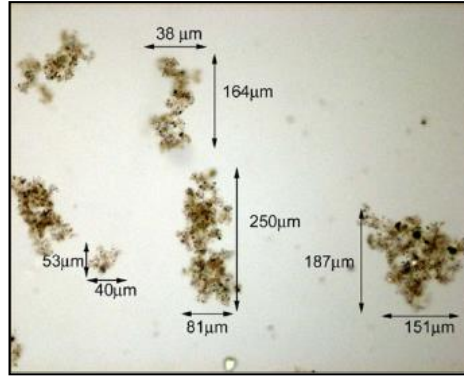
Figure 2.15: Microscopic image of aggregates from EC reactor at 12 minutes (10x).

On the other hand, the reaction at the cathode side is very important because of the producing of gas bubbles which lift the pollutant particles to the surface by a flotation process. Another advantage of the producing of gas bubbles is encouraging the contact between pollutant particles and coagulant by providing a certain amount if mixing action.

2.4.3.1.1. A Brief Description of the EC Mechanism with Aluminium Anodes

EC technique uses a direct current source between metal electrodes, which is usually made of iron or aluminium immersed in wastewater. The EC process features electrochemical dissolution of a sacrificial anode and simultaneous hydrogen gas evolution at the cathode according to Faraday's Law. In this study, aluminium electrodes are used in the EC process. This is caused by electro-dissolution of the anode and the reduction of water at the cathode which generates aluminium and hydroxide ions according to the following reactions [Daneshvar et al., 2006], [Can et al., 2003]:

Anode reactions:

$$Al \rightarrow Al^{3+} + 3e^{-} \tag{2.15}$$

$$O_{2(g)} + 4H^{+} + 4e^{-} \rightarrow 2H_2O, (E^{o} = +1.229\,V) \tag{2.16}$$

Cathode reaction:

$$3H_2O + 3e^- \rightarrow \frac{3}{2}H_{2(g)} + +3OH^- \qquad (2.17)$$

Solution reactions:

$$Al^{3+} + 3OH^- \rightarrow Al(OH)_{3\downarrow} \text{ (at alkaline conditions)} \qquad (2.18)$$

$$Al^{3+} + 3H_2O \rightarrow Al(OH)_{3\downarrow} + 3H^+ \text{ (at acidic conditions)} \qquad (2.19)$$
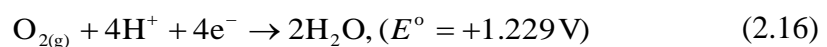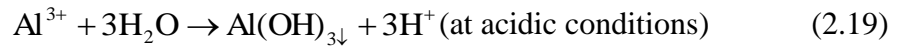
The standard potential of aluminum dissolution is lower (E_1^o = -1.662 V), than the standard potential of hydrogen evolution (E_2^o = -0.828 V). The dissolution of aluminum is thermodynamically favored ($E_2^o \gg E_1^o$) and it should proceed spontaneously.

The speciation of the aluminium hydroxides formed during EC is highly variable and is strongly influenced by pH [Can et al., 2003], [Canizares et al., 2006]:

$$xAl^{3+} + yOH^- \rightarrow Al_x(OH)_y^{3x-y} \qquad (2.20)$$
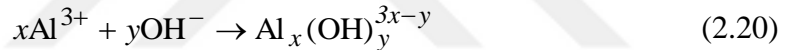
The Al^{3+} and hydroxide ions (OH^-) produced at the electrodes react to form monomeric species such as $Al(OH)^{2+}$, $Al(OH)_2^+$, $Al_2(OH)_2^{4+}$, $Al(OH)_4^-$ at low pH values and polymeric species such as $Al_6(OH)_{15}^{3+}$, $Al_7(OH)_{17}^{4+}$, $Al_8(OH)_{20}^{4+}$, $Al_{13}O_4(OH)_{12}^{7+}$, and $Al_{13}(OH)_{34}^{5+}$ (Figure 2.16), transformed initially into $Al(OH)_{3(s)}$ in the solution according to reaction (2.20) and finally into solid $Al(OH)_3$ according to complex precipitation kinetics [Can and Bayramoglu, 2014], [Canizares et al., 2006], [Mollah et al., 2001], [Rebhun and Lurie, 1993].
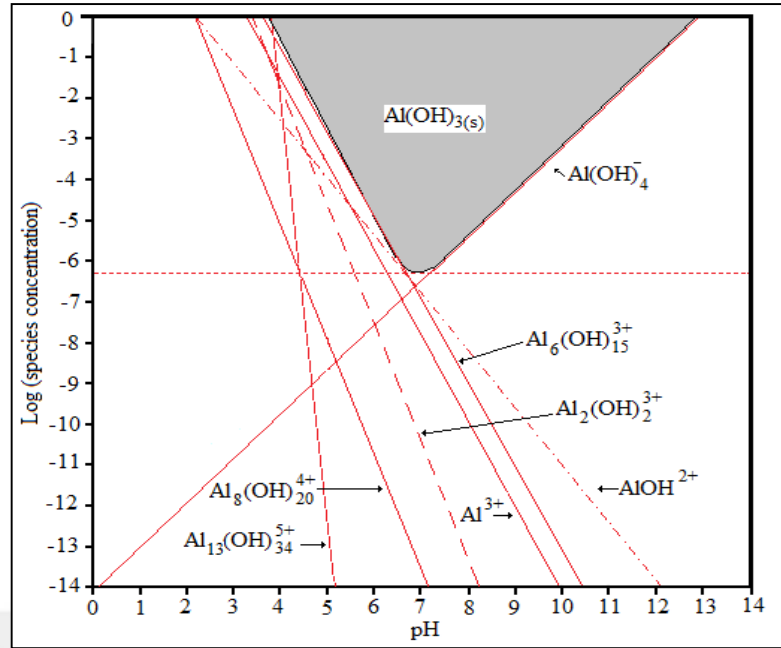
Figure 2.16: Solubility of Al species as a function of Al concentration and pH.

In electrocoagulation process, different species of aluminum hydroxide compounds are formed in the reaction environment at different pH values. Cationic monomeric species of aluminum, such as $Al(H_2O)_6^{3+}$, are the dominant species at pH< 4. In the pH of between 5.2 to 8.8, polymeric species and insoluble $Al(OH)_3$ are dominant species. In the pH> 9, $Al(OH)_4^-$ is the dominant species and in pH> 10, $Al(OH)_4^-$ is only species in solution. At pH in the range of 4-5, neutralization of opposite charges and elimination are due to reaction of pollutants such as humic substances with monomeric aluminum species such as $Al(OH)_2^+$ and $Al(H_2O)_6^{3+}$.

$$Pollutant + Monomeric\,Al\,species \rightarrow [Pollutant - monomeric\,Al\,species]_{(s)} \quad (2.21)$$

At pH in the range of 5 to 6, neutralization of opposite charges and elimination are due to reaction of pollutant molecules with polymeric aluminum species, such as $Al_3(OH)_4^{5+}$, $Al_6(OH)_{15}^{3+}$, and $Al_7(OH)_{17}^{4+}$.

$$Pollutant + Polymeric\,Al\,species \rightarrow [Pollutant - Polymeric\,Al\,species]_{(s)} \quad (2.22)$$

At pH more than 6.5, pollutant molecules adsorbed on Al(OH)$_3$ flocs and produced suspended particles. Surface of Al(OH)$_3$ flocs could attract dissolved organic compounds or trapped colloid particles and caused their separation and removal of them from solution through precipitation or flotation by hydrogen bubbles.

$$Al^{3+} + 4OH^- \rightarrow [\text{monomeric or dimeric Al species}] + Al(OH)_4^-$$
$$\rightarrow [Al_{13} \text{ polymeric species}] + OH^- \rightarrow [\text{colloid and precipitated Al species}] + OH^- \rightarrow Al(OH)_{3\downarrow} \quad (2.23)$$
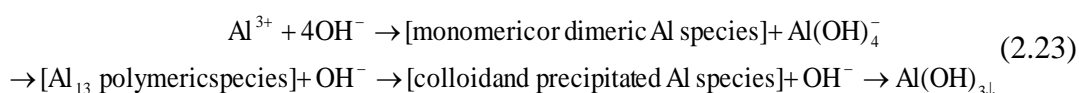
At pH values below 3.5, the aluminium ion is the predominant species. The predominant aluminium chemical species at pH values of 4.0-9.5 was Al(OH)$_{3(s)}$. The pH of minimum solubility of solid Al(OH)$_{3(s)}$ is about 6.5, and total soluble Al^{3+} concentration is 3×10^{-6} to 3×10^{-4} M (or 0.025-2.5 mg/L) between pH 6 and 9. However, it is interesting to note that a new aluminium complex forms as Al(OH)$_4^-$ at pH values greater than 10.0. This ion is soluble and directly affects the pollutant removal. On the other hand, the cathode may be chemically attacked by hydroxyl ions generated during H$_{2(g)}$ evolution at high pH values [Picard et al., 2000]:

$$2Al + 6H_2O + 2OH^- \rightarrow 2Al(OH)_4^- + 3H_2 \quad (2.24)$$

The positively charged polyhydroxo-complexes such as Al$_8$(OH)$_{20}^{4+}$ are the effective flocculants in the pH range 4-7. Freshly formed amorphous Al(OH)$_{3(s)}$ "sweep flocs" have large surface areas, which are beneficial for a rapid adsorption of soluble organic and inorganic compounds and trapping of colloidal particles. Simultaneously, the hydroxyl ions produced at the cathode increase the pH in the electrolyte and may induce precipitation and co-precipitation of metal ions in wastewater in the form of their corresponding hydroxides. Moreover, there is a possibility of oxidation and reduction of polluting substances in the wastewater at the anode and cathode, respectively. This acts synergistically to remove pollutants from water. The sweep flocs are removed easily from aqueous medium by sedimentation or H$_2$ flotation [Daneshvar et al., 2006]. The solubility boundary denotes the thermodynamic equilibrium that exists between the dominant aluminium species at a given pH and solid aluminium hydroxide. The minimum solubility of aluminium,

0.03 mg/L, occurs at pH 6.3, with solubility increasing as the solution becomes more acidic or alkaline [Holt et al., 2002]. However, as the aluminium concentration increases and/or the solution 'ages', polynuclear aluminium complexes are formed and aluminium hydroxide precipitates.

2.4.3.1.2. A Brief Description of the EC Mechanism with Iron or Steel Anodes

When an iron or steel anode is utilized in EC, Fe^{2+} is dissolved in the wastewater from metalic iron oxidation at the anode (standard electrode potential; $E^{\circ} = -0.44\,\text{V}$) as follows:

$$Fe \rightarrow Fe^{2+} + 2e^{-} \tag{2.25}$$

whereas hydroxide ion and H_2 gas are generated at the cathode from the reaction (standard electrode potential; $E^{\circ} = -0.828\,\text{V}$):

$$2H_2O + 2e^{-} \rightarrow 2OH^{-} + H_{2(g)} \tag{2.26}$$
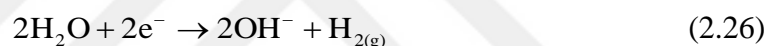
OH^{-} production from reaction (2.26) causes an increase in pH during electrolysis. As can be seen in Fig. 3a, insoluble $Fe(OH)_2$ precipitates at pH>5.5 and remains in equilibrium with Fe^{2+} up to pH 9.5 or with monomeric species such as $FeOH^{+}$, $Fe(OH)_2$ and $Fe(OH)_3^{-}$ at higher pH values. The formation of insoluble $Fe(OH)_2$ can be written as:

$$Fe^{2+} + 2OH^{-} \rightarrow Fe(OH)_{2(s)} \tag{2.27}$$

and the overall reaction for the electrolytic process from the sequence of reactions (2.25)-(2.27) is:

$$Fe^{2+} + 2OH^{-} \rightarrow Fe(OH)_{2(s)} + H_{2(g)} \tag{2.28}$$
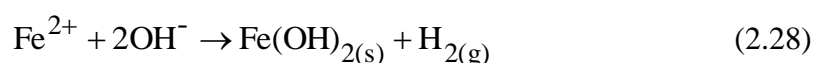
In the presence of dissolved O_2 in water, dissolved Fe^{2+} is oxidized to insoluble $Fe(OH)_{3(s)}$

$$4Fe^{2+} + 10H_2O + O_{2(g)} \rightarrow 4Fe(OH)_{3(s)} + 8H^+ \qquad (2.29)$$

and protons can be directly reduced to H_2 gas at the cathode:

$$8H^+ + 8e^- \rightarrow 4H_{2(g)} \qquad (2.30)$$

The corresponding overall reaction obtained by combining reactions (2.25), (2.29) and (2.30) is:

$$4Fe^{2+} + 10H_2O + O_{2(g)} \rightarrow 4Fe(OH)_{3(s)} + 4H_{2(g)} \qquad (2.31)$$
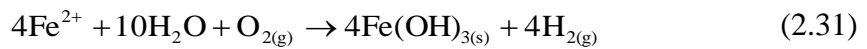
In acidic media of pH<5, however, a greater quantity of Fe anode than that expected from Faraday law following reaction (1) is dissolved owing to the chemical attack of protons [Sharp et al., 2006a].
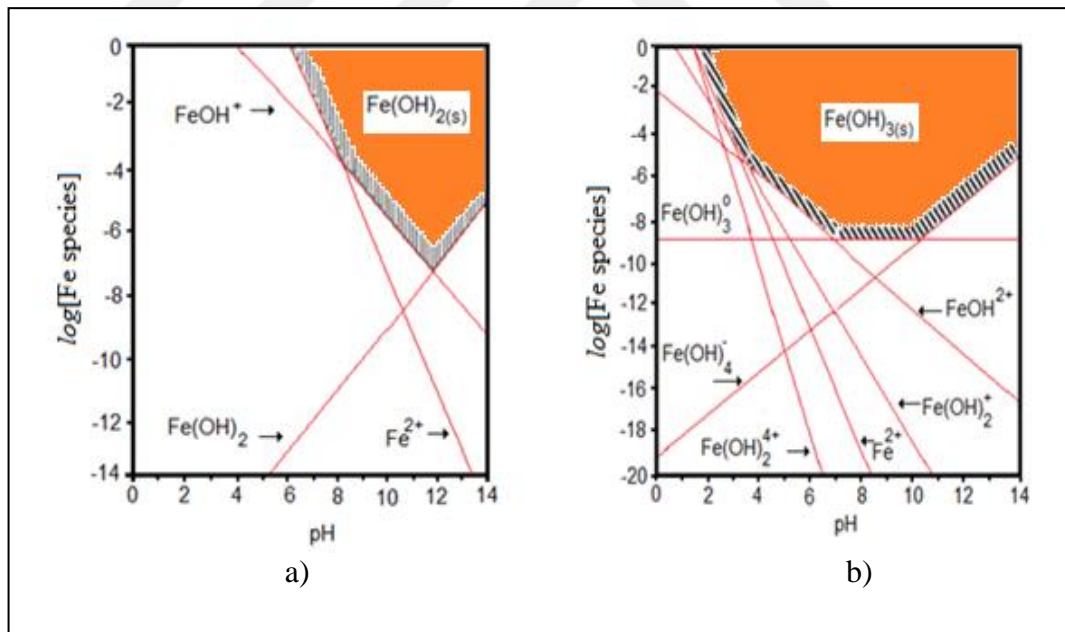
Figure 2.17: Solubility of Fe species as a function of Fe concentration and pH a) the pH range of $Fe(OH)_{2(s)}$, b) the pH range of $Fe(OH)_{3(s)}$.

Figure 2.17.b) shows that $Fe(OH)_{3(s)}$ coagulates from pH> 1, i.e., it is present in much stronger acidic media than $Fe(OH)_{2(s)}$ (see Figure 2.17.b). Then, this precipitate can be in equilibrium with soluble monomeric species like Fe^{3+},

$Fe(OH)^{2+}$, $Fe(OH)_2^+$, $Fe(OH)_3$ and $Fe(OH)_4^-$ as a function of the pH range. Among them, hydroxo iron cations have a pronounced tendency to polymerize at pH 3.5-7.0 to give polymeric cations such as $Fe_2(OH)_2^{4+}$ and $Fe_2(OH)_4^{2+}$.

Once the insoluble flocs of $Fe(OH)_3$ are produced, they can remove dissolved pollutants by surface complexation or electrostatic attraction. The first mechanism considers that the dye can act as a ligand to bind a hydrous iron moiety of the floc yielding a surface complex:

$$[\text{Pollutant molecule} - H] + (HO)OFe_{(s)} \rightarrow [\text{Pollutant molecule} - OFe_{(s)}] + H_2O \quad (2.32)$$
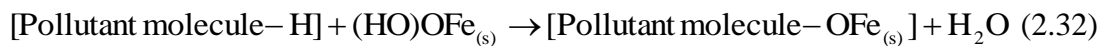
and the second one supposes that $Fe(OH)_3$ flocs with surface complexes contain areas of apparent positive or negative charge that attract the opposite regions of the pollutant molecule. Coagulation of these flocs forms particles that are separated from the wastewater by sedimentation or electroflotation.

2.4.3.2. Factors Affecting EC Process

The electrocoagulation process is a quite complex for treatment of wastewaters and may be affected by several operating parameters, namely, current density, operating time, initial pH, electrode connection mode and pollutants concentrations.

2.4.3.2.1. Effect of Electrode Material

Different materials could be used as the electrodes for the present electrocoagulation and the type of electrode pair has been known to be an important factor influencing the performances of the electrocoagulation process. The performance of electrocoagulation reactor is affected significantly by the electrode material used in the process. The complexities of many electrode processes make it impossible to select an optimum electrode material on a theoretical basis. The electrodes in the electrocoagulation cell must have adequate mechanical strength and resistant to erosion and other types of physical attack by the electrolyte, the reactant and the products. Several researchers have studied the choice of electrode material with a variety of theories as to the performance of a particular material [Holt et al.,

1999]. At its simplest, an electrocoagulation system consists of an anode and a cathode made of metal plates, both submerged in the aqueous solution being treated. The electrodes are usually made of aluminum, iron, or stainless steel (SS), because these metals are cheap, readily available, proven effective, and non-toxic [Chen et al., 2007]. Aluminium and iron electrodes have both been used successfully in EC processes. Aluminium dissolves in all cases as Al(III) whereas there is some controversy as to whether iron dissolves as Fe(II) or Fe(III) [Moreno et al., 2009], [Sasson et al., 2009]. Most results indicate that iron dissolves as Fe(II), such as [Sasson et al., 2009], [Linares-Hernández et al., 2009], [Bagga et al., 2008], and is oxidised in bulk solution to Fe(III) if there are oxidants, such as oxygen, present in sufficient concentration and pH is alkaline. Fe(II) is a poor coagulant compared to Fe(III) due to higher solubility of hydroxides and lower positive charge, which explains some poor results obtained with iron electrodes, such as in the study of Bagga et al. [Bagga et al., 2008]. Optimal material selection depends on the pollutants to be removed and the chemical properties of the electrolyte. In general, aluminium seems to be superior compared to iron in most cases when only the efficiency of the treatment is considered. However, it should be noted that aluminium is more expensive than iron.

Inert electrodes, such as metal oxide coated titanium, are used as cathodes in some constructions. When water has significant amounts of calcium or magnesium ions, the inert cathode material is recommended [Chen, 2004]. There are also some studies where combinations of aluminium and iron electrodes have been used. Linares-Hernández et al. [2009] obtained high removal of colour with aluminium electrodes, while iron was more effective than aluminium in reducing COD from industrial wastewater. A combination of iron and aluminium removes both colour (71%) and COD (69%) with high efficiency. Similar results were obtained when paper mill wastewaters were treated with various aluminium and iron electrode combinations [Katal et al., 2011]. Aluminium electrodes were most effective in removing colour of the wastewater, whereas iron electrodes removed COD and phenol from the wastewater more effectively than aluminium electrodes. A combination of aluminium and iron electrodes removed colour, COD and phenol with high efficiency. Combination electrodes have been studied for arsenic removal from groundwater [Gomes et al., 2007]. Iron electrodes and a combination of iron and aluminium electrodes gave the highest arsenic removal efficiencies. Similar

results were obtained for copper, chromium and nickel removal from metal plating wastewater [Akbal and Camcı, 2011]. Fe-Al pair has been most effective in removing indium from water.

Electrode passivation has been considered as one of the main operational issues with electrocoagulation process. In this process, oxidation will cause the anode material to under-go electrochemical corrosion, whereas the cathode will be subjected to passivation when the cell is connected to an external power source [Mollah et al., 2004]. Electrode passivation, specifically of aluminum electrodes, has been widely observed and recognized as detrimental to reactor performance. This formation of an inhibiting layer, usually an oxide on the electrode surface, will prevent metal dissolution and electron transfer, thereby limiting coagulant addition to the solution. Over time, the thickness of this layer increase, reducing the efficiency of the electrocoagulation process [Liu et al., 2010]. The methods of preventing and/or controlling electrode passivation include: (i) Changing polarity of the electrode, (ii) Hydromechanical cleaning, (iii) Introducing inhibiting agents and (iv) Mechanical cleaning of the electrodes. According to these researchers, the most efficient and reliable method of electrode maintenance was to periodically mechanically clean the electrodes which for large-scale, continuous processes is a non-trivial issues [Holt et al., 1999].

2.4.3.2.2. Current Density or Charge Loading

In most electrochemical processes, current (i) and electrolysis time (t_{EC}) are the most important parameters for controlling the reaction rate in the EC reactor. The current density (j, A/m^2) is determined by dividing each current (i) by the corresponding effective electrode surface area ($S_{electrode}$, m^2). Current not only determines the coagulant dosage but also the mixing rate within electrocoagulation. Electrolysis or EC time (t_{EC}) determines the rate of dissolution of metal ions (i.e. Al^{3+} and Fe^{2+}) from anodes, as it strongly depends on the current value [Emamjomeh and Sivakumar, 2006]. For aluminum anodes, the electrochemical equivalent mass is 335.6 mg/(Ah). For iron anodes, the value is 1041 mg/(Ah). A large current means a small electrocoagulation unit. However, when too large current is used, there is a high chance of wasting electrical energy in heating up the water. More importantly, a

too large current density would result in a significant decrease in current efficiency. In order for the electrocoagulation system to operate for a long period of time without maintenance, its current density is suggested to be 20-25 A/m^2 unless there are measures taken for a periodical cleaning of the surface of electrodes [Chen, 2004]. The current density selection should be made with other operating parameters such as pH, temperature as well as flowrate to ensure a high current efficiency. The current efficiency for aluminum electrode can be 120-140% while that for iron is around 100%. The over 100% current efficiency for aluminum is attributed to the pitting corrosion effect especially when there are chlorine ions present. The current efficiency depends on the current density as well as the types of the anions. Significantly enhanced current efficiency, up to 160%, was obtained when low frequency sound was applied to iron electrodes [Kovatchva and Parlapanski, 1999]. The quality of the treated water depends on the amount of ions produced (mg) or charge loading, the product of current and time (Ah). The operating current density or charge loading can be determined experimentally if there are not any reported values available. There is a critical charge loading required. Once the charge loading reaches the critical value, the effluent quality does not show significant improvement for further current increase.

Current density is directly proportional to the rate of electrochemical reactions taking place on the electrode surface and it also has an influence on the electrode potential, which defines the reactions taking place on the electrode surface. It seems that on iron and aluminium anodes, dissolution reaction is the primary reaction, and the proportion of other reactions is insignificant at the typical current densities and electrode potentials when pH is neutral or acidic. At alkaline pH the dissolution rate of iron anodes can be lower than the value calculated by Faraday's law, which indicates that there can be other reactions at the anode in these conditions. The anode metals most commonly used are aluminum or iron because when electrochemically oxidized they produce the most commonly used ionic coagulants, Al^{3+} and Fe^{3+} (or Fe^{2+}) respectively. The dissolution of coagulant into solution is governed by Faraday's Law [Scott, 1995]:

$$w = \frac{i \times t_{EC} \times M_{Me}}{z \times F} \qquad (2.4)$$

where, w: metal dissolving (g), i: current intensity (A), t_{EC}: EC time (s), M_{Me}: molecular weight of metal (g/mol), z: number of electrons involved in the oxidation/reduction reaction, and F: Faraday's constant (96,487 C/mol e⁻).

Charge loading is the most important parameter for controlling the reaction rate within the EC reactor and it may also serve as a design parameter for the process [Chen et al., 2000]. Charge loading is defined as the charges transferred in electrochemical reactions for a given amount of water treated and is calculated as the applied current in the EC process multiplied by the operating time in the EC process:

$$q\ (\text{C/L}) = \frac{i \times t_{EC}}{v} \ \text{ or } \ q\ (\text{F/m}^3) = \frac{i \times t_{EC}}{F \times v} \tag{2.5}$$

where q is the charge loading (C/L or F/m³ water), i is the applied current (A), t_{EC} is the EC time (min), F is the Faraday's constant (1 F = 96487 Coulomb) and v is the solution volume (L or m³) in the EC reactor. Too high charge loading produces more iron hydroxide flocs leading to higher concentration of Fe^{2+} ions. Excessive iron hydroxide flocs are difficult to float and separate due to the high density and poor affinity between the hydroxide flocs and the gas bubbles. Moreover, high charge loading results in high-energy consumption, a prime concern of operating cost. Therefore, the charge loading needed to be optimised.

2.4.3.2.3. Effect of Initial pH

pH of the solution plays an important role in the electrochemical and chemical coagulation process. It has an effect on dissolution of the electrodes, speciation of hydroxide and ZP of colloidal particles. As discussed in Sections xx and yy, aluminium and iron cations and hydroxides cause destabilization of colloids. Effective coagulant species are formed in acidic, neutral and slightly alkaline conditions. In highly alkaline pH $Al(OH)_4^-$ and $Fe(OH)_4^-$ ions are formed and these ions have poor coagulation performance. It is also known that competing anions have an effect on the optimum pH of the coagulation. The effect of water pH on the efficiency of pollutant removal can mostly be explained by the before mentioned mechanisms. However, pH increases during the EC treatment, making it a constantly

chaning parameter; therefore mechanistic studies of EC systems are difficult to conduct.

In pHs lower that 3, the release rate of aluminium during electrolysis with a constant charge per volume was lowe than in pHs above 3 [Mouedhen et al., 2008]. Chemical dissolution of aluminium cathodes occurs because pH increases to a level where aluminate is formed. It is probable that acidic bulk solution inhibits this reaction because produced hydroxyl ions are consumed by the acid in the solution. In acidic pH the dissolution of iron electrodes was significant even without electricity, whereas oxidation of Fe(II) to Fe(III) occurs only at pHs above 5 [Sasson et al., 2009]. The dissolution rate decreases at high pH, which is understandable as the corrosion rate of iron decreases in alkaline pH in the presence of oxygen because a passive layer forms on the surface.

There are also some pollutants which have specific optimum pHs of treatment, such as phosphorus and metal cations [Irdemez et al., 2006], [Yu et al., 2005]. As with aluminium and iron, other metal cations can also form hydroxides in water. Most non-inonic hydroxides have low solubility in water and can be removed by precipitation and co-precipitation with EC [Akbal and Camel, 2011].

2.4.3.2.4. Electrode Connection Modes

In a simple electrocoagulation cell two electrodes are used. But to improve the electrocoagulation process it may be necessary to interchange the polarity of the electrode intermittently. Usually, using two-electrode electrocoagulation cell is not suitable for wastewater treatment because of a workable rate of metal dissolution. The conductive metal plates used in EC fabrication are commonly known as "sacrificial electrodes. " The sacrificial electrode and the cathode may be made up of the same or of different materials [Liu et al., 2010]. To improve the performance of the electrocoagulation cell, the use of electrodes with large surface area is required. The performance improvement has been achieved also by using electrocoagulation cell either with monopolar electrodes or with bipolar electrodes [Ghosh et al., 2008]. The schematic diagram of monopolar and bipolar electrodes is shown in Figure 2.18. This arrangement of monopolar electrodes with cells in series is electrically similar to a single cell with many electrodes and interconnections. The experimental setup

also requires a resistance box to regulate the flow of current and a multimeter to read the current values. In a bipolar arrangement, the sacrificial electrodes are placed between the two parallel electrodes without any electrical connection. The two bipolar electrodes are connected to the electric power source with no interconnections between the sacrificial electrodes. This cell arrangement provides a simple setup, which facilitates easy maintenance. When an electric current is passed through the two electrodes, the neutral sides of the conductive plate will be transformed to charged sides, which have opposite charge compared with the parallel side beside it. The sacrificial electrodes are known as bipolar electrodes [Modirshahla et al., 2007]. The pollutant removal efficiencies and operating costs of monopolar and bipolar configurations have been compared in several studies [Ghosh et al., 2008], [Asselin et al., 2008].

Many systems and reactors (batch or continuous mode) contain parallel or series plate electrodes with monopolar or bipolar connection. The electrode configuration scheme is presented in Figure 2.18. The arrangements illustrated in the figure differ in the manner of electrical connection to the DC power source. In monopolar pharalel (MP-P) configuration, alternative electrodes were joined to the power supply terminals of opposite polarity, giving a number of individual reactor units of monopolar pharalel electrode arrangement. In this system each unit operates at the same voltage and the total current in the reactor (cell current) is the sum of the individual unit currents. In the case of MP-P, a voltage U is connected between n pairs of anodes and cathodes, connected in parallel via copper bus bars, causing a current ni to pass across electrode/solution interfaces via the bulk solution, i being the current that passes between an individual anode/cathode pair. Monopolar electrodes in serial connections (MP-S) for each pair of sacrificial electrodes is internally connected with each other, because the cell voltages sum up, a higher potential difference is required for a given current.
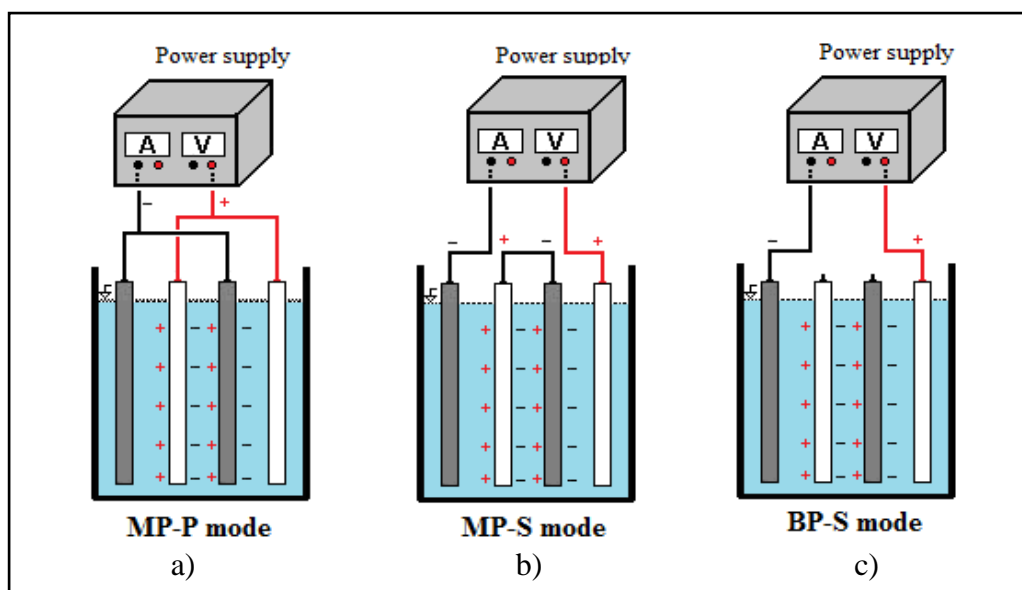
Figure 2.18: Electrode connection modes in the EC reactors. a) MP-P b) MP-S and c)BP-S.

In bipolar series (BP-S) arrangement, only the extreme electrodes are connected to the power source (Figure 2.18.c)). There is no electrical connection between iner electrodes for bipolar electrodes in serial connections. Outer electrodes are monopolar and iner ones are bipolar. The voltage applied between the latter electrodes by the power supply causes the polarization of the in termediate bipolar electrodes, which then present different polarities in the opposite faces. Every electrode excluding the electrodes at the end acts as an anode on one side and cathode on the other side. Each adjacent electrode pair acts as single unit. The total voltage drop in the system is the sum of the individual unit voltages. In the case of BP-S connection electrodes, if a voltage nU is applied between two feeder electrodes, between which (n-1) bipolar electrodes are interposed, current would flow across one feeder/solution interface, through the solution, sequentially into and out of each of the bipoles, and finally to the second feeder electrode. As the same current passes through n electrode pairs, the maximum theoretical current efficiency is also n; rather than unity. Bipolar reactors have advantages of being easier to engineer, as electronic connections need be made only to the feeder electrodes, so inter-electrode gaps can be smaller, and costs of higher voltage/lower current transformer rectifiers are lower for the same total power output than for the lower voltage/higher current required for monopolar reactors. However, the large terminal

voltage between a pair of feeder electrodes also causes a proportion of the current to flow in the solution, bypassing the bipolar electrodes, as shown in Figure 2.18.

As shown in Figure 2.18.a) and 2.18.b), anodes and cathodes are in monopolar paralel connection, the current is divided between all the electrodes in relation to the resistance of the individual cells. Hence, a lower potential difference is required in parallel connection, when compared with serial connections.

2.4.3.2.5. Effect of the Distance Between the Electrodes

Once distance between the electrodes increases, the electrical current decreases. To achieve a certain current density, the voltage must be increased. On the other hand the IR-drop increases as the distance between electrodes increases. With increasing distance, less interaction of ions with hydroxide polymers is expected. In other words, decreasing both local concentration and electrostatic attraction are the reasons for decreasing the removal of Tartrazine. When the distance of the electrodes is increased from 0.5 to 3 cm, the removal efficiency decreases by about 26.64% [Modirshahla et al., 2007]

2.4.3.2.6. Effect of Temperature

Although electrocoagulation has been around for over 100 years, the effect of temperature on this technology was not very much investigated. For water treatment, the literatures from former USSR show that the current efficiency (CE) of aluminum increases initially with temperature until about 60 $°C$ where a maximum CE was found. Further increase in temperature results in a decrease in CE. The increase of CE with temperature was attributed to the increased activity of destruction of the aluminum oxide film on the electrode surface. When the temperature is too high, there is a shrink of the large pores of the $Al(OH)_3$ gel resulting in more compact flocs that are more likely to deposit on the surface of the electrode. Similar to the CE, the power consumption also gives a maximum at slightly lower value of temperature, 35 $°C$, for treating oil-containing wastewater. This was explained by the opposite effects of temperature on CE and the conductivity of the wastewater. Higher temperature gives a higher conductivity hence a lower energy consumption.

2.4.3.3. The Application of EC in Surface Water and Wastewater

The recent most of the published studies on the removal of organic pollutants from surface water, wastewater or synthetic water were shown Table 2.4, and 2.5. Electrode configuration, process time, initial pH, electrode material, and current density are the most focused operating parameter in EC process.

In this study, the treatment performance of NOM from surface waters by EC process was investigated. The studies in which EC technology and CC process have been used for NOM removal from surface water are presented in Table 2.4 under optimum conditions. Also, a few articles that are about comparison of EC and CC were given in Table 2.4.

Bagga et al. found similarly NOM removal efficiency between EC and CC for surface water that includes low concentration of DOC [Bagga et al., 2008].

Staaks et al., determined 52% removal efficiency at pH of 6 and optimum alum dosage [Staaks et al., 2011].

Mahvi et al., was compared the performance of composite polyaluminum silicate chloride (PASiC) and electrocoagulation process by aluminum electrodes in NOM removal from raw surface water [Mahvi et al., 2011]. PASiC coagulant at optimum concentration of 1–5 ml/L was capable of removing TOC, COD, UV, and turbidity from raw water by 93.77, 93.5, 63 and 95 %, respectively. EC process removed TOC, COD, UV and turbidity from raw water by 89, 99.75, 37 and 50% respectively. It was concluded that PASiC and EC process are reliable, efficient and cost effective methods for removal of NOM from surface water.

A lot of researchers have conducted a series of experimental assays to determine the optimal operating conditions for humic acid removal from surface water. Humic matter was removed from water with high removal efficiency by using Al electrodes at optimum condition [Feng et al., 2007], [Yıldız et al., 2007].

Vepsäläinen et al., [Vepsäläinen M., et al. 2012] investigated the effect of electrocoagulation cell constructions on NOM removal. Three combinations of electrodes were tested: one that only had aluminium electrodes, one that had aluminium anodes and inert cathodes, and one that had inert anodes and aluminium cathodes. NOM destabilization mechanism was double layer compression at low pH, in contrast to adsorption and bridging at higher pH [Vepsäläinen M., et al. 2012].

Purifications of surface waters from metals, microorganisms, nitrate, phosphates and phosphorus removal have been studied, as well as NOM removal. Practically, the complete removal of phosphates and phosphorus [Vasedevan et al., 2009], [Janpoor et al., 2011], [Attour et al., 2014] and microbes [Uduman et al., 2011], [LIanos et al., 2014] is possible. Al electrodes were slightly more effective than Fe electrodes for these pollutants. When the operating parameters of EC process are optimized, the total removal or high removal efficiency of metal ions (arsenic, chromium, cobalt, iron as Fe (III), mercury as Hg (I)) could be obtained [Parga et al., 2005], [Shafaei et al., 2011], [Kobya et al., 2011b], [Kobya et al., 2015]. Also, the treatment of wastewater including mixed different metal was studied [Heidmann et al., 2008], [Akbal et al., 2011].

Electrocoagulation technology has been used for treatment of different types of wastewater. This technology has used as a tertiary treatment [Zodi et al., 2011] and pre-treatment [Coskun et al., 2012]. Table 2.5 shows the recent studies about NOM removal by EC technology from wastewater/industrial water.

Generally, chemical oxygen demand (COD) removal efficiency was given in Table 2.4 for different studies. The treatment performance of process was evaluated in terms of biochemical oxygen demand (BOD$_5$), total suspended solid (TSS), and total nitrogen (TN), as well as COD.

The articles about treatment of textile and dyes wastewater by EC process were not given in Table 2.4. Khandegar et al., [Khandegar et al., 2013] published a review article that including a lot of studies about treatment of textile and various types of dyes.

Table 2.4: The recent studies about NOM removal by EC technology and CC from surface water, groundwater and synthetics water.

Matrix	The parameter which present NOM	Electrode Material/ Coagulant Matter	Optimum process conditions	Removal efficiency	References
Natural Surface water- Lake Houston Canal-	DOC_i=5.0–5.6 mg/L	Fe electrode	pH= 6.4 CD= 21 mA/cm^2 ~20 mg Fe^{+3}/L	~37%	Bagga et al., 2008
Natural Surface water- Lake Houston Canal-	DOC_i=5.0–5.6 mg/L	Iron (III) chloride (FeCI$_3$)	pH= 6.4 ~ 20 mg Fe^{3+}/L	~ 42%	Bagga et al., 2008
Real surface water	DOC	Iron (III) chloride (FeCI$_3$)	pH=4.5-6.0	29-70%	Yu et al., 2007 Bond et al., 2010 Uyak et al., 2007
Real surface water	DOC	Alum	pH=5.0-6.5 5-100 mg/L	60%	Yu et al ., 2007 Uyguner et al., 2007 Soh et al., 2008
Ground water (synthetic)	Humic acid	Al electrode	CD=4.76 m A/cm^2 pH=3.0-5.5	97.8%	Feng et al., 2007
High NOM concentration (synthetic)	Humic matter	Al electrode and 5-15 mM Na$_2$SO$_4$	pH=5.0 t_{EC}= 9 min.	97.2%	Yıldız et al., 2007
Real water (South Aust ralia)	DOC_i=13.6 mg/L	Aluminium chlorohydrate (ACH) / Alum	pH=6 at optimum dosage	43% 52%	Staaks et al, 2011
Raw surface water	TOC	Al electrode	pH=6.5 30 V t_{EC}=60 min	89%	Mahvi et al., 2011

Table 2.4: The recent studies about NOM removal by EC technology and CC from surface water, groundwater, synthetics water (Continue).

Matrix	The parameter which present NOM	Electrode Material/ Coagulant Matter	Optimum process conditions	Removal efficiency	References
Real surface water	Permanganate index	Al	1 A	47%	Ricordel et al., 2010
Natural water (Canada)	DOC_i=13.31 mg/L	Al/Fe/Zinc	CD= 24.3 A/m^2 t_{EC}= 1 min. no pH adjustment	70.2%/83.0%/84.0%	Dubrawski et al. 2013
Synthetic (Suwannee River NOM isolate)	DOC_i=13.79 mg/L	Al/Fe/Zinc and electrolyte=150 mg/L Na_2SO_4	CD= 24.3 A/m^2 t_{EC}= 1 min.	68.7%/72.6%/64.5%	Dubrawski et al. 2013
Synthetic (Nordic area NOM isolate)	DOC_i=9.03 mg/L	Al/Fe/Zinc and electrolyte=150 mg/L Na_2SO_4	CD= 24.3 A/m^2 t_{EC}= 1 min.	54.2%/64.7%/55.2%	Dubrawski et al. 2013
Raw surface water (Finland)	TOC_i=18.29 mg/l	Only Al/ Al anode and inert cathodes*/ Inert anodes and Al cathodes	pH=4 Electric charge (C/I)=144	78% Similar removal efficiency with all constructions tested.	Vepsäläinen M., et al. 2012

[*]Commercially available dimensionally stable anode (DSA) electrodes

Table 2.5: The recent studies about NOM removal by EC technology from wastewater/industrial water.

Matrix	The parameter which present NOM	Electrode Material	Optimum process conditions	Removal efficiency	References
Synthetic aqueous wastewater solution	0.5 g/L tannic acid 600 mg O_2 /L COD	Al plate and (0,1 M NaCI)	CD=7.0 mA/cm^2 pH=7.0	>80%	Mansouri et al., 2012
Synthetic wastewater	100 mg/L HA (27-32 mg/L DOC)	Al and Fe electrodes and combinations	pH=4 CD=100 A/m^2 t_{EC}=10 min anode/cathode=Al/Fe	80%	Kuokkanen et al., 2015
Peat bog drainage water	14-25 mg/L DOC	Al and Fe electrodes and combinations	pH=6.4-7.0 CD=70 A/m^2 t_{EC}=60-90 min Fe	71-75%	Kuokkanen et al., 2015
Pulp and paper wastewaters	1450 mg O_2 /L COD 270 mg C/L TOC	Al plate	CD=10.0 mA/cm^2 pH=7.0	>60%	Mansouri et al., 2012
Pulp and paper wastewaters	75 mg/L DOC	Al and Fe electrodes and combinations	CD=15 mA/cm^2 Al	46%	Zodi et al., 2011

Table 2.5: The recent studies about NOM removal by EC technology from wastewater/industrial water (Continue).

Matrix	The parameter which present NOM	Electrode Material	Optimum process conditions	Removal efficiency	References
Raw pulp and paper wastewaters	Colour 0.34 (absorbance at 600 nm)	Al and Fe electrodes and combinations	pH=5-7 CD=70 mA/cm^2 Al-Al	99.9%	Katal et al., 2011
Pulp and paper wastewaters	Lignin, BOD, phenol	Al and Fe electrodes and combinations	Al	>80%	Kamali and Khodaparast, 2015
Leachate water (stable)	380 mg O2/L COD	Al plate	pH=7.2 ~ 1.4 Al g/L	~42%	Labanowski et al., 2010
Textile wastewater	530 mg/L COD	Mild steel	pH=8.04 CD=25 mA/cm^2 t_{EC}=10 min.	54%	Bhaskar et.al., 2009
Olive mill wastewaters	COD	Al and Fe electrodes	25 mA/cm^2 t_{EC}=40 min. Al	30%	García-García et al., 2014
Olive mill wastewaters	COD	Al and Fe electrodes	t_{EC}=45 min., 1A Al	58.7%	Coskun et al., 2012
Slaughterhouse wastewaters	COD	Al and Fe electrodes	pH=2 CD=150 A/m^2 t_{EC}=25 Al	93%	Kobya et al., 2006

Table 2.5: The recent studies about NOM removal by EC technology from wastewater/industrial water (Continue).

Matrix	The parameter which present NOM	Electrode Material	Optimum process conditions	Removal efficiency	References
Slaughterhouse wastewaters	COD	Al and mild steel electrodes	0.3 A Mild steel t_{EC}=60 or 90 min	82±2%	Asselin et al., 2008
Slaughterhouse wastewaters	COD	Al elctrodes	pH=3 CD=1 mA/cm^2	85%	Bayar et al., 2011
Slaughterhouse wastewaters	COD	Al electrodes	pH=8.74 CD~30 mA/cm^2 t_{EC}=55 min	85%	Awang et al., 2011
Slaughterhouse wastewaters	COD	Fe electrodes	pH=7.1 CD=25 A/m^2 t_{EC}=50 min	93%	Ahmedian et al., 2012
Slaughterhouse wastewaters	COD	Al and Fe electrodes	pH=4 CD=100 A/m^2 t_{EC}=20 min Al	78.3%	Ozyonar et al., 2014
Oily wastewaters, petroleum refinery wastewater	COD	Al, Fe and stainless steel electrodes	pH=8 A constant current density Al	63%	El-Naas et al., 2009

3. MATERIAL AND METHODS

3.1. Materials

3.1.1. Humic Acid Solutions

Humic acids of different origins (commercial, terrestrial) were used in electrocoagulation experiments. Two different synthetic aqueous solutions were prepared by using commercial humic acid (CHA) and soil humic acid (SHA). CHA were supplied by Sigma-Aldrich (Lot No. BCBG7429V). CHA was used for representative water sample including high concentration of organic matter. SHA standard as a terrestrial source was purchased from the International Humic Substance Society (IHSS) (Lot No. 1S102H). The SHA was selected for this investigation because it shows terrestrial properties of NOM source. It is typical of the fertile prairie soils of the U.S. states of Indiana and extracted from an undisturbed area. Physico-chemical properties of CHA and SHA solutions are provided in Table 3.1.

Table 3.1: Physico-chemical properties of CHA and SHA.

Parameter	Unit	CHA	SHA
DOC	mg/L	16.17	25.33
UV_{254}	1/cm	2.3143	3.6764
VIS_{436}	1/cm	0.31	1.10
$SUVA_{254}$	L/(m mg)	14.31	14.51
Zeta potential	mV	-40.7	-27.4
Particle size	nm	220	1100

A stock solution of 1000 mg L^{-1} was prepared by dissolving 1 g of humic acid and soil humic acid in 0.1 M NaOH, then diluted in 1 L of deionized water, and stored in a cold room after mixing well. The solution was diluted to 50 mg L^{-1} for each experiment. All solutions were prepared with high quality pure water using Millipore Water Purification System. The initial pH of stock CHA and SHA solution was ranged from 10.15 to 10.72, 10.12 to 10.66, respectively. Before every an

experiment, these parameters were measured again due to changes in chemical conditions of solutions. The synthetic samples had low conductivity (67.2 μS cm^{-1} for CHA, and 83.8 μS cm^{-1} for SHA).

The pH of solutions was adjusted to desired level with H_2SO_4 and NaOH. Initial pH (pH_i) showed ± 0.1 deviation. Conductivity was enhanced to a nominal value of 300 μS cm^{-1}, typical of surface water, using 150 mg L^{-1} Na_2SO_4.

3.1.2. Aquatic Natural Organic Matter

The natural water samples were taken from Lake Saimaa and Lake Terkos as representative aquatic NOM source in September 2013, and in May 2014, respectively. Lake Saimaa situated in the southeastern Finland (Figure 3.1). At approximately 4,400 square kilometers, it is the largest lake in Finland, and the fourth largest natural freshwater lake in Europe. Its average depth is 17 m. and maximum depth 82 m. The length of the entire coastline is 15,000 kilometers and there are over 13,700 islands in the lake. [Web 1, 2015].

The evolution of Lake Saimaa is very complex. The basis for the Saimaa landscape was born at the bottom of an ancient sea over 1,900 million years ago. Clay, silt and mud stratified at the bottom of the sea to form mica gneiss and related rocks. As time passed, the mountain range wore down and is now sand on the shores of Lake Saimaa. The fragmented remainders of the mountain range can still be seen in the landscape as a colourful mosaic of water, rock and fertile ground [Web 2, 2015].

Lake Saimaa was formed by glacial melting at the end of the Ice Age. Originally the waters of Saimaa drained into the Gulf of Bothnia. The land that was released from under the ice sheet rose quicker in the Gulf of Bothnia and the land started to lean towards South-East Finland. In Saimaa, the waters flooded against the Salpausselkä ridges and approximately 5,700 years ago the spectacular terminal moraines of Salpausselkä broke. As a result, Saimaa flowed as a wide torrent onto the dry lands. The Vuoksi, Saimaa's effluent river, was born. These days the Vuoksi, which flows into Lake Ladoga, is the largest river in Finland in terms of volume. Imatra, the largest rapids on the Vuoksi, has attracted visitors to its banks for centuries [Karels and Niemi, 2002].

Humans arrived in Saimaa over 10,000 years ago. Great waters for fishing and land for hunting attracted people to this new area that had been revealed from under the ice. The most popular settlement spots were near the sunny beaches. Cities and small villages grew up near the water. Bridges and ferry boats connect those that live in the fragmented archipelago. Life in the countryside relies on agriculture, forestry and the service industry. Major towns on the lakeshore include Lappeenranta, Imatra, Savonlinna, Mikkeli, Varkaus, and Joensuu. In places in the Saimaa basin, the most of the lake is spotted with islands, and narrow canals divide the lake in many parts The Saimaa Canal from Lappeenranta to Vyborg connects Saimaa to the Gulf of Finland. Other canals connect Saimaa to smaller lakes in Eastern Finland and form a network of waterways. These waterways are mainly used to transport wood, minerals, metals, pulp and other cargo, but also tourists use the waterways [Web 2, 2015].

A legacy of the isolation brought about by the Ice Age is the endemic species of Lake Saimaa. An endangered freshwater seal, the Saimaa Ringed Seal, lives only at Saimaa. Another of the lake's endangered species is the Saimaa salmon. [Web 1, 2015]

The water samples collected the around of Mikkeli shoreline. Raw Lake Saimaa water (LSW) samples were collected from 1 m below the surface into glass bottles. Every week a fresh water sample was taken and stored at +4 ^{0}C, without pH adjustment.
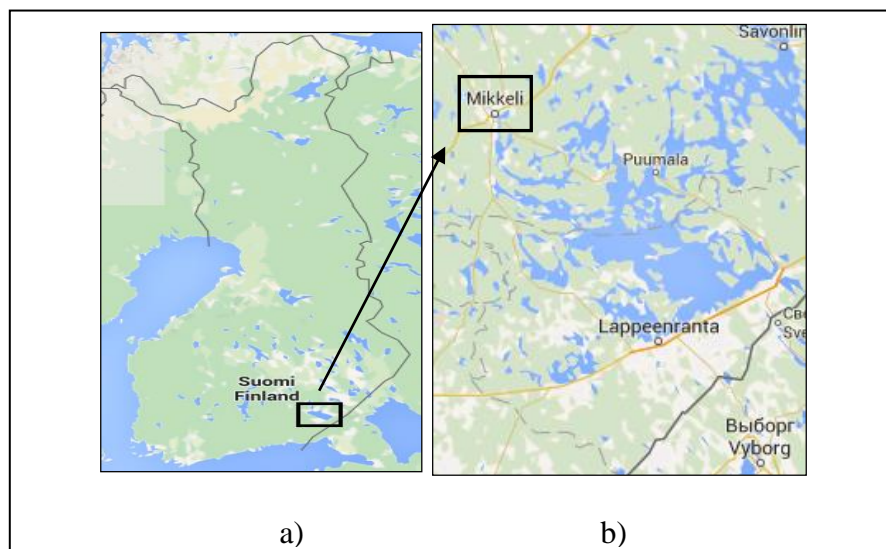
Figure 3.1: Location of sample point in a) Finland, b)Lake Saimaa Bay.

Lake Terkos is the one of the drinking water supplies in Istanbul/Turkey (Figure 3.2.). Kagıthane Treatment Plant takes its water from this lake. With its population over 10 million and significant centres of industry and commerce, Istanbul is one of the important mega-cities of Turkey and the world. Lake Terkos is very important since it is the cleanest water supply of Istanbul and provides 25% of the water demand of this Metropolitan Area [Baykal et al. 2000]. Lake Terkos has a 39 km² water area and a maximum depth of 11 meters.

The lake is located in the north-west of Istanbul. Terkos Dam is a lake-dam near the village of Durusu in the Çatalca district of Istanbul. Terkos Lake, being rich in terms of feeding rivers, has fresh-water characteristics despite its proximity to the Black Sea. Istranca Creek is the stream that carries the maximum amount of water to the lake [Sümeyra, 2015]. The control of pollution in lakes, which are important sources of food and water, is significant for the sustainability of lake ecosystem as well as human health.

The geological foundation of the lake's surroundings is composed of metamorphic rocks of the Paleozoic and Mesozoic era. The cover rocks, young sediments and Ergene group in the upper part can be found on metamorphic rocks. The limited areas on the bottom of rivers that pour into the lake are covered with the current Quaternary alluvium [Akşiay et al., 1990]. Geological units in the lake's surroundings are Eocene-aged Kirklareli, Miocene-aged Ergene Formation, Pliocene-aged Belgrade Formation, alluviums and sand dunes [Baki, 1997]. These are also the units that mainly carry the groundwater. The rocks located in the water section that limits the Terkos Basin are generally impermeable or less permeable. This prevents the water exchange with neighboring basins. The conclusion that no water leakage from the lake into the Black Sea would be possible can be reached due to width and geological structure of sand dunes in some regions between the Black Sea and the lake. However, it was discovered that the coastal strip, which separates the lake from the Black Sea, is dangerously narrowed because of unauthorized sand removal from the area and erosion [Maktav et al., 2002].
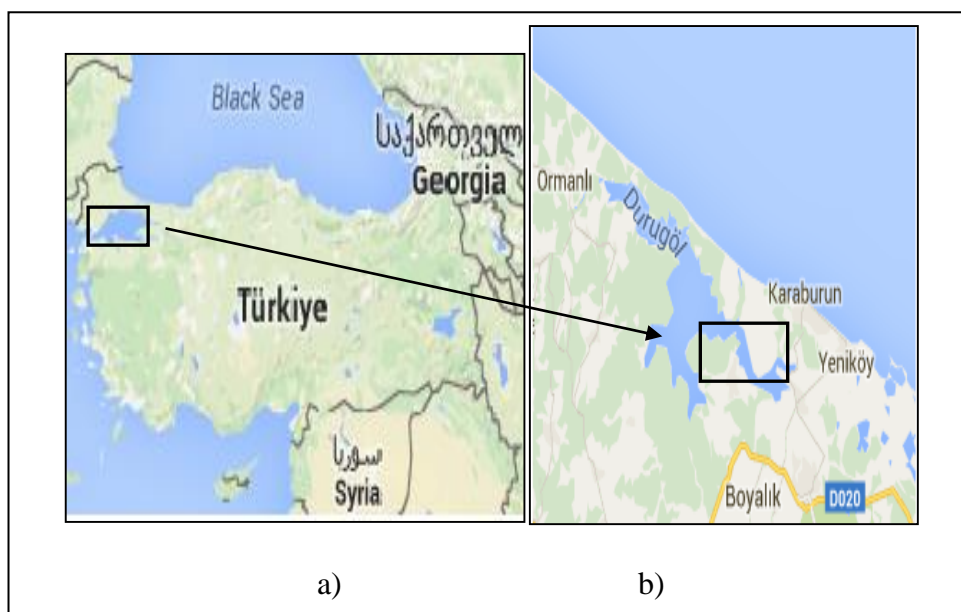
Figure 3.2: Location of sample point in a) Turkey, b) in Lake Terkos

Raw Lake Terkos water (LTW) samples collected and were stored at glass containers and kept +4 ^{0}C. Besides, samples were transported to the laboratory, and the physicochemical properties of the raw waters, LSW and TLW, immediately determined. Physicochemical properties (at original pH of raw water) of aquatic NOM samples are provided in Table 3.2. Anion and cation concentration of LTW were shown in Table 3.3. The SUVA values of raw waters were less than 3 L/(m mg) that shows the water is composed hydrophobic and mainly of hydrophilic material. It is mixture of aquatic humic and other NOM. The SUVA of LTW was the lowest among studied NOM sources.

The raw Lake Terkos samples and treated samples at optimum conditions were characterized using HPSEC technique. The distilled water was used to as eluent (mobile phase). Apparent molecular weight was derived by calibration with standard protein which is pullulan molecular weight standards of in the range of 342-708,000 Da.

Table 3.2: Physico-chemical properties of LSW and LTW

Parameter	Unit	Lake Terkos Water	Lake Saimaa Water
pH	-	7.78±0.02	7.30±0.02
Turbidity	NTU	1.2	4.13
Conductivity	µS/cm	344	142
DOC	mg/L	6.58	14.86
UV_{254}	1/cm	0.1363	0.4122
VIS_{436}	1/cm	0.004	0.022
$SUVA_{254}$	L/(m mg)	2.07	2.77
Zeta potential	mV	-8.7	-20.4
Particle size	nm	1369	752

Table 3.3: Anion and cation concentration of LTW

Anions and cations	Concentration mg L^{-1}
Cl^-	19.61
F^-	0.148
SO_4^{2-}	12.21
Na^+	19.48
K^+	2.043
Ca_2^+	41.33
Mg_2^+	3.05

3.2. Methods

3.2.1. Experimental Set-up and Procedure

The EC process experiments were conducted in laboratory scale. An EC batch cell consisted of a plexiglass reactor that had dimensions of 150 mmx100 mm x100 mm. The electrodes were made of high purity aluminum and iron plates with dimensions of 130 mmx80 mm. The EC experiments were conducted with using only aluminium as one anode and cathode, only iron as one anode and cathode and hybrid electrodes which were designed using one aluminum and one iron electrodes together as anode and cathode. There was 10 mm gap between electrodes, and they were connected to a digital power supply (GW Instek PSP-405 Programmable DC) in monopolar connection mode (Fig. 3.3). Currents were held constant for each run. All water samples were allowed to equilibrate to room temperature before experiments. In each run, the ranges of 1000-1300 mL of water samples were placed into the EC

reactor. During operating time, water was stirred with a magnetic stirrer at a speed of 150 rpm. The samples at the different operating times were taken from the EC reactor. The pH and initial conductivity were determined using WTW Inolab Multi 9310 IDS pH meter and CON6 Conductivity Meter (Ecoscan), respectively. The initial turbidity of samples was measured with turbidimeter Hach Lange. They were filtered through 0.45 µm pore size membrane before UV/VIS, DOC and HPLC analysis. When the experiments were repeated for zeta and particle size measurement, the samples filtered through filter. Afterwards, filtered samples drawn from a depth of almost 4 cm below the water surface. Prior to experiments, electrodes were washed with 0.25 M H_2SO_4-solution for 2 min and rinsed with deionized water, then dried in the drying-oven and placed in a desiccator to cool down. The same process was also applied after each experiment.

Different current densities were applied to see the effect. Current densities were calculated for each applied current by dividing the applied current by the active anode surface area (S). The active anode surface area (S) of the electrodes was determined depending on submerged part of electrodes in solution.
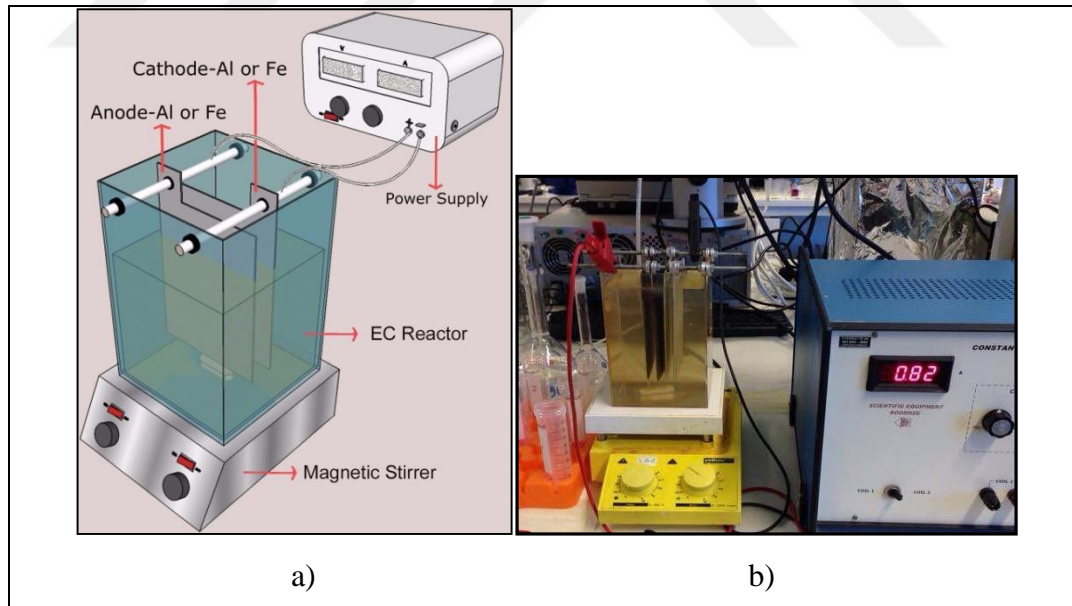
Figure 3.3: EC reactor in experiments a) schematic, b) laboratory desings.

3.2.2. Analytical Methods

3.2.2.1. UV/vis Measurements

UV/vis absorption spectra were recorded by Perkin Elmer Lambda 45 UV/VIS Spectrophotometer. The absorbance values of the samples were measured at 254 nm (UV_{254}, cm^{-1}) and 436 nm (VIS_{436}, cm^{-1}) wavelength. The color of samples was determined by using absorbance value of samples at 436 nm.

3.2.2.2. DOC and Inorganic Matter Analysis

DOC content of samples was measured using a TOC analyzer (TOCVCPH, Shimadzu, Japan) as Non-purgeable Organic Carbon NPOC (mg/L). DOC analysis of samples was done using calibration curve of potassium hydrogen phthalate.

Dionex ICS-3000 Ion Chromatography, Perkin-Elmer AAnalyst 300 atomic Absorption were used for measurement of concentration of anion and cation.

3.2.2.3. Zeta Potential and Particle Size Measurements

The magnitude of the ZP [50] is determined from electrophoretic measurement of particle mobility in an electric field [Malvern, 2008]. The relationship between dispersion of colloidal and ZP is shown according to D4187-82 ASTM Zeta Potential of Colloids in Water and Wastewater in Table 3.4.

The ZP values of samples were determined based on Smoluchowki model using a Malvern Zetasizer Nano-ZS (Malvern, USA). The green cell was used. The measurement was done at temperature 22 ± 1 ^{0}C. The number of sub-runs was set to be automatic. If the results are not stable, the number of sub-runs will increase until obtain stable measurements but not using more than 100 sub-runs. Number of measurements was ten. Only results meeting "Malvern quality criteria" were used. Standard solution was "ZP Transfer Standard", a latex standard having a zeta potential -50mV-+5 mV. The ZP of colloids was measured in all raw waters and the treated waters.

Table 3.4: The relationship between dispersion of colloidal and ZP.

State of Stability	Zeta Potential, MV
Strong coagulation-floculation	+5/-5
Incipient instability	-10/-30
Moderate strength in stability	-30/-40
High strength in stability	-41/-60
Very high strength in stability	-61 and more

The floc size measurements were done depend on the dynamic light scattering measurement using a Zetasizer (Nano-ZS, Malvern, USA). The size of particles measured in the polystyrene cuvette. This cell was washed by deionized water and ethanol before the measurements. All measurements were carried out at $22 \pm 1\ ^0C$. Each result was an average of three readings.

3.2.2.4. Molecular Weight Fractionation by HPLC Technique

HPSEC was used to derive weight and number average molecular weight (M_W and M_N, respectively) of NOM. The measurement of molecular weight of organic matter was carried out with an Agilent HPLC 1260 Series. The HPLC system comprises of detector, column, mobile phase reservoir, pump, injection valve, data recorder, and collector for separated substance. Figure 3.4 shows the used HPLC system in this study. Two different columns were used. PL aquagel-OH 30 (100-60,000 MW (Da)) and PL aquagel MIXED-H (6,000-10,000,000 MW (Da)). The columns have a pH range 2-10, compatibility with organic solvent (up to 50% methanol), mechanical stability up to 140 bar.
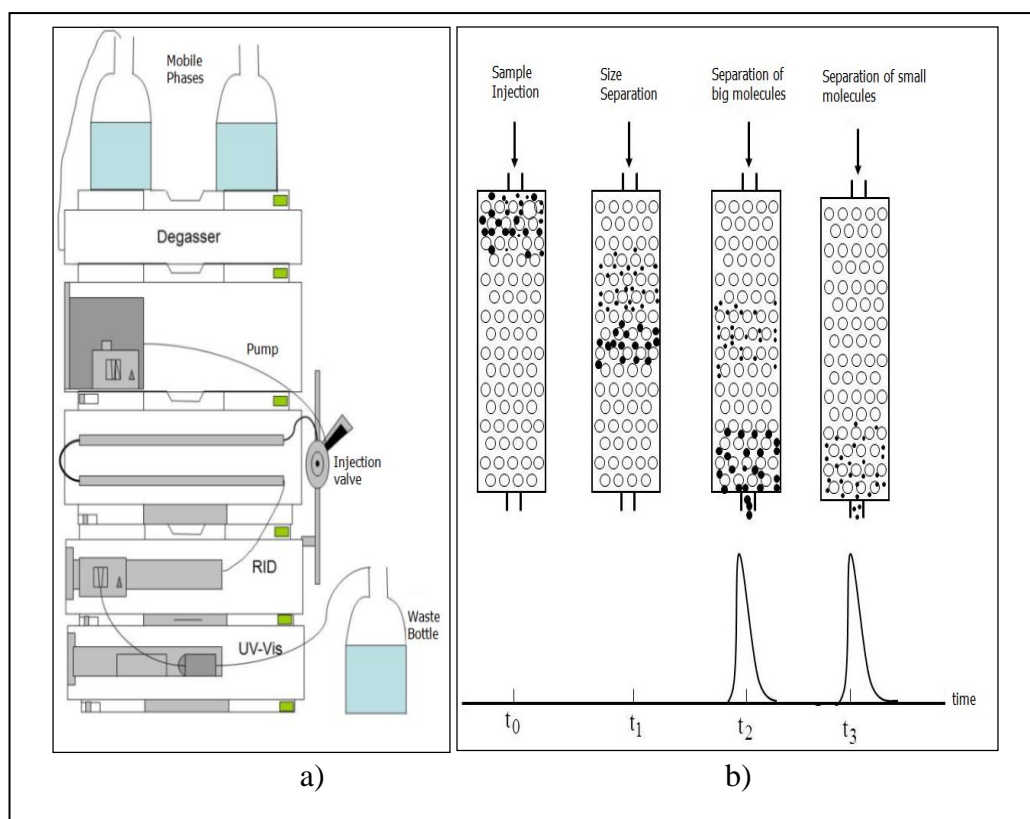
Figure 3.4: a) Schematic diagram of HPSEC, b) the mechanism by means of the column in the HPSEC operation.

Prior to chromatographic separation, all samples were filtered through 0.45 µm membrane filter. The water was used to as eluent with a flow rate of 1 mL/min. The injection volume was 25 µL. The mobile phase is pumped through the column at high pressure with pumps. Separated molecules leave column with mobile phase.

The column effluent was detected by UV and RI detector. DAD was based on UV absorbance (254 nm cm^{-1}). The deviation that takes place in detector for eluent of per molecule is recorded on a PC monitor in real time. Thus, chromatographic separation is obtained. It is determined as a narrow band or a peak. ChemStation software was used to explanation of obtained results.

The molecular weight of organics was determined by size calibration using ten pullulan standards with different molecular weights; 708,000, 344,000, 194,000, 107,000, 47,100, 21,100, 9,600, 6,100, 1,080 and 342 Daltons. A regression coefficient of determination 0.999 was achieved.

4. RESULTS and DISCUSSION

4.1. The Effect of Operating Parameters on Removal of Humic Substances and Natural Organic Matter by EC

The first part of study, the effect of the main parameters which are initial pH, current density, electrode material, operating time on removal of humic substance and organic matter from CHA aqueous solution and natural surface waters was investigated during EC process, respectively. The optimum conditions were determined depend on these parameters. The effect of electrode material and operating time on removal of humic substance from SHA aqueous solution was studied. At optimum conditions, the treatability of water samples (commercial, terrestrial and aquatic NOM) that has different physico-chemical structures was evaluated using different electrode configurations.

4.1.1. The Effect of Operating Parameters on Removal of HS from CHA Aqueous Solution

The investigated parameters were initial pH (pH_i), current density, electrode material and operating time for CHA aqueous solution.

4.1.1.1. Effect of Initial pH on HS Removal

pH is one of the most important parameters in treatment by EC process due to the effect on both metal hydroxide species and pollutant parameters in wastewater. In experiments, initial pH values ranged from 3 to 8 for two different metal anodes, aluminum and iron. The operating time means that electrolysis time of EC process. It was 25 min.

Figure 4.1.a) shows the removal efficiency of HS with aluminium electrodes at current density 1.2 mA/cm^2. The pH_i 4, 5, 6, and 8 were studied. As it is seen in Figure 4.1.a), for Al electrodes the best performance was obtained after 25 min at pH_i 4 with 87.5% removal efficiency and residual DOC concentration of 2.02 mg/L.

The final concentration of DOC after 25 min was 3.06 mg/L and 4.41 mg/L, with removal efficiency 81.1% and 72.7% at pH_i 5 and 6, respectively. At pH_i 8, the removal efficiency was 59.5% with final concentration of 6.55 mg/L. The pH value was changed depend on each of pH_i during EC process (Section 2.4.3.).

Figure 4.1.b) shows the DOC removal efficiency of HS with respect to produced Al in-stu at current density of 1.2 mA/cm² for different initial pHs. The amount of Al or Fe dissolved from aluminium or iron anodes (ELC) was calculated according to the Faraday's law (Equation 2.4). The DOC removal efficiency increased with the increasing the amount of aluminium coagulant produced in the EC process. At 4 of pH_i, the maximum removal efficiency was obtained with 14.7 mg Al. The maximum DOC reduction per Coulomb or mg Al were 0.0900 mg HS removed/C and 963.8 mg HS removed/g Al produced (Table 4.1), according to equation 2.6 and 2.7, respectively.

$$q_{t\,(c)} = (DOC_i - DOC_t)*v/ELC \qquad (2.6)$$

$$q_t = (DOC_i - DOC_t)*1000/ELC \qquad (2.7)$$

where DOC_t is the residual concentration of DOC at 25 min of EC process and v is the volume of water treated.

The overall reactions in EC process result in excess hydroxyl ions $(OH)^-$ in relation to hydrogen ions (H^+) the outcome is that a transient pH rise over time.

Figure 4.1: The effect of initial pH on DOC removal efficiency. with a) operating time, b) the amount of coagulant generated (Al electrode, j=1.2 mA/cm²).

The UV_{254} reduction data showed the parallel results to DOC removal efficiency. As it is seen in Figure 4.2, the pH_i 4 and 5 showed the best treatment performance. The best short term performance in UV_{254} removal was achieved with Al anode, reducing to 0.084 cm^{-1}, or 91.1% reduction after 2 min at pH_i 4 shown in Figure 4.2. The UV_{254} removal was over 90% after 10 min and 25 min electrolysis, 0.089 cm^{-1} and 0.101 cm^{-1} at pH_i 5 and 6, respectively. At the 25 min, the removal efficiency reached 78.01% with 0.442 cm^{-1} at pH_i 8.

The drop region can be defined as the ''reactive'' stage of the three proposed stages of EC pollutant removal: the ''lag'' stage, ''reactive'' stage, and ''stabilizing'' stage [Holt et al., 2005]. The ''lag'' stage was not observed as shown by Dubrawski [Dubrawski et al., 2013] probably due to the faster generation rate of coagulant in the current investigation. The reactive stage continued until 4 min electrolysis time for pH_i 4. Stabilizing stage was observed after this time. The reactive stage continued until almost the end of the process for pH 5, 6 and 8. Obviously, the lower pH values led to faster removal and better efficiency in both DOC and UV_{254}. Feng et al. [Feng et al., 2007] found that given a small electrode interval and/or a high current density, the lower pH value leads to a better removal rate of humic acid with Al electrodes. This study supports the results of our investigation. At acidic conditions obtained high removal yield compared to pH_i of 8. The optimum conditions and dominate removal mechanism was verified by zeta potential measurement in further sections (4.2). Figure 4.3 shows that Al electrodes were successful for removal of color from water at studied pH_i values. Color removal efficiency was reached 99.6%, 98.9%, 95.9% and 79.8% with Al electrodes at pH_i 4, 5, 6 and 8 respectively.

Figure 4.2: The effect of initial pH on UV_{254} reduction during the EC process with Al electrode ($j=1.2$ mA/cm^2).

Figure 4.3: The effect of initial pH on color removal efficiency during the EC process with Al electrodes ($j=1.2$ mA/cm^2)

.

Figure 4.4 illustrates the removal efficiency of HS with iron electrodes at current density 3 mA/cm^2. The DOC removal efficiency was increased at lower pH_i. The best removal efficiency was 86.5% ($DOC_{treated}$ 2.19 mg/L) at pH_i 3, and 85.9% ($DOC_{treated}$ 2.29 mg/L), 66.6% ($DOC_{treated}$ 5.40 mg/L) and 41.9% ($DOC_{treated}$ 9.02 mg/L) after 25 min of EC process time at pH_i 4, 5, and 8 respectively.
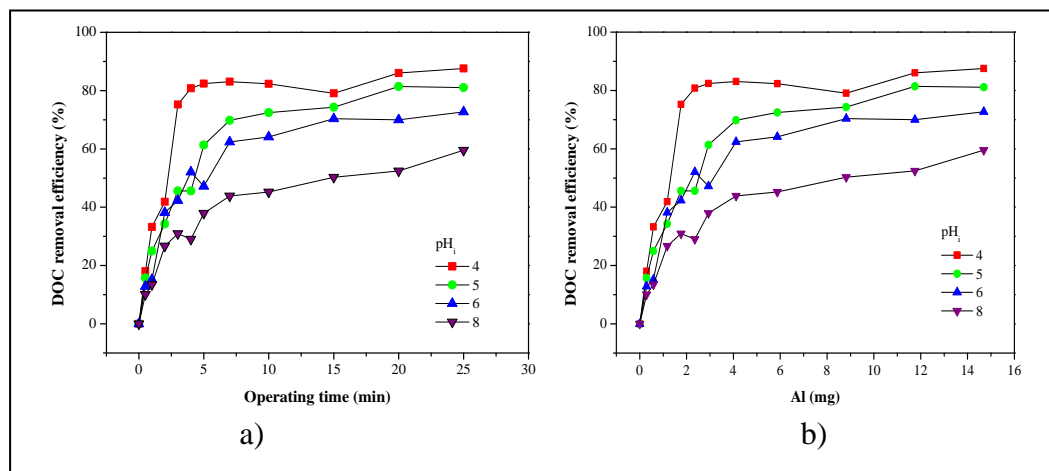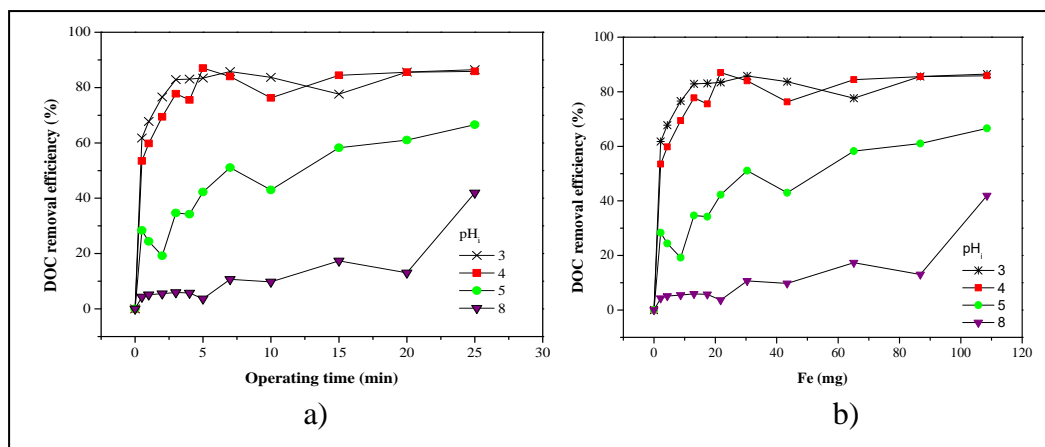
Figure 4.4: The effect of initial pH on DOC removal efficiency. with a) operating time, b) the amount of coagulant generated (Fe electrode, j=3 mA/cm^2).

Figure 4.4.b) shows the DOC removal efficiency of HS with respect to produced Fe in-stu at current density of 3 mA/cm^2 for different initial pHs. The produced Fe amount was calculated according to the Faraday's law (Equation 2.4). The DOC removal efficiency increased with the increasing the amount of iron coagulant produced in the EC process. At 3 of pH_i, the maximum removal efficiency was obtained with 108.51 mg Fe and 128.8 mg HS removed/g Fe produced (Table 4.1).

As it is seen in Figure 4.5, apart from the aluminum anodes, the UV_{254} was higher than initial UV_{254} values at initial stage of treatment for all pH_i applied. For example, $UV_{254}/UV_{254\ (i)}$ value was 1.20 and 1.14 at pH_i 4 and 5 at 5 min of process time, respectively. This difference was probably seen because of the UV at 254 wavelength absorbing orange color produced by iron particles [Dubrawski et al., 2013]. At the same condition, color removal efficiency was 13.18% and -11.29% at 5 min of process time because of iron particles as mentioned above. After 25 min electrolysis, effective removal efficiency was obtained by reducing the UV_{254} to 0.039 cm^{-1}, 0.026 cm^{-1} at pH_i 3 and 4, with 84.7% and 97.2% respectively. The removal efficiency was 68.2% and 71.6% with 0.380 cm^{-1} and 0.571 cm^{-1}, at pH_i 5 and 8, respectively. The acidic conditions showed effective HS removal for both DOC and UV_{254}. At lowest pH_i, the negatively charged iron species, such as $Fe(OH)_4^-$, are occur. It can be concluded that the high HS removal efficiency can be attributed to anionic Fe-hydroxides and afterwards $Fe(OH)_3$ with increasing pH.
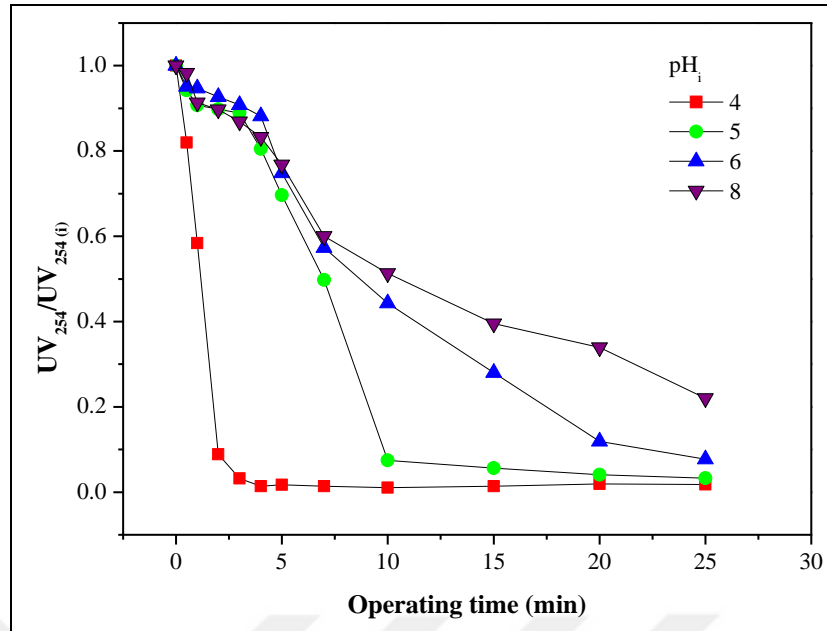
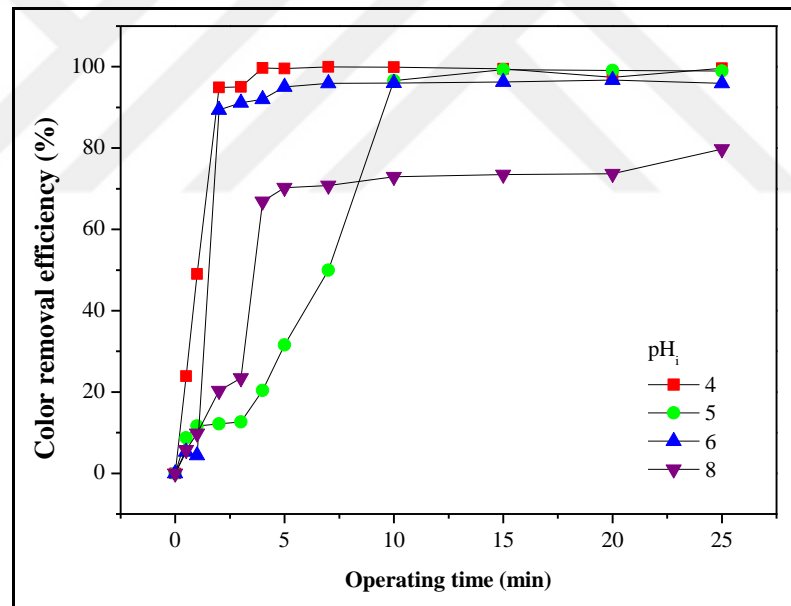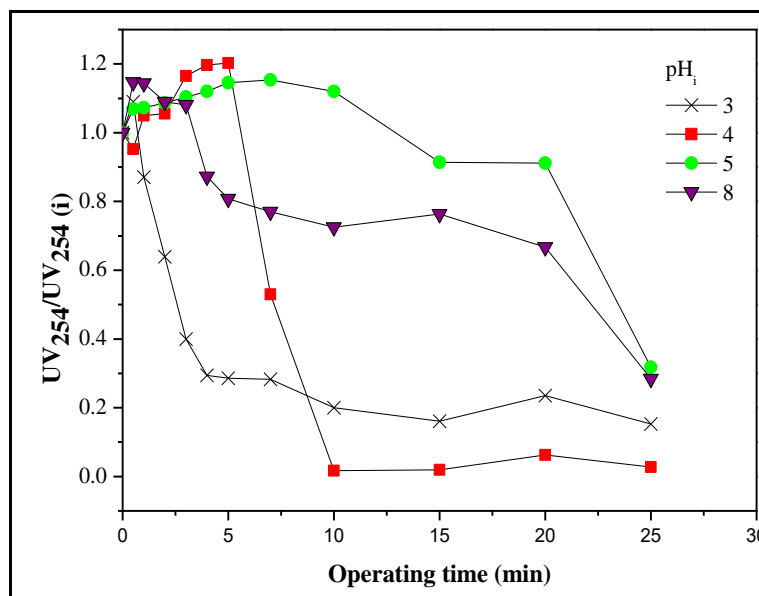Figure 4.5: The effect of initial pH on UV_{254} reduction during the EC process with Fe electrodes ($j=3$ mA/cm^2).
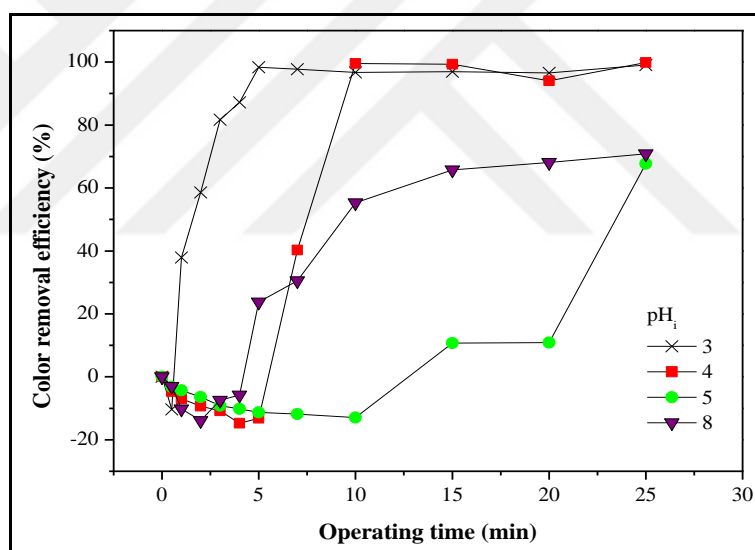
Figure 4.6: The effect of initial pH on color removal efficiency during the EC process with Fe electrode ($j=3$ mA/cm^2).

The EC treatment process efficiently removes color [Kliaugatie et al., 2013]. The removal of color and DOC by EC could be attributed to precipitation of dissolved organic molecules and aluminum and iron compounds. The color removal efficiency dropped negative value while VIS_{436} absorbance value increased until 1, 7, 15 and 5 min at pH_i 3, 4, 5 and 8, respectively as shown in Figure 4.6. After 5 min and 15 min, color removal performance changed through positive way at pH_i 4 and 5, respectively. This time is shorter at the lower pH values. The excessive amount of

Fe^{2+} and Fe^{3+} species result in diminished color removal. Also, the complex reactions that are between dissolved organic compounds and dissolved Fe ions can induce color formation. According to the increase in UV_{254} values and reduction of color removal efficiency, a certain time is necessary for the flocculation of the particles to take place before sedimentation and filtration. At acidic and neutral conditions, Fe^{3+} ions are oxidized easily to $Fe(OH)_3$. $Fe(OH)_3$ has a shape of yellowish-small particles and its sedimentation is difficult [Can et al., 2006]. When iron electrode was used as anode, the solution had red color at the initial stage of treatment, as seen in Figure 4.6. Afterwards yellowish-small particle was occurred in the reactor. When the process continued, the floc-foam layer was observed on the surface of water due to flotation after a certain time. The produced H_2 gas by redox reactions can be remove dissolved or suspended particle with flotation mechanism. It contributes to removal of pollutant. The pH value increases depending on EC period and initial pH due to hydroxyl ions produced from cathodes. While increasing pH of solution during EC process, functional groups of humic acid has more negatively charged and humic matter react with the positively charged iron hydroxide complexes. After a certain time it causes precipitation of occurred more polymeric humic-metal hydroxide structures. After 10 min, the color removal efficiency was 96.7%, 99.6%, and 55.2% at pH_i 3, 4, and 8, respectively. At pH_i 5, the longer electrolysis time was necessary for the sufficient color removal efficiency. After 25 min, the color removal efficiency reached 67.7% at pH_i 5. Hence, it could be concluded that the removal of color (VIS_{436}) depends on initial pH and process operating time. Under alkali conditions, organic matter removal was not successful. It can be concluded that $Fe(OH)_6^+$ and $Fe(OH)_4^+$ species are not so effective on removal of NOM. The results show iron electrodes for organic removal is better in more acidic conditions compared to optimum conditions for aluminum electrode.

Table 4.1: The effect of pH_i on removal of HS by Al and Fe electrodes, t_{EC}=25 min, j=1.2 mA/cm^2 for Al and j=3 mA/cm^2 for Fe.

Electrode type	pH	q (C/L)	ELC (mg)	q_t, Removed mg HS/C	q_t, Removed mg HS/g Al or Fe
Al	4	157.5	14.69	0.0900	963.8
Al	5	157.5	14.69	0.0830	892.4
Al	6	157.5	14.69	0.0750	800.5
Al	8	157.5	14.69	0.0610	654.8
Fe	3	375	108.51	0.0373	128.8
Fe	4	375	108.51	0.0370	127.9
Fe	5	375	108.51	0.0287	99.3
Fe	8	375	108.51	0.0181	62.5

4.1.1.2. Effect of Current Density on HS Removal

Current density means that applied current (Ampere or milliamp) per effective surface area (m^2 or cm^2). The amount of dissolving metal from anode electrodes increase with enhancement current density and the higher removal efficiency of pollutant can obtain. But, a limited current density value is recommended in order to avoid excess amount of O$_2$ produced because when oxygen evolution takes place in the anode surface, dissolution of anode reduces. At high current density, the heating of solution can be a problem. Current density effects density and size of gas bubbles (H$_2$). While current density increases, density of bubbles increases but the size of their decreases. Consequently, it is observed the greater upstream and faster reduction of contaminants and flotation sludge. On the other hand, high CD can result in breaking of occurred flocs. The effect of current density in the range of 0.42-4.5 mA/cm^2 on removal of organic matter with EC process using Al and Fe electrodes was investigated. The pH_i 4 of solution was selected depend on optimum condition for each electrode type.

The effect of different current densities on HS removal is shown in Figure 4.7-4.9 and 4.10-4.12, for Al and Fe, respectively. Consumption of the anode material in the EC process is directly related to the charge density as stated in Faraday's law. At high current density, a significant amount of anode dissolves and so the removal of

pollutant increases (Figure 4.7.b). Charge loading is the most important parameter for controlling the reaction during EC process. It was defined in equation 2.5. Also, too high charge loading produces more coagulant. Higher charge loading led to more HS removal efficiency. For a given time, 87.5% ($DOC_{treated}$ 2.02 mg/L) of humic acid removal can be achieved with a current density of 1.2 mA/cm^2 (157.5 C/L), but 81.6% ($DOC_{treated}$ 2.97 mg/L) of removal was obtained when the current density was reduced to 0.42 mA/cm^2 (67.5 C/L) with Al electrodes at pH_i 4, as it is seen in Figure 4.7 and Table 4.2.

Figure 4.7: The effect of current density on DOC removal efficiency. with a) operating time, b) the amount of coagulant generated (Al electrode).

Figure 4.7.b) shows the coagulants generated from anode surface at current density of 1.2 mA/cm^2. The produced species are sufficient for the removal of pollutants. At low current density, the DOC removal efficiency was similar initial operating time. It can result from dissolution of cathode, as well as dissolution of anode. There were no sufficient coagulants reacting with all of the HA molecules at current density 0.42 mA/cm^2.

The reduction of UV_{254} was noticeably different for high and low current density at initial stage of electrolysis (Figure 4.8). At 2 min, UV_{254} removal efficiency was 67.6% (0.306 cm^{-1}), 91.10% (0.084 cm^{-1}), 81.7% (0.173 cm^{-1}) while current density was 0.42 mA/cm^2, 1.2 mA/cm^2 and 3 mA/cm^2 for Al electrode, respectively. Over a period of 5 min, humic acid removal with respect to UV_{254} was reached over 95% for all current densities studied.

Figure 4.8: The effect of current density on UV_{254} reduction during the EC process with Al electrode.
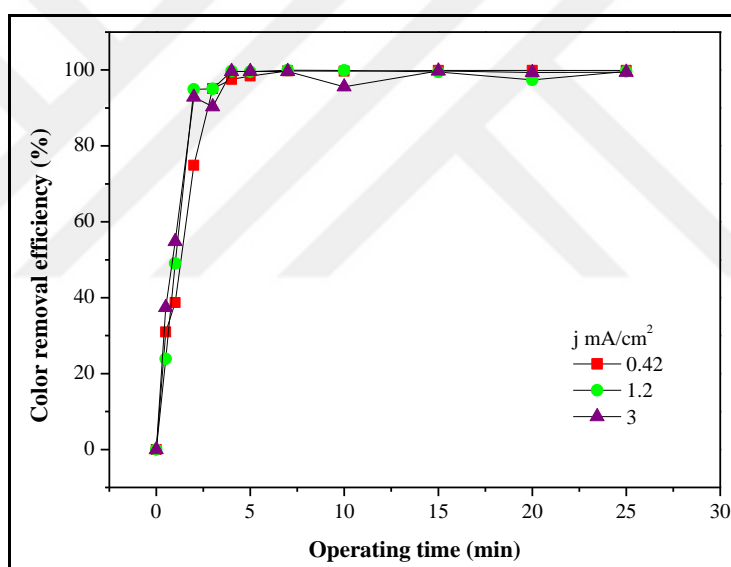
Figure 4.9: The effect of current density on color removal efficiency during the EC process with Al electrode.

As it is seen in figure 4.10.a), the maximum removal efficiency was 86.5% ($DOC_{treated}$ 2.19 mg/L) at current density 3 mA/cm^2 with iron electrodes during EC process. At current density 1.2 mA/cm^2, the best removal efficiency was 74.9% using iron electrodes. But end of the operating time (25 min), the DOC removal efficiency was reduced for all studied current density (Figure 4.10.a). The DOC removal efficiency was 74.9%, 85.9% and 73.8% for current density of 1.2, 3 and 4.5 mA/cm^2, respectively, for iron electrode. On the other hand, at a higher current

density ((3 mA/cm^2 (394 C/L) for Al; 4.5 mA/cm^2 (555 C/L) for Fe)) DOC reduction were 82.1% (DOC$_{treated}$ 2.9 mg/L) and 78.3% (DOC$_{treated}$ 3.5 mg/L) for Al and Fe, respectively (Table 4.2). It can be concluded that the DOC removal efficiency would not increase after a certain current density (optimum current density), as it is seen in Figure 4.7.a) and Figure 4.10.a). Current density and the charge loading needed to be optimized.
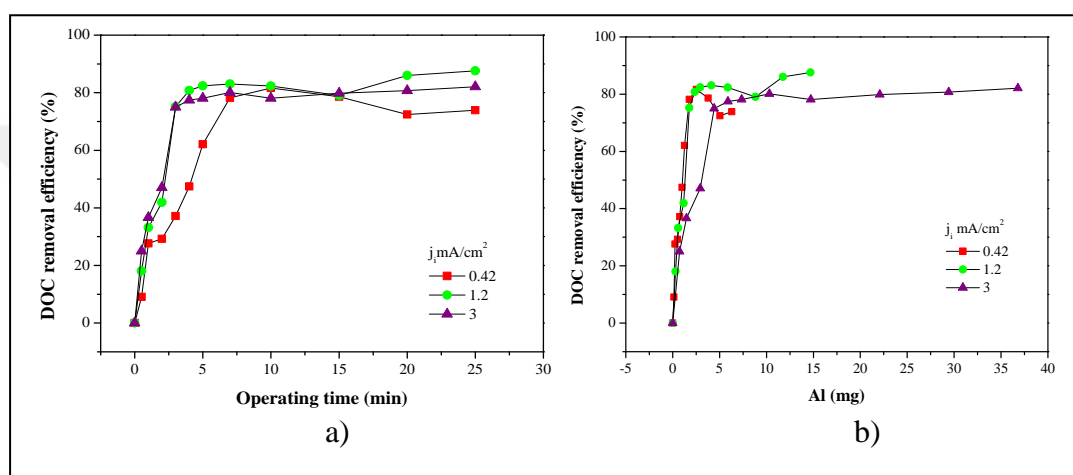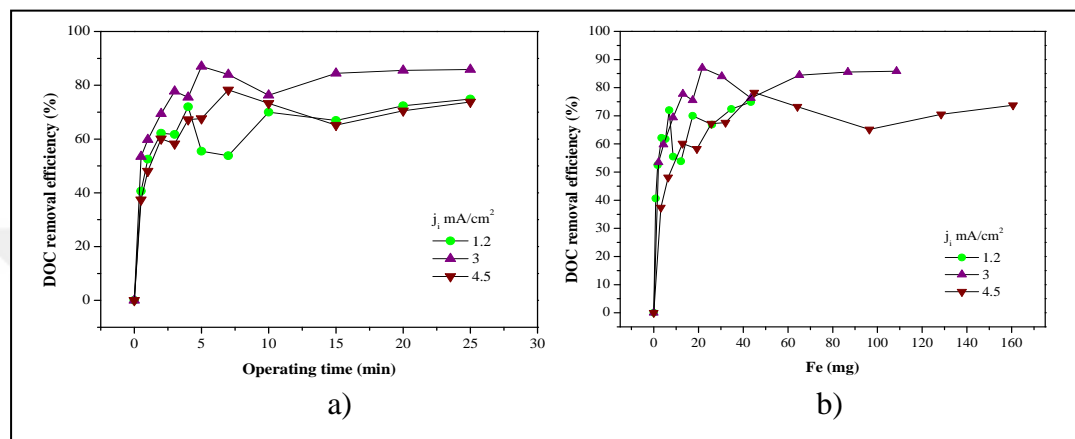

Figure 4.10: The effect of current density on DOC removal efficiency. with a) operating time, b) the amount of coagulant generated (Fe electrode).

The best performance in UV$_{254}$ removal was achieved at current density of 3 mA/cm^2 with iron electrode, the removal efficiency was 98.3% (0.016 cm^{-1}), as shown in Figure 4.11. It can be obviously seen in Figure 4.12, while the UV$_{254}$ values increasing initial stage of process for Fe electrode, color removal efficiency was diminished at all applied current density values. The best reduction of VIS$_{436}$ was 0.0002 cm^{-1} with 99.8% color removal efficiency with iron electrode after 25 min at current density 3 mA/cm^2 and at pH$_i$ 4. The color removal efficiency was above 99% in 10 min of reaction time, while current density was in the range of 0.42–3 mA/cm^2 with Al electrode (Figure 4.9). It can be concluded that UV$_{254}$ reduction would not increase after a certain current density (optimum current density) as DOC removal efficiency. The produced gas bubbles increase at higher current density and can destroy formed humic-metal hydroxide complexes. Afterwards, it can result in release of humic matter in solution.
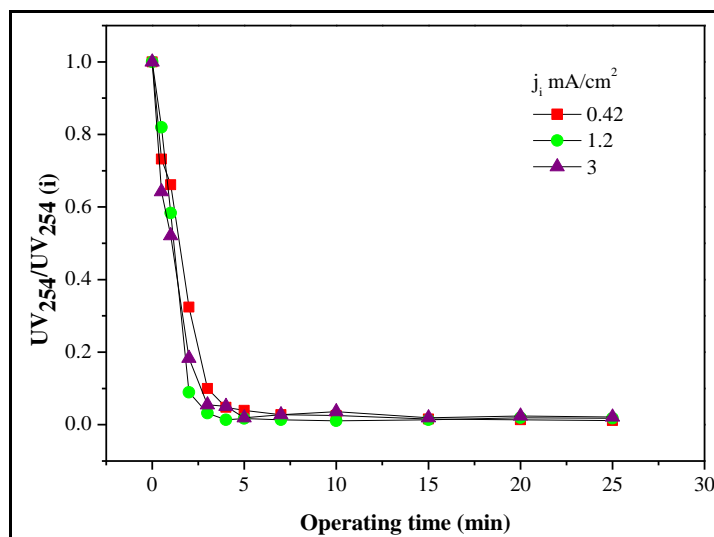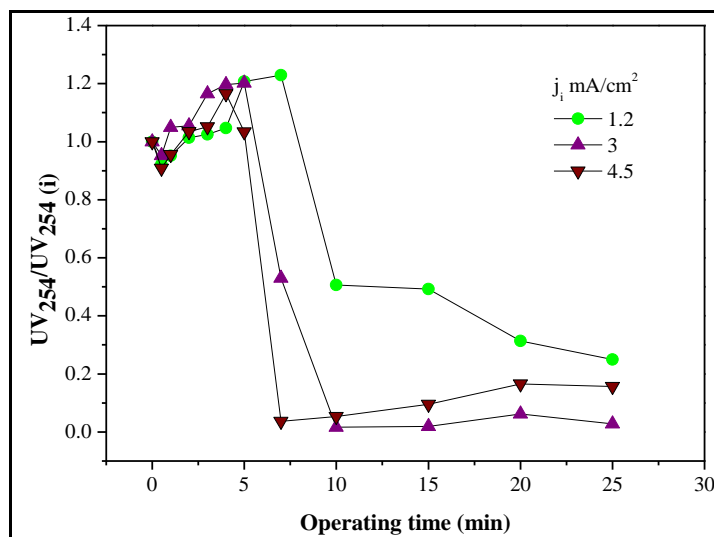
Figure 4.11: The effect of current density on UV_{254} reduction during the EC process with Fe electrode.
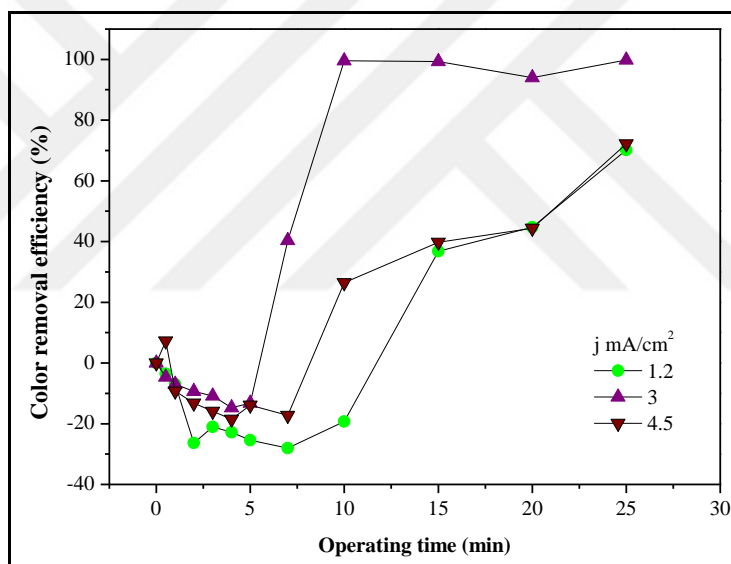
Figure 4.12: The effect of current density on color removal efficiency during the EC process with Fe electrode.

When iron electrode was used as anode, the solution had red color at the initial stage of treatment. As it is seen in Figure 4.12, the color removal efficiency dropped negative value and color of solution gradually was getting more dark brown until a certain operating time. The excessive amount of Fe^{2+} and Fe^{3+} species result in diminished color removal. After 10 min, 5 and 7 min the color removal was occurred at 1.2, 3 and 4.5 mA/cm^2, respectively. The end of the process time, the best color removal efficiency was obtained at 3 mA/cm^2 with 99.8%.

Table 4.2: The effect of current density on removal of HS, t_{EC}= 25 min, pH_i= 4 for Al and Fe.

Electrode type	j_i mA/cm^2	q (C/L)	ELC (mg)	q_t, Removed mg HS/C	q_t, Removed mg HS/g Al or Fe
Al	0.42	67.5	6.30	0.1770	1898.0
Al	1.20	157.5	14.69	0.0900	963.8
Al	3	394.5	36.80	0.0336	360.6
Fe	1.2	150	43.40	0.0807	278.9
Fe	3	375	108.51	0.0370	127.9
Fe	4.5	555	160.60	0.021	74.29

4.1.1.3. Effect of Electrode Material on HS Removal

The effect of different electrode types on humic acid removal by EC process was shown in Figure 4.13-4.15. The treatment performances of aluminum, iron and hybrid electrodes was compared in terms of DOC removal efficiency and UV_{254} reduction and color removal efficiency. The optimum conditions were used in experiments. The conditions of EC process were the pH_i 5 and current density 3 mA/cm^2 for hybrid, the pH_i 4 and current density 1.2 mA/cm^2 for Al, and the pH_i 4 and current density 3 mA/cm^2 for Fe electrode configuration.

Iron anode electrode showed the best short term performance until 3 min of electrolysis (Figure 4.13). At this time, DOC removal efficiency was 77.8%. Further electrolysis, Al electrodes reached iron electrode's performance almost at 7 min with 83% reduction. Iron and aluminum electrodes showed similarly DOC removal efficiency after 15 min. Afterwards, the removal of organic matter continued more slowly both iron and aluminum. DOC removal efficiency was 87.6% and 85.9% for aluminum and iron electrode, respectively, at the end of electrolysis time of 25 min, as it is seen in Figure 4.13. On the other hand, the removal rate of DOC by hybrid electrodes was decreased beyond 10 min of operating time (Figure 4.13). The removal efficiency by hybrid electrode was 73.2% at 25 min. Al anodes succeed the best DOC removal efficiency of CHA by EC process. The effluent concentration of humic acid was 2.02 mg/L, 2.29 mg/L and 4.33 mg/L for Al, Fe and hybrid electrodes, respectively, end of the EC process.
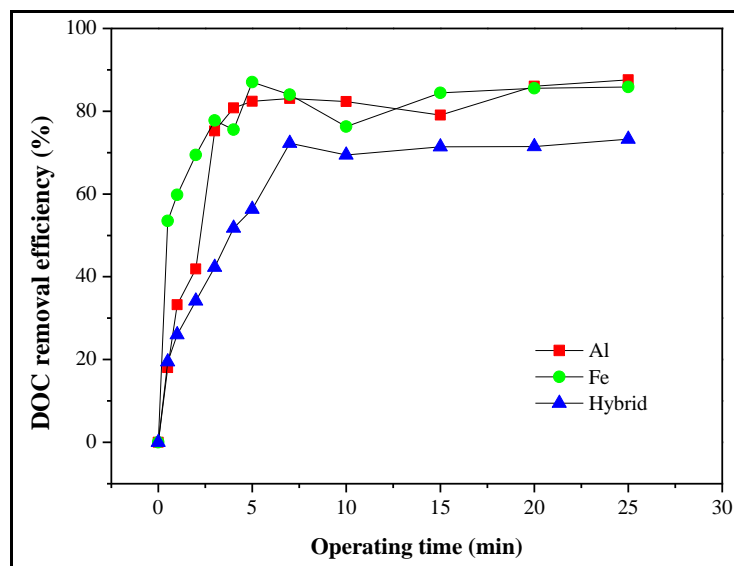
Figure 4.13: Effect of electrode types on DOC removal efficiency during EC process at optimum conditions.

The UV_{254} reduction data was shown for three electrode type in Figure 4.14. At 2 min, UV_{254} removal efficiency was 91.1% (0.084 cm^{-1}), while current density was 1.2 mA/cm^2 for Al electrode. UV_{254} reduction by the hybrid electrodes was approached almost after 10 min Al electrode's UV_{254} removal efficiency. As it is seen in Figure 4.14, the UV_{254} was observed after 7 min by Fe electrodes. The best performance in UV_{254} removal was achieved at current density 3 mA/cm^2 with iron electrode; the removal efficiency was 98.3% (0.016 cm^{-1}) at 10 min. The UV_{254} removal efficiency of HA was 98.2% (0.017 cm^{-1}), 97.2% (0.026 cm^{-1}), 98.2% (0.021 cm^{-1}) for Al, Fe and hybrid, respectively, by EC process the end of 25 min. During the EC process time, hybrid electrode had higher performance than Fe electrode until a certain time, as it is seen in Figure 4.14. Also, the increasing UV_{254} did not observed with hybrid electrodes, as opposed to, Fe electrode.

As it is seen in Figure 4.15, the color removal efficiency $-VIS_{436}-$ was above 99% for Al, Fe and hybrid electrode at given optimum conditions. When Fe and hybrid electrodes were used, the solution had red color until a certain time. As it is seen in Figure 4.15, color removal efficiency dropped negative value. This duration was 5 min and 1 min for Fe and hybrid. It would result in the UV_{254} enhancement at initial stage of EC process for iron electrode, as it is seen in Figure 4.14. As mentioned above (4.1.1), the increment did not exactly reflect the removal efficiency of humic acid in terms of UV_{254} [Dubrawski et al., 2013]. Al electrodes showed

faster removal of color compared to Fe and hybrid. The color removal efficiency was 95.0% at 3 min by Al electrode, as it is seen in Figure 4.15. Adhoum [Adhoum and Monser, 2004] found that Al electrode was more effective than Fe electrode on color removal.

Figure 4.14: Effect of electrode types on UV_{254} reduction during EC process at optimum conditions.
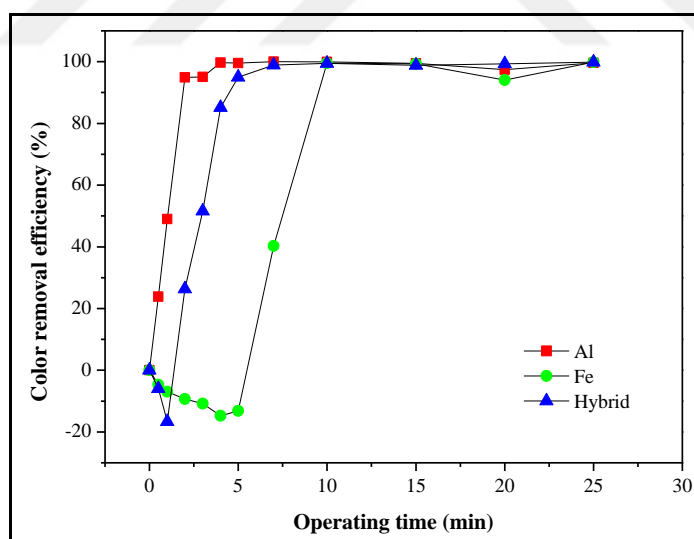
Figure 4.15: Effect of electrode types on color removal efficiency during EC process at optimum conditions.

The SUVA value of treated samples were 1.1 L/(m mg), 0.8 L/(m mg), and 0.5 L/(m mg) for Fe, Al and hybrid, respectively, at maximum DOC reduction for CHA. It can be concluded that he high MW fraction of hydrophobic humic matter was removed.

4.1.2. The Effect of Electrode Type and EC Time on Removal of HS from SHA Aqueous Solution

The treatability of terrestrial NOM source was investigated with different electrode types by EC process. The experiment conditions –pH_i, CD and operating time- were decided depend on preliminary studies, and the obtained results from CHA. The pH_i of solution adjusted 4; and applied current density was 3 mA/cm^2 for Al, Fe, and hybrid electrode.

The effect of electrodes types on DOC removal efficiency, UV_{254} reduction and color removal efficiency was shown in Figure 4.16, 4.17, and 4.18, respectively. The DOC removal efficiency was increased significantly until 3 min by aluminum electrodes. It was reached 85.7% ($DOC_{treated}$ 3.6 mg/L) initial stage of electrolysis at current density 3 mA/cm^2. After 20 min, the DOC removal efficiency showed a major increment by Al electrodes while after 15 min, Fe and hybrid electrodes get through stabilizing phase until end of the electrolysis. The maximum DOC removal efficiency was obtained at 15 min and 20 min with 89.2% ($DOC_{treated}$ 2.74 mg/L) and 79.5% ($DOC_{treated}$ 5.18 mg/L) for Fe and hybrid electrode, respectively. But the end of operating time the DOC removal efficiency was slightly reduced for Fe and hybrid electrodes, as it is seen in Figure 4.16. It could be concluded that almost 20 min electrolysis time is enough for effective treatment of SHA with using Fe and hybrid electrode. When electrolysis time protracted, the DOC removal efficiency would not so much increase. The end of the 25 min, the DOC removal efficiency was 90% ($DOC_{treated}$ 2.52) for Al electrode. At 10 min. it was 87.6 % ($DOC_{treated}$ 3.34 mg/L) with Al electrode.
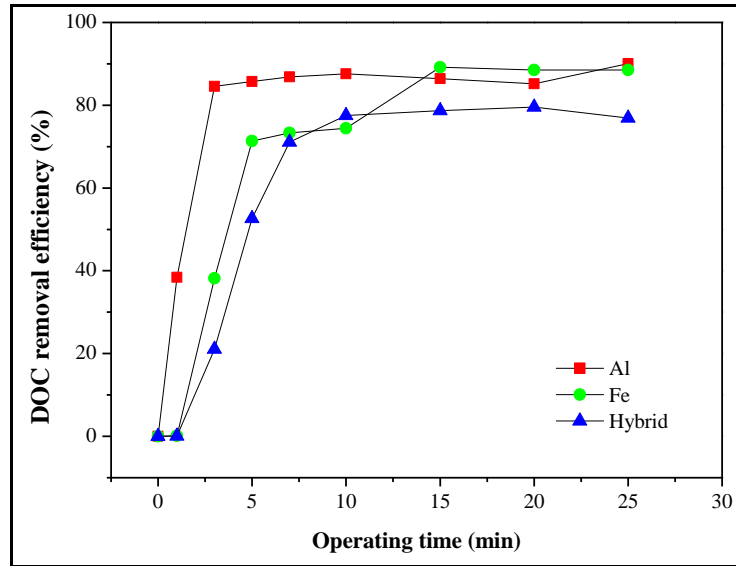
Fig 4.16: Effect of electrode type on DOC removal efficiency during EC process.

As it is seen in Figure 4.17, hybrid anode showed the best performance for UV_{254} reduction with 0.012 cm^{-1}. The lowest UV_{254} value was 0.022 cm^{-1} and 0.056 cm^{-1} for Al and Fe, respectively. Aromatic fraction that presents high amount in terrestrial HA source was removed almost 99% by using Al and hybrid electrodes in EC process in terms of UV_{254}. While the UV_{254} removal efficiency was 96.6% at the end of 25 min, the increment UV_{254} was seen during 5 min of operating time because of increment VIS_{436}, as CHA.
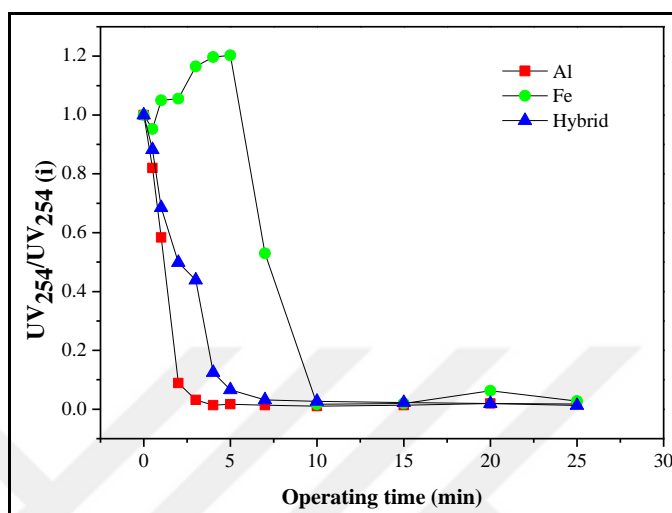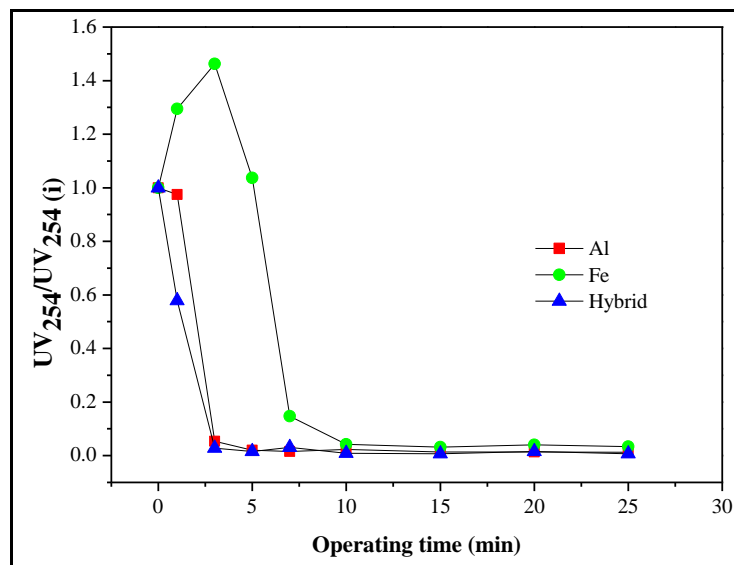

Figure 4.17: Effect of electrode type on UV_{254} reduction during EC process.
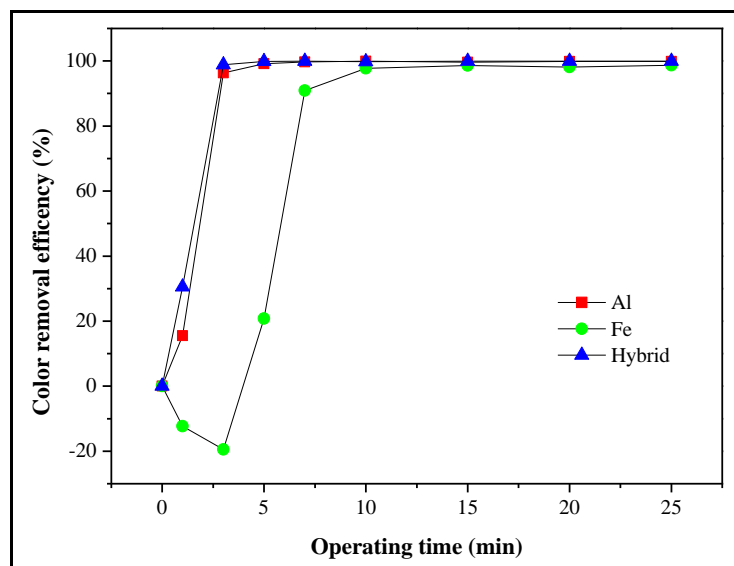
Figure 4.18: Effect of electrode type on color removal efficiency during EC process.

The color removal efficiency by EC process using Al, Fe and hybrid electrode was given in Figure 4.18. The color removal of SHA could be occurred after 3 min due to the increasing VIS_{436} by Fe electrode. At 25 min, the color removal efficiency was 98.6% by Fe electrode. Al and hybrid electrodes showed more effective performance than Fe and the color removal efficiency was above almost 99% with Al and hybrid electrode for treatment of soil humic acid by EC process.

As it is seen in Figure 4.16, 4.17, and 4.18, the EC operating time were 25 min for all studied electrode type. At the 15 min of electrolysis time was succeeded effective UV_{254} reduction for Al, Fe and hybrid. After this time, the performance of these electrodes was not increased until 25 min. The optimum EC operating time is 10 min and 15 min for Al and hybrid, and Fe, respectively, considering decolorization of soil humic acid. The 20 min of electrolysis seems optimum time for treatment of SHA in terms of effective removal of DOC, color, and UV_{254} by using Al electrode, while the 15 min process time is enough for Fe, and hybrid. Slavik found that the increase in pH after an initial coagulation resulted in a considerable release of dissolved organic substance even at very small pH changes of 0.2 (Slavik et al., 2012). Very small amount reduction in removal efficiency of DOC was observed a few conditions after a certain operating time (Figure 4.7; 4.10; 4.16). It can result from release of humic acid from metal-HA complexes.

The SUVA value of treated samples were 2.0 L/(m mg), 0.87 L/(m mg), and 0.21 L/(m mg) for Fe, Al and hybrid, respectively, at maximum DOC reduction. The

high MW fraction of hydrophobic humic matter was removed. The minimum SUVA value was obtained both CHA and SHA when using hybrid electrodes because hybrid electrodes achieved best removal efficiency of UV_{254} both CHA and SHA, while Al was succeed best DOC reduction for CHA and SHA.

4.1.3. The Effect of Operating Parameters on Removal of NOM from Natural Surface Waters

The effect of operating parameters on removal of aquatic organic matter was investigated. Lake Saimaa and Lake Terkos was selected as studied area.

4.1.3.1. The Treatment of Lake Saimaa Water

The location of Lake Saimaa and sample point was given in Figure 3.1.

4.1.3.1.1. Effect of Initial pH on NOM Removal

Firstly, Lake Saimaa water was treated by EC process. The pH_i of 4, 5, 7.30±0.02 (the original pH of lake) with Al electrode; pH of 4, 5, 7.3 and 8 with Fe electrode and pH of 4, 7.3 and 8.5 with hybrid electrode were studied for LSW at 3 mA cm^{-2} current density. The EC operating time was 25 min.

As it is seen in Figure 4.19.a) for Al electrodes the best performance was obtained after 25 min at pH_i 4 with 71.1% removal efficiency and effluent DOC concentration of 4.29 mg/L of LSW. At 3 mA cm^{-2}, q(C/L) was 303.5 for all initial pHs. The maximum DOC reduction per Coulomb or mg Al were 0.0348 mg HS removed/C and 287.2 mg HS removed/g Al produced (Table 4.3), according to equation 2.6 and 2.7, respectively. The final concentration of DOC after 25 min was 5.38 mg/L and 5.68 mg/L, with removal efficiency 63.8% and 61.7% at pH_i 5 and 7.3, respectively. The maximum DOC removal efficiency was 62.9% at 20 min at pH_i 7.3. At the lowest pH_i, the rate of DOC removal increased faster than pH_i 5 and original pH of water. At just 5 min, 62.5% DOC reduction was obtained by Al anode at pH_i 4. But after a certain time, DOC removal efficiency was not significantly increased at this pH_i, as it is shown Figure 4.19.a). At pH_i 7.3 and 4, DOC reduction

was closed each other after 15 min. At pH_i 5, DOC removal efficiency increased until end of the EC process time. At water' original pH, reactive phase was continued almost 20 min.   The initial pH_i 4 value was changed during EC process, as it is seen in Figure 4.56. The increase in pH value can result in reduction or go to stabilizing phase of DOC removal efficiency. At high pH values, polymeric Al^{3+} hydroxides as monomeric and polymeric occur. It could be concluded that complex at high pH value was not so effective for removal of NOM. This difference was investigated by zeta potential trend and particle size growth rate in further sections.

Figure 4.19: The effect of initial pH on DOC removal efficiency. with a) operating time, b) the amount of coagulant generated (LSW, Al electrode, $j=3$ mA/cm^2).
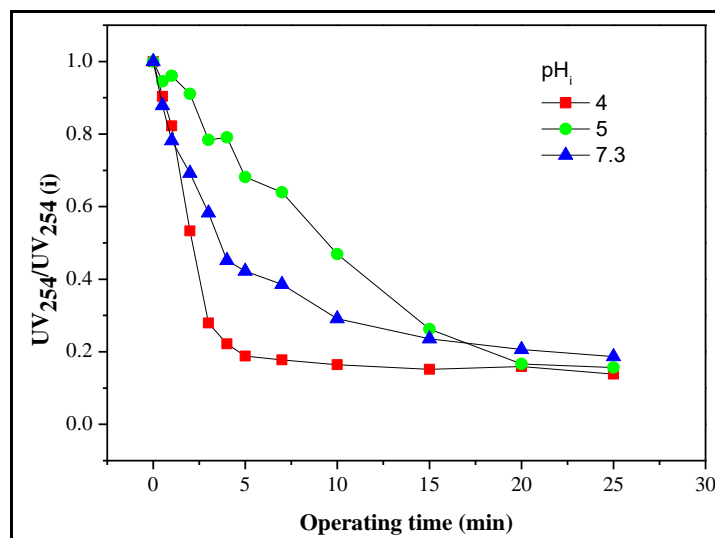
Figure 4.20: The effect of initial pH on UV_{254} reduction during the EC process with Al electrode ($j=3$ mA/cm^2).
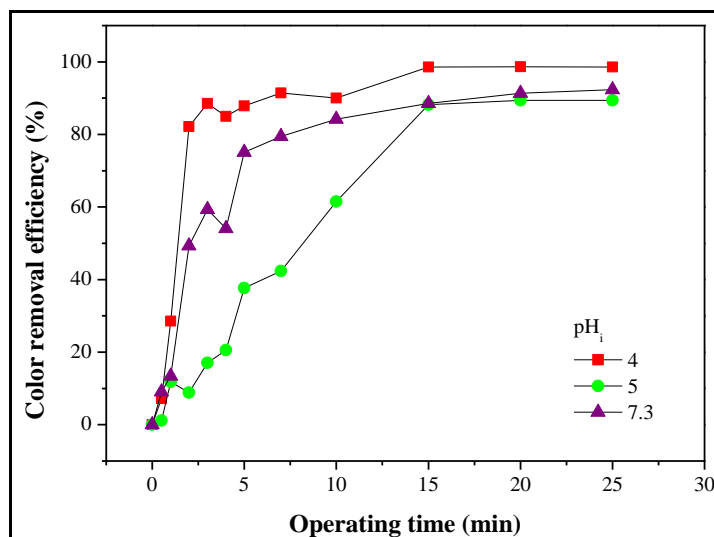
Figure 4.21: The effect of initial pH on UV_{254} reduction during the EC process with Al electrode (j=3 mA/cm^2).

The UV_{254} reduction data was given for studied initial pHs in Figure 4.20. The pH_i 4 showed the best UV_{254} reduction with 86.2% (0.053 cm^{-1}). At initial stage of electrolysis, the UV_{254} removal efficiency showed a similar tendency at the pH_i 7.3 and 4. At 3 min, the removal efficiency was 46.7% and 30.8% for pH_i 4 and 7.3, respectively. The end of the process, the UV_{254} reduction was obtained 84.9% (0.063 cm^{-1}) and 81.3% (0.077 cm^{-1}) for pH_i 5 and 7.3, respectively. As it is seen in Figure 4.19.a) and Figure 4.20, the end of the process, the pH_i 5 showed higher DOC removal efficiency and UV_{254} reduction compared to the pH_i 7.3. But for effective removal of DOC and UV_{254} at pH_i 5, more operating time is needed.

Figure 4.21 shows Al electrodes were successful for removal of color from water. The color removal efficiency was above 90% at studied pH values. The best color removal efficiency was 98.6% at pH_i 4. The color removal efficiency reached 89.4%, 92.3% with Al electrodes at pH_i 5 and water's original pH, respectively.

Iron anode electrodes were more effective on the DOC removal efficiency at acidic initial pHs, as it is seen in Figure 4.22. The DOC removal efficiency was 58.8%, 48.7%, and 44.0% at pH_i 4, 5, 7.3, respectively, at 15 min. At pH_i 8, the removal of DOC was so slowly occurred by using Fe electrodes, at initial stage of electrolysis (4 min). The final DOC concentration was 9.27 mg/L with removal efficiency 37.6% at pH_i 8. The best DOC removal efficiency was obtained at the original pH of water with 61.6% (DOC$_{treated}$ 5.71 mg/L) at 25 min. The produced Fe amount was 114.15 mg at current density of 3 mA/cm^2. The removed NOM per the

amount of Fe produced was 80.1 and 77.9 at the original pH of raw water and pH_i 4, respectively, at 25 min. Also, the end of the process at pH_i 4, the DOC removal efficiency was 59.8% (5.97 mg/L). It was needed more time to reach effective DOC removal for its original pH.
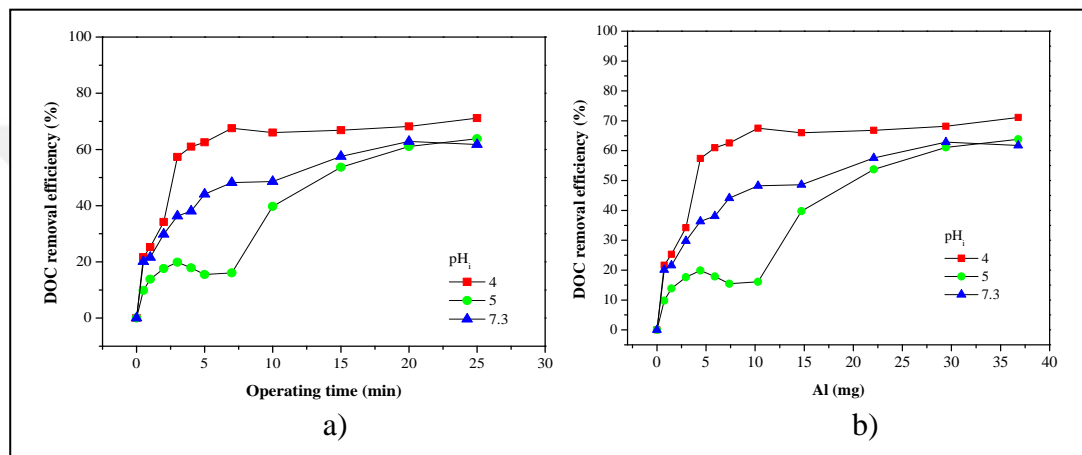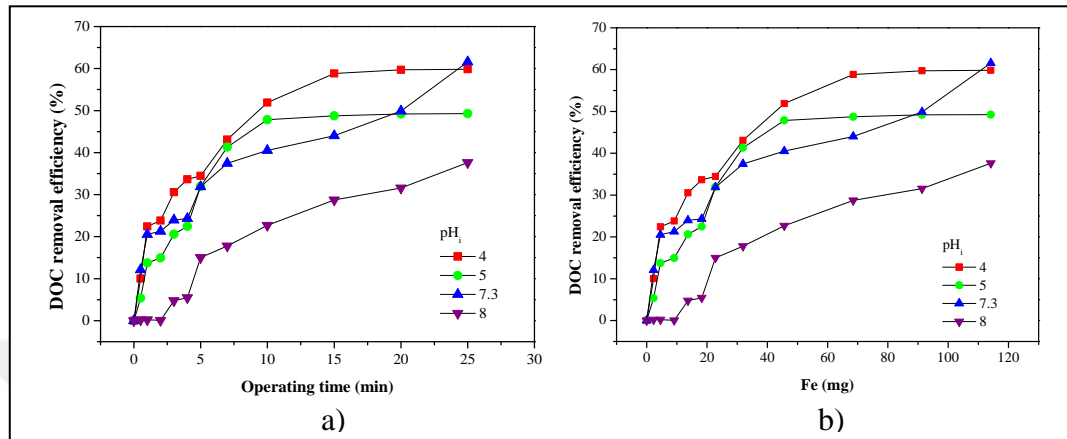

Figure 4.22: The effect of initial pH on DOC removal efficiency. with a) operating time, b) the amount of coagulant generated (Fe electrode, j=3 mA/cm^2).

When iron electrode was used as anode, the UV_{254} reduction was not observed initial stage of treatment, as it is seen in Figure 4.23. At the pH_i 4 and 5, the UV_{254} removal efficiency was 91.9% (0.031 cm^{-1}), and 83.3% (0.086 cm^{-1}), respectively. When initial pH value was increased, the UV_{254} reduction diminished. The UV_{254} removal efficiency was 79.1% (0.086 cm^{-1}) and 82.1% (0.080 cm^{-1}), at pH_i 7.3 and 8, respectively.

Figure 4.23: The effect of initial pH on UV_{254} reduction during the EC process with Fe electrode (j=3 mA/cm^2).

Figure 4.24: The effect of initial pH on color removal efficiency during the EC process with Fe electrode ($j=3$ mA/cm^2).

The color removal efficiency by Fe electrode was shown in Figure 4.24. The color of water gradually was getting first time brown and the green until a certain EC process time. The accumulation of the flocs on the water surface was observed almost after this EC process time. Figure 4.5.c) shows the best color removal efficiency was obtained at pH$_i$ 4 with 98.9%. Also, at this pH value the decreasing in color removal efficiency was short compared the other studied pHs. The end of the process time, the color removal efficiency was 96.5%, 92.35, and 97.5% for pH$_i$ 5, 7.3 and 8, respectively.

Table 4.3: The effect of pH$_i$ on removal of NOM, $t_{EC}=25$ min, $j_i=3$ mA/cm^2.

Electrode type	pH	q (C/L)	ELC (mg)	q_t, Removed mg NOM/C	q_t, Removed mg NOM/g Al or Fe
Al	4	303.5	36.80	0.0348	287.2
Al	5	303.5	36.80	0.0312	257.6
Al	7.3	303.5	36.80	0.0302	249.4
Fe	4	303.5	114.15	0.0293	77.9
Fe	5	303.5	114.15	0.0241	64.1
Fe	7.3	303.5	114.15	0.0301	80.1
Fe	8	303.5	114.15	0.0184	49.0

As it is seen in Figure 4.25, the increase trend for DOC removal efficiency was observed until 20 min electrolysis time for all studied pHs by hybrid electrodes. At pH_i 4, this reactive stage continued until the end of the EC process. It was reached maximum DOC removal efficiency with 68.6% ($DOC_{treated}$ 4.66 mg/L) at pH_i 4. The effluent concentration of DOC was 4.74 mg/L and 6.12 mg/L at pH_i 7.3 and 8, respectively. The optimum operating time seems 20 min for these initial pHs (Figure 4.25).
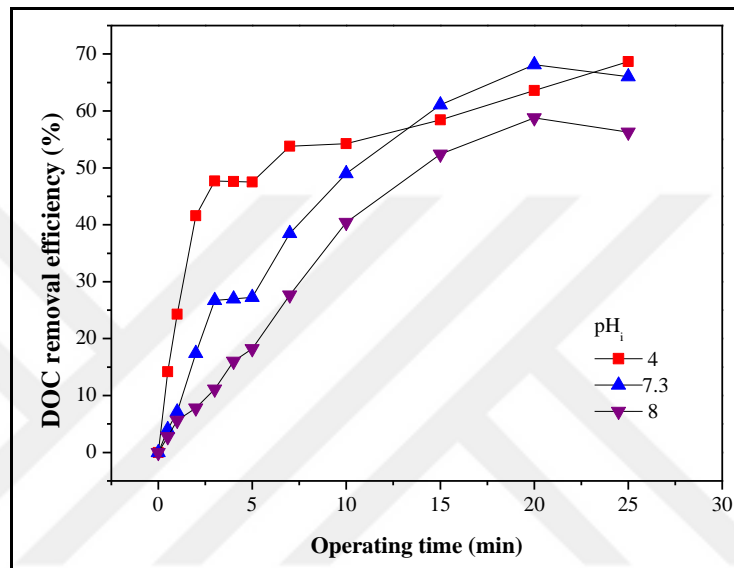
Figure 4.25: The effect of initial pH on DOC removal efficiency during the EC process with hybrid electrode ($j=3$ mA/cm^2).

The UV_{254} reduction was given in Figure 4.26. The best short term performance was obtained at pH_i 4. At 5 min, the UV_{254} removal efficiency was 82.8% (0.084 cm^{-1}) this pH_i. The end of the EC process time, the UV_{254} removal efficiency was 90.9% (0.035 cm^{-1}), 92.4% (0.031 cm^{-1}), and 91.4% (0.035 cm^{-1}) at pH_i 4, 7.3, and 8, respectively.

The color was effectively removed at all initial pHs by hybrid electrodes, as it is seen in Figure 4.27. The color removal efficiency was above 95% at 20 min for all pH_i. Hybrid electrodes resulted in a drop at color removal until just 1 min at initial stage of operating time.
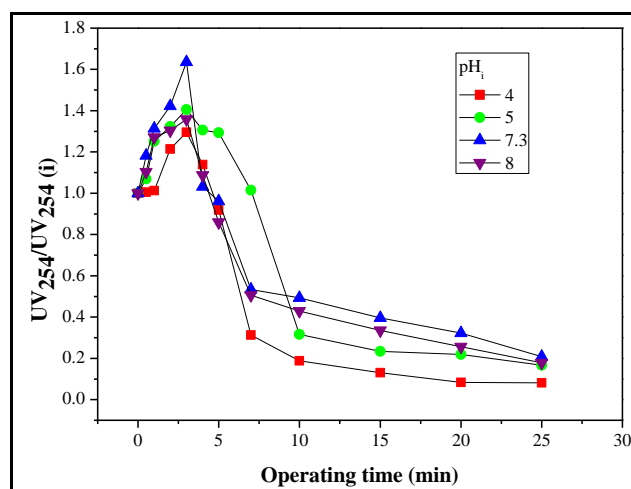
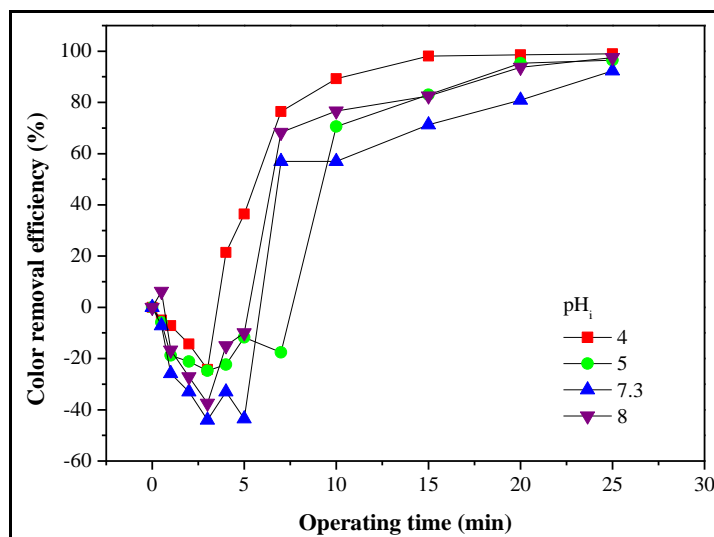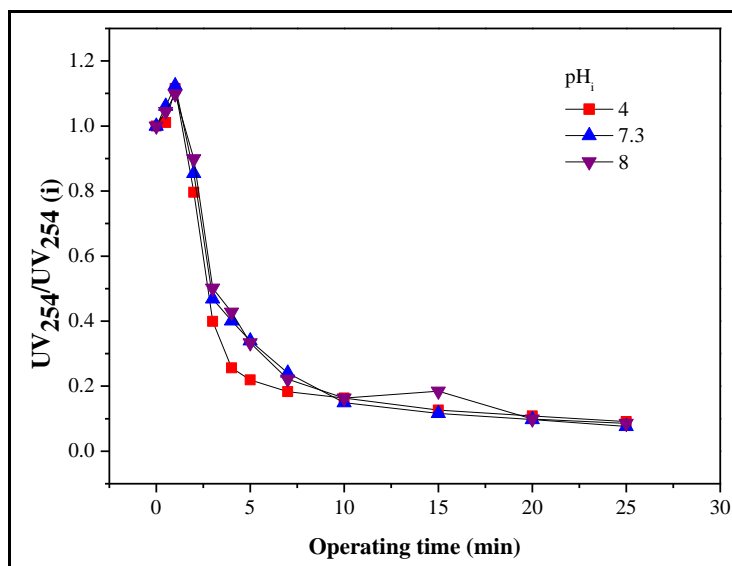Figure 4.26: The effect of initial pH on UV_{254} reduction during the EC process with hybrid electrode (j=3 mA/cm^2).
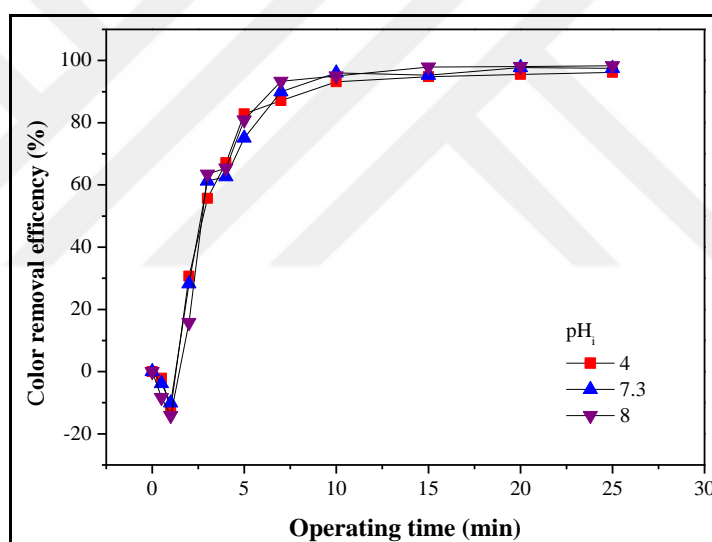
Figure 4.27: The effect of initial pH on color removal efficiency during the EC process with hybrid electrode (j=3 mA/cm^2).

4.1.3.1.2. Effect of Current Density on NOM Removal

The aluminum and iron electrodes were selected for investigate effect of current density on DOC removal efficiency, UV_{254} reduction and color removal efficiency (Figure 4.28; 4.29; 4.30) by EC process for LSW. The studied current density values were 1.2 mA/cm^2, 3 mA/cm^2, and 4.5 mA/cm^2. The pH$_i$ was original pH value of water for Al electrode and 4 for Fe in the experiments.

Figure 4.28.a) shows the best DOC removal efficiency was obtained at current density 3 mA/cm^2 with 61.7% (DOC$_{treated}$ 5.68 mg/L) for LSW, by Al electrode. The DOC removal efficiency was 53.2% (DOC$_{treated}$ 6.96 mg/L), 55.8% (DOC$_{treated}$ 6.60 mg/L), at 1.2 mA/cm^2 and 4.5 mA/cm^2, respectively. The 0.0652, 0.0302, and 0.0153 mg NOM were removed per C, at 1.2, 3, and 4.5, respectively (Table 4.4). It can be conclude that the removal efficiency not increased after a certain current density.

At original pH of water, Al dosage was 14.69, 36.80 and 65.76 mg at 1.2, 3 and 4.5 mA/cm^2, respectively, at 25 min (Figure 4..28.b).The amount of removed NOM per g Al was found to decrease (537.8-126.1 mg/g) with increase in Al dosage (Table 4.4). The concentration of removed NOM was 7.9, 9.18 and 8.29 mg/L at 1.2, 3 and 4.5 mA/cm^2, respectively. It seemed that adsorption site of Al-hydroxides for Al complexes- solute interaction was increased by increasing the amount of Al dosage due to increased available surface charges which favored functional sides of organic matter for attachment and decreasing in the electrostatic repulsive.
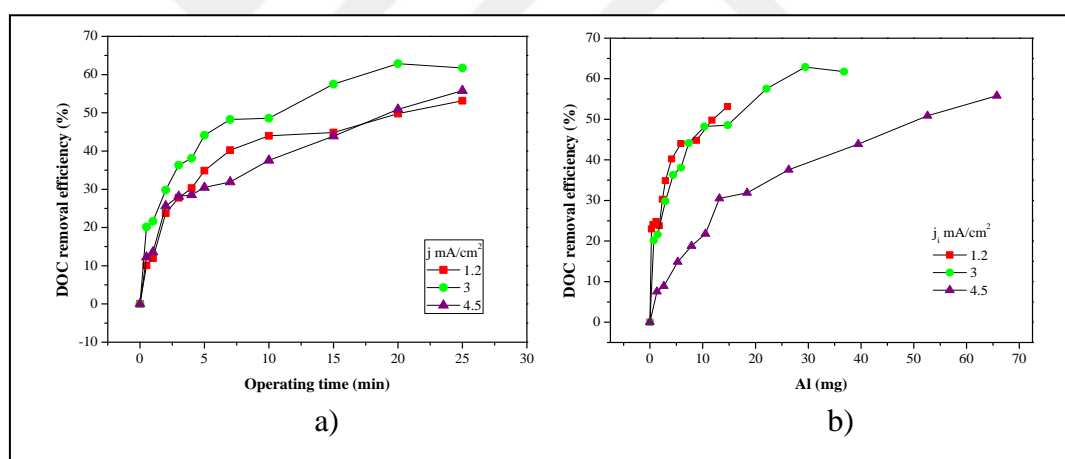
Figure 4.28: The effect of current density on DOC removal efficiency with a) operating time, b) the amount of coagulant generated (Al electrode, pH$_i$=7.3).

The reduction of UV$_{254}$ was clearly different for low and high current density during operating time (Figure 4.29). The UV$_{254}$ removal efficiency was 68.5% (0.130 cm^{-1}) and 84.5% (0.064 cm^{-1}) and at current density of 1.2 mA/cm^2 and 4.5 mA/cm^2, respectively. As it is seen in Figure 4.29, at current density of 3 mA/cm^2, the effective removal efficiency was obtained with 81.3% (0.0771 cm^{-1}) at the end of the process.

As it is seen in Figure 4.30, the best color removal efficiency was obtained at current density of 3 mA/cm² with 92.3% by Al electrode. At current density of 1.2 mA/cm² and 4.5 mA/cm², the color removal efficiency was 75.6% and 60.7%, respectively.
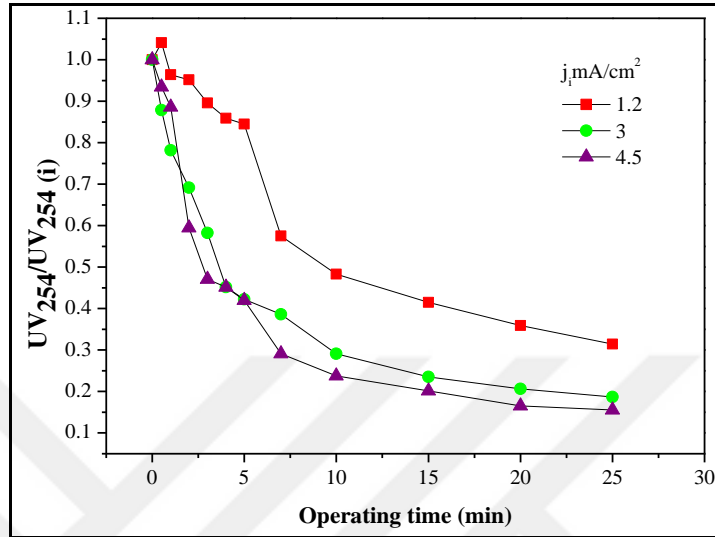
Figure 4.29: The effect of current density on UV_{254} reduction during the EC process with Al electrode (pH_i=7.3).
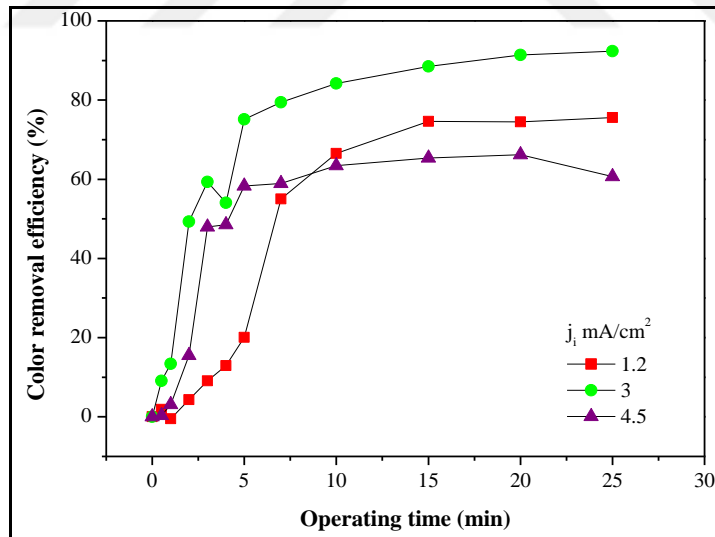
Figure 4.30: The effect of current density on color removal efficiency during the EC process with Al electrode (pH_i=7.3).

As it is seen in Figure 4.31.a), the DOC removal efficiency was 50.7% (7.33 mg/L mg/L), 59.8% (5.97 mg/L), and 59.3% (6.05 mg/L) for at 1.2 mA/cm², 3 mA/cm² and 4.5 mA/cm², by Fe electrode, respectively. Figure 4.31.b) shows the DOC removal efficiency with respect to Fe dosage during Ec process. The removed

mg NOM per g generated Fe at 1.2, 3 and 4.5 mA/cm² was calculated as 165.3, 77.9, and 43.17. The q_t decreased with increasing the amount of Fe (mg) (Table 4.4).

It seemed that the removal capacity of occurred coagulant (iron-hydroxides) was increased. At the end of the treatment, DOC reduction was similar for 3 and 4.5 mA/cm². The DOC removal efficiency showed increasing trend until 25 min, while the removal efficiency moved towards stabilizing trend at current density 3 mA/cm². The current density of 1.2 mA/cm² was not so effective of organic matter removal from LSW.
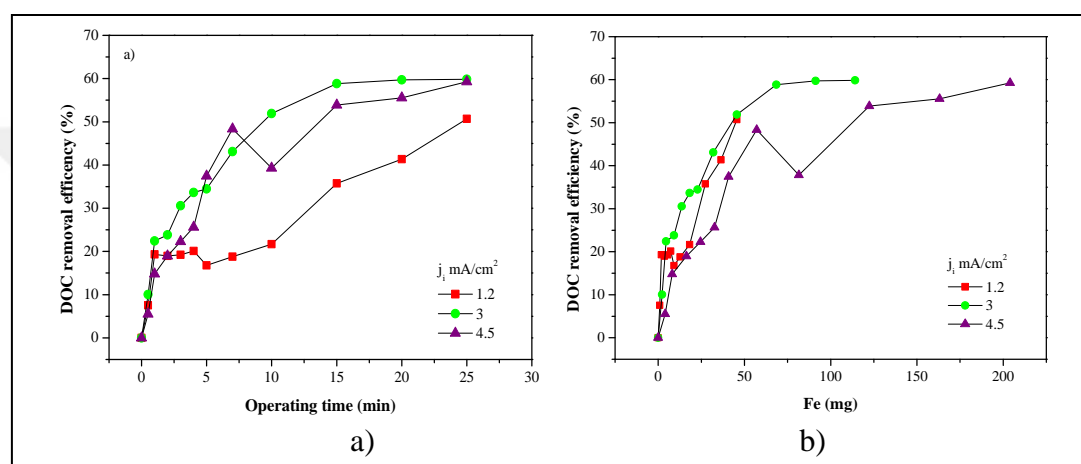
Figure 4.31: The effect of current density on DOC removal efficiency. with a) operating time, and b) the amount of coagulant generated (Fe electrode, pH_i=4).

The best UV_{254} reduction was obtained at current density of 3 mA/cm² with 91.9% (0.031 cm⁻¹), as it is seen in Figure 4.32. The lowest current density (1.2 mA/cm²) showed the lowest the UV_{254} removal efficiency among the studied current densities by EC process. At current density of 4.5 mA/cm² the removal efficiency was 85.6% (0.055 cm⁻¹). At given operating time, the current density of 3 mA/cm² was optimum for treatment of aromatic fraction LSW at pH_i 4.

As it is seen in Figure 4.33, the end of the electrolysis the color removal efficiency was above 90% for all studied current densities, while initial stage of electrolysis color removal efficiency showed negative values. The best color removal efficiency was 98.9% at 3 mA/cm² by Fe electrodes.
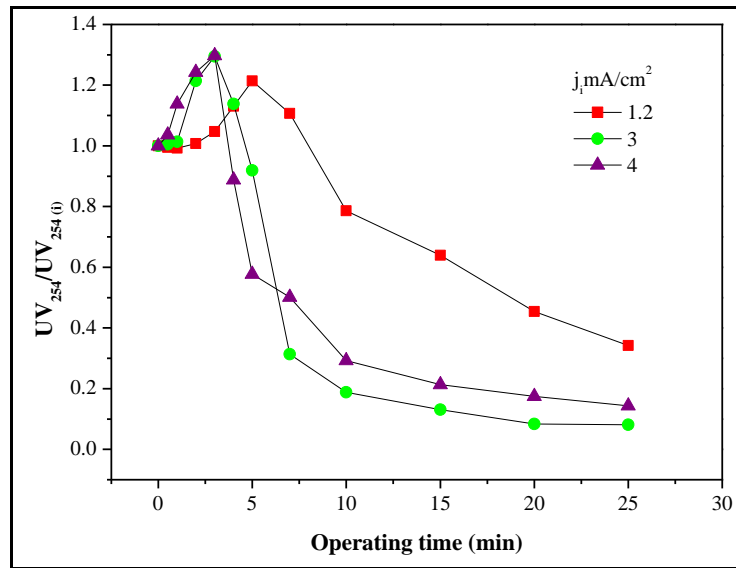
Figure 4.32: Effect of initial current density on UV_{254} reduction during EC process using Fe electrode ($pH_i=4$).
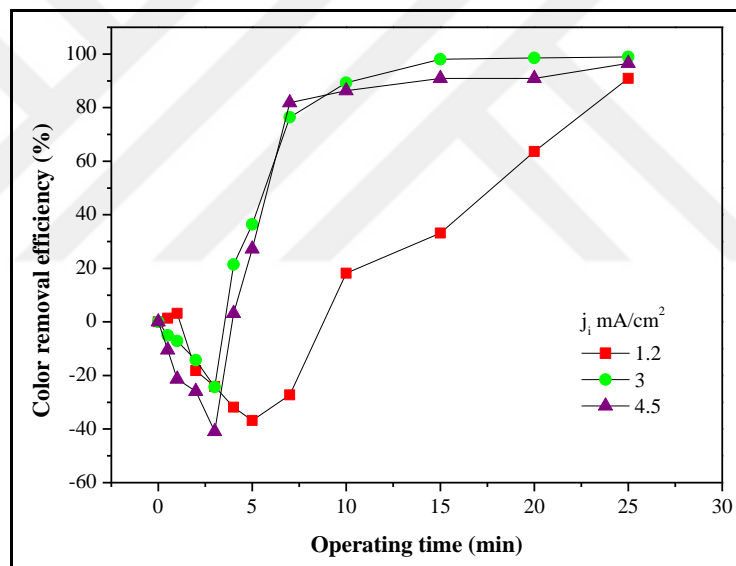
Figure 4.33: Effect of initial current density on color removal efficiency during EC process using Fe electrode ($pH_i=4$).

Table 4.4: The effect of current density on removal of NOM by Al and Fe electrodes, t_{EC}=25 min, pH_i=7.3 for Al and pH_i=4 for Fe.

Electrode type	j_i mA/cm^2	q (C/L)	ELC (mg)	q_t, Removed mg NOM/C	q_t, Removed mg NOM/g Al or Fe
Al	1.2	121.2	14.69	0.0652	537.8
Al	3	303.2	36.80	0.0302	249.4
Al	4.5	542.3	65.76	0.0153	126.1
Fe	1.2	121.2	45.58	0.0622	165.3
Fe	3	303.5	114.15	0.0293	77.9
Fe	4.5	542.3	204.00	0.016	43.17

The SUVA shows LSW had both low and high MW NOM. The SUVA value of Lake Saimaa decreased from 2.77 to 1.2, 1.5, and 0.75 for Al, Fe, and hybrid, respectively. The results show the high MW fraction was removed by EC.

4.1.3.1.3. Effect of Electrode Material on NOM Removal

The effect of different electrode types (aluminum, iron and hybrid) on NOM removal from Lake Saimaa is shown in Figure 4.34-4.36. Aluminum anode showed the best short term performance until 7 min of electrolysis (Figure 4.44). Further electrolysis, hybrid electrodes reached aluminum electrode's performance with 61.1% reduction at 15 min and then hybrid electrode showed higher DOC removal efficiency. DOC removal efficiency by iron anode was 61.6% at the end of the electrolysis time of 25 min. The reactive stage was continued during 25 min of EC process for all electrodes. On the other hand, DOC reduction was increased more slowly beyond 7 min by both aluminum and iron electrodes. The lowest effluent concentration was obtained as 5.05 mg L^{-1} with hybrid electrode.
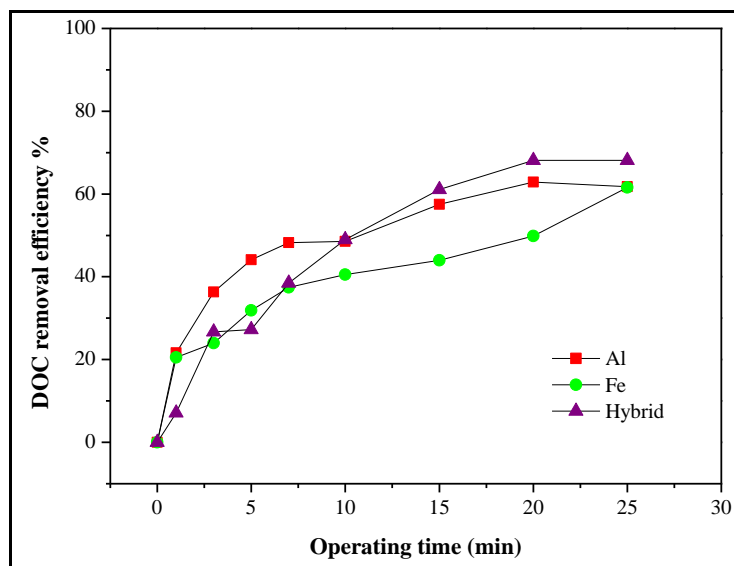
Figure 4.34: Effect of electrode types on DOC removal efficiency during EC process
$(pH_i = 7.3, j = 3$ mA cm$^{-2})$.

The UV$_{254}$ reduction data was shown for three electrode type in Figure 4.35. As it is seen in Figure 4.35, hybrid electrode has slightly higher performance than Al electrode. For two electrodes type, initial 10 min was reactive phase and beyond this time stable stage was observed during operating time.

After 3 min of electrolysis, UV$_{254}$ removal efficiency was over 50% by hybrid electrode. Among the electrodes, the best UV$_{254}$ removal efficiency was obtained as 92.4% with 0.0312 cm^{-1} by hybrid electrode at the end of the process. When iron electrodes were used as anode in EC process, the UV$_{254}$ value increased during 3 min of electrolysis as it is seen in Figure 4.45. But the increment did not exactly reflect the aromatic structure of NOM [Dubrawski et al., 2013]. In addition, the color removal efficiency showed a negative performance until 5 min, when using iron electrodes, as it is seen in Figure 4.36. It would result in the UV$_{254}$ enhancement at initial stage of EC process [Katsumata et al., 2008], [Dubrawski and Mohseni, 2013] because it can be concluded that Fe^{2+}/Fe^{3+} metal hydroxide flocs that occur at early stage of process do not precipitate immediately and adsorption of NOM on flocs are weak at this stage. The subsequent DOC reduction was 61.6% with 5.71 mg L^{-1} for aquatic NOM (LSW) and the UV$_{254}$ removal efficiency was 79.3%, with 0.086 cm^{-1} by iron electrode.
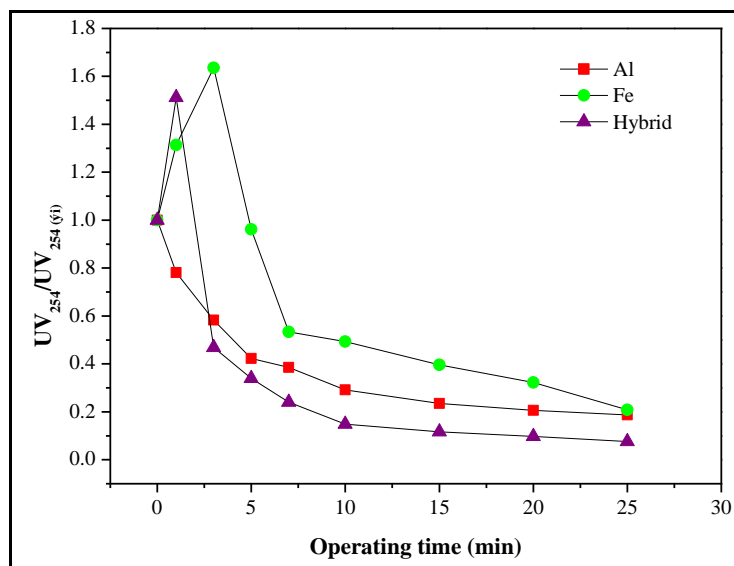
Figure 4.35: Effect of electrode types on UV_{254} reduction during EC process
$(pH_i = 7.3, j = 3$ mA cm^{-2}).
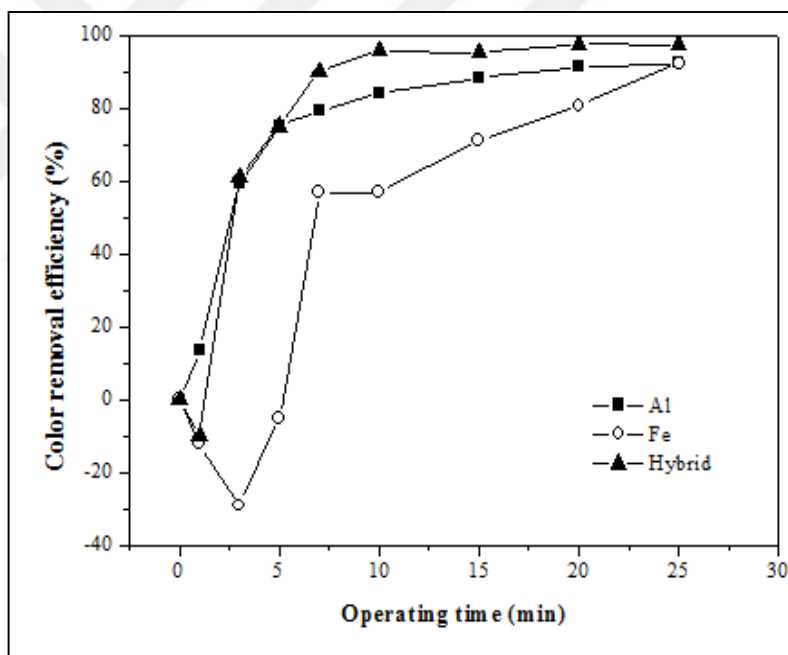
Figure 4.36: Effect of electrode types on color removal efficiency.

More effective DOC and UV_{254} reduction and color removal were obtained
by hybrid electrodes than the other electrodes. Aluminum electrodes were more
effective in removing color of the aquatic NOM than iron electrodes at the point of
short term performance, whereas color removal efficiency was 92.3% both aluminum
and iron end of process as it is seen in Figure 4.36.

4.1.3.2. The Treatment of Lake Terkos Water

The effect of current density on DOC removal efficiency, UV_{254} reduction and color removal efficiency was determined at original pH of LTW by Al, Fe and hybrid anode electrode. The operating time was studied 25 min. But, this process time was not enough for removal of NOM at low current density. As it is seen in Figure 4.37, the DOC removal efficiency was 27.2%, 35.3% and 34.8% at 3 mA/cm^2, 6 mA/cm^2 and 10 mA/cm^2, respectively, at 25 min. Then, higher current density was studied. The more effective removal efficiency was obtained with 70.7% at current density of 15 mA/cm^2. But, the temperature of solution was increased during process and reached 32.8 ^{0}C. Several researchers have investigated the effect of temperature on NOM removal from water. Vepsalainen et al. studied the effect of temperature and found that high NOM removal was obtained a temperature of 22.25 ^{0}C using an Al electrode. Temperature had a significant effect on the dissolving speed of Al and the impact of on NOM removal was minor compared to that of initial pH [Vepsalainen et al., 2009]. This current density was eliminated due the increasing in temperature. The removal efficiency was similar at 6 mA/cm^2 and 10 mA/cm^2. At current density 6 mA/cm^2 succeed the increment after 5 min, while at current density 3 mA/cm^2 the removal of NOM raised after 10 min. The process continued until 60 min in order to increase removal efficiency of DOC at current density of 6 mA/cm^2 and 3 mA/cm^2, as it is seen in Figure 4.38. At 60 min, the removal efficiency of DOC was 50.2% (DOC$_{effluent}$=3.28 mg/L) and 40.3% (DOC$_{effluent}$=3.93 mg/L) for 6 mA/cm^2 and 3 mA/cm^2, respectively. The optimum removal efficiency was 50.2% (DOC$_i$=6.58; DOC$_{effluent}$=3.28 mg/L) by Al electrode at pH original and 6 mA/cm^2. At original pH of water, Al dosage was 157.15 mg at 60 min, at 6 mA/cm^2 (Figure 4.38.b). The amount of removed NOM was calculated as 21 mg NOM/g Al or 0.0026 mg NOM/C at optimum removal efficiency (Table 4.6).
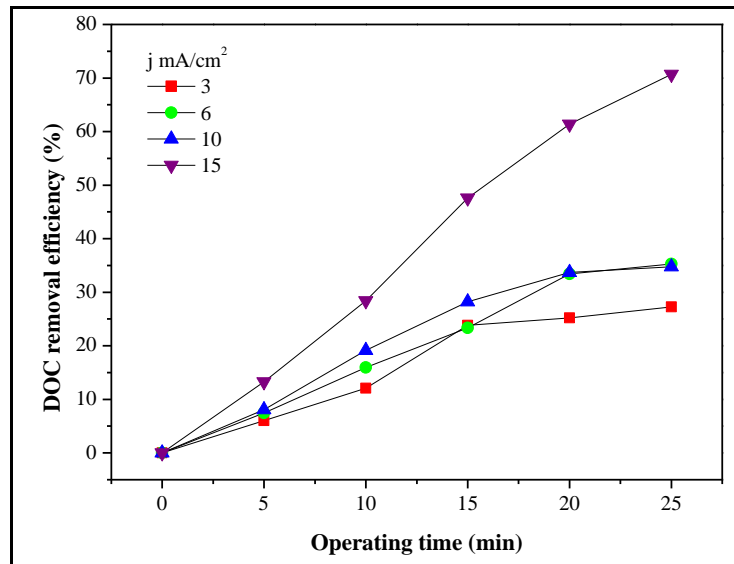
Figure 4.37: The effect of current density on DOC removal efficiency during the EC process with Al electrode (LTW, pH_i=7.76).
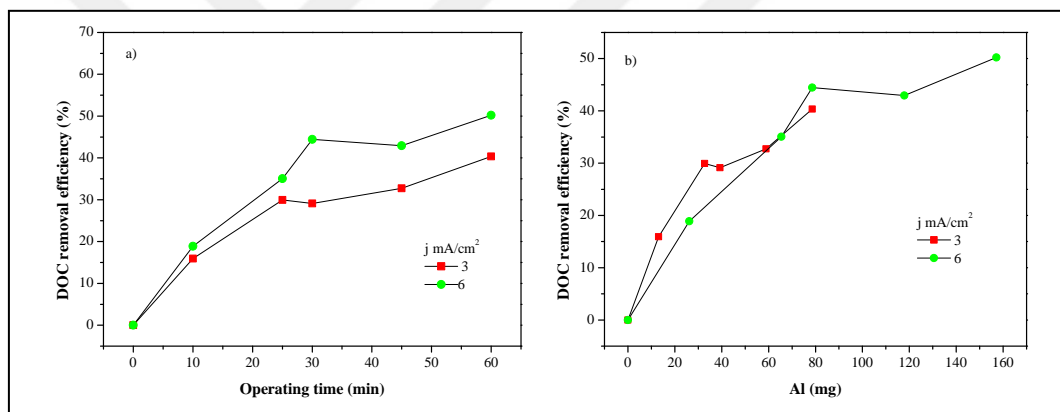
Figure 4.38: The effect of current density on DOC removal efficiency. with a) operating time, and b) the amount of coagulant generated (Al electrode, pH_i=7.76).

The UV_{254} reduction was 87.4% and 70.4% at current density 15 mA/cm^2 and 10 mA/cm^2, respectively, at 25 min. As it is seen in Figure 4.39, the removal efficiency of removal of UV_{254} was 76.1% (0.034 cm^{-1}) and 60.6% (0.056 cm^{-1}) at current density 6 mA/cm^2 and 3 mA/cm^2 by Al electrode. The initial SUVA was 2.07 L/(m mg). At optimum current density that was 6 mA/cm^2 the SUVA value was determined 1.04 L/(mg m) the end of the process. At 3 mA/cm^2, the SUVA was reduced to 1.42 L/(m mg). The character of sample was changed after treatment. The SUVA value is under 2, indicating removal of high MW fractions.
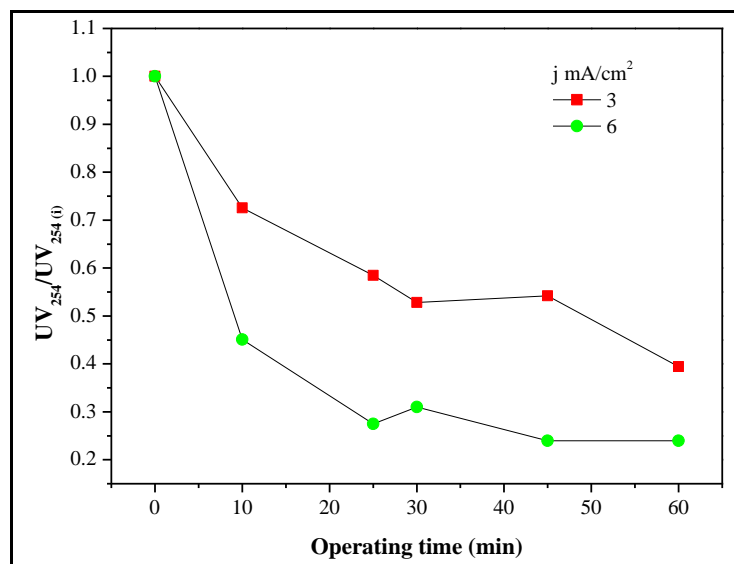
Figure 4.39: The effect of current density on UV_{254} reduction during the EC process with Al electrode (pH_i=7.76).

The color removal efficiency was observed 75.2% and 29.7% at current density 6 mA/cm^2 and 3 mA/cm^2, respectively, at 60 min. The high current density had significant influence on color removal efficiency. When the current density 10 mA/cm^2 and 15 mA/cm^2 were studied, the color reduction was 10% and 55%, respectively, at 25 min.

Figure 4.40, shows the effect of current density on DOC removal efficiency when using Fe electrodes at the original pH_i of sample. The operating time was 60 min. The maximum removal efficiency was 60.5% ($DOC_{effluent}$=2.61 mg/L) and 40.1% ($DOC_{effluent}$=3.97 mg/L) at 6 mA/cm^2 and 3 mA/cm^2, respectively, end of the process. At original pH of water, Fe dosage was 487.52 and 243.76 mg at 6 mA/cm^2 and 3 mA/cm^2, respectively, at 60 min (Figure 4..40.b).The amount of removed NOM per g Fe was found to decrease (10.8-8.2 mg/g) with increase in Fe dosage (Table 4.6). It seemed that adsorption site of iron-hydroxides for iron complexes-organic molecules interaction was increased by increasing the amount of Fe dosage due to increased available surface charges which favored functional sides of organic matter for attachment.
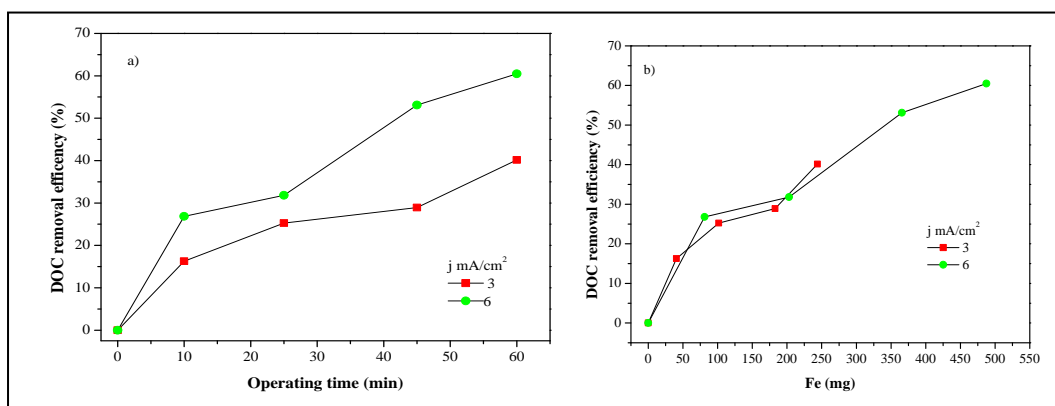
Figure 4.40: The effect of current density on DOC removal efficiency. with a) operating time, b) the amount of coagulant generated (Fe electrode, pH_i=7.72).

As it is seen in Figure 4.41, the removal efficiency of UV_{254} was similar until 25 min at 3 mA/cm^2 and 6 mA/cm^2, respectively. The removal efficiency of UV_{254} was 73.5% (0.036 cm^{-1}) and 61.0% (0.053 cm^{-1}) the end of the operating time and SUVA was 1.38 L/(m mg) and 1.34 L/(m mg), at 6 mA/cm^2 and 3 mA/cm^2, respectively. It can be concluded that the hydrophobic fraction was mainly removed.
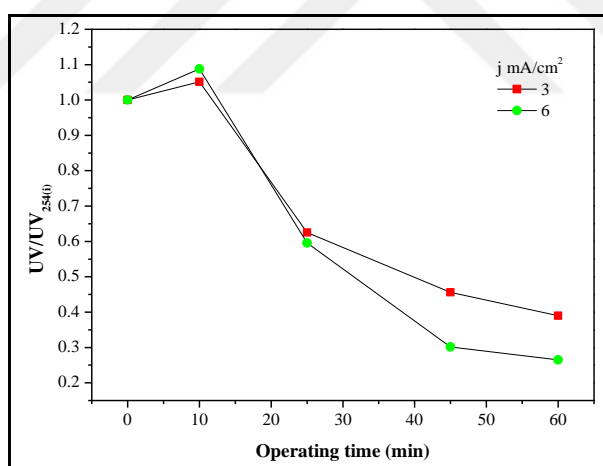
Figure 4.41: The effect of current density on UV_{254} reduction during the EC process with Fe electrode (pH_i=7.72).

Figure 4.42 shows the effect of current density on the removal efficiency of DOC by using hybrid electrode. The low current density showed higher DOC removal efficiency during process time. The reduction in DOC was 48.7% and 43.9% at current density of 3 mA/cm^2 and 6 mA/cm^2, at 45 min, respectively. The removal efficiency was 52.4% (DOC$_{effluent}$=3.13 mg/L) and 45.9% (DOC$_{effluent}$=3.56 mg/L) at 3 mA/cm^2 and 6 mA/cm^2, respectively, the end of the process. The

optimum current density was 3 mA/cm^2. At this current density, color removal efficiency was 76.4% the end of the process.
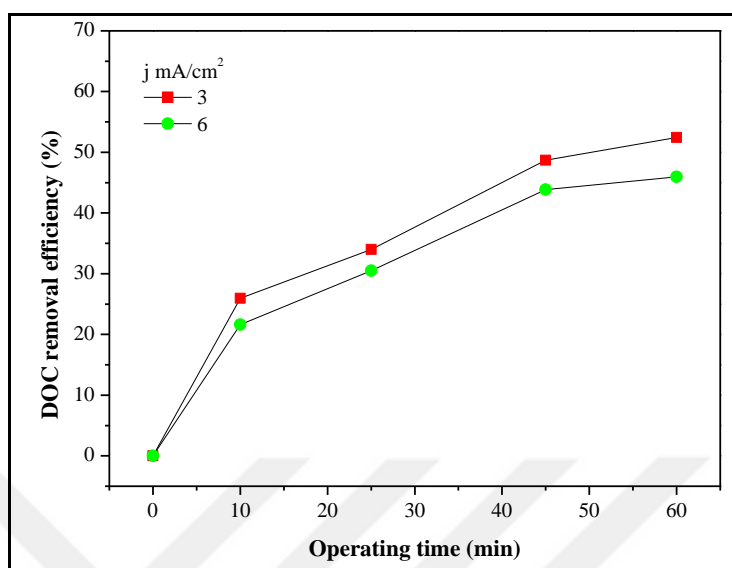
Figure 4.42: The effect of current density on DOC removal efficiency during EC process with hybrid electrode (pH$_i$=7.60).

As it is seen in Figure 4.43, The UV$_{254}$ reduction was obtained 68.4% (0.043 cm^{-1}) and 62.5% (0.051 cm^{-1}) at 3 mA/cm^2 and 6 mA/cm^2, respectively. The SUVA values decreased from 2.05 to 1.37 and 1.43 for at 3 mA/cm^2 and 6 mA/cm^2, respectively. The maximum DOC and UV$_{254}$ reduction was obtained by hybrid electrodes at the lower current density. At this current density, color reduction was 76.4%.
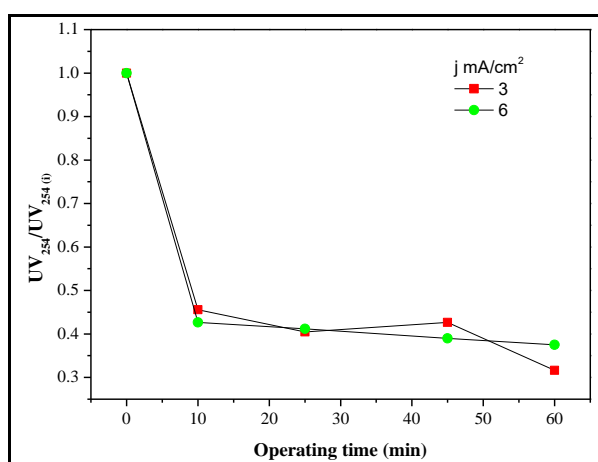
Figure 4.43: The effect of current density on UV$_{254}$ reduction during the EC process with Hybrid electrode (pH$_i$=7.60).

The Figure 4.44 shows the effect of pH_i on removal efficiency of NOM was investigated in terms of the reduction in DOC removal at 6 mA/cm^2 using Fe electrode. Figure 4.44.b) shows Fe dosage was 487.52 for all pHs, at 60 min. The pH_i 4 and 8 was studied for aquatic NOM, as well as, original pH of raw water, as it is seen in Figure 4.44. The original pH of sample was the best condition for effective removal of NOM with 60.5% ($DOC_{effluent}$=2.61 mg/L) and the removed mg NOM per Fe dosage (g) was 8.2. At alkaline pH, the removal efficiency of DOC was 51.4% ($DOC_{effluent}$= 3.22 mg/L). At acidic conditions, while the removal efficiency DOC was 45.4% ($DOC_{effluent}$= 3.61 mg/L), during the operating time the reduction in DOC appeared similar with pH_i 8. q_t was calculated as 6.1 and 6.9 mg/g (Table 4.5).
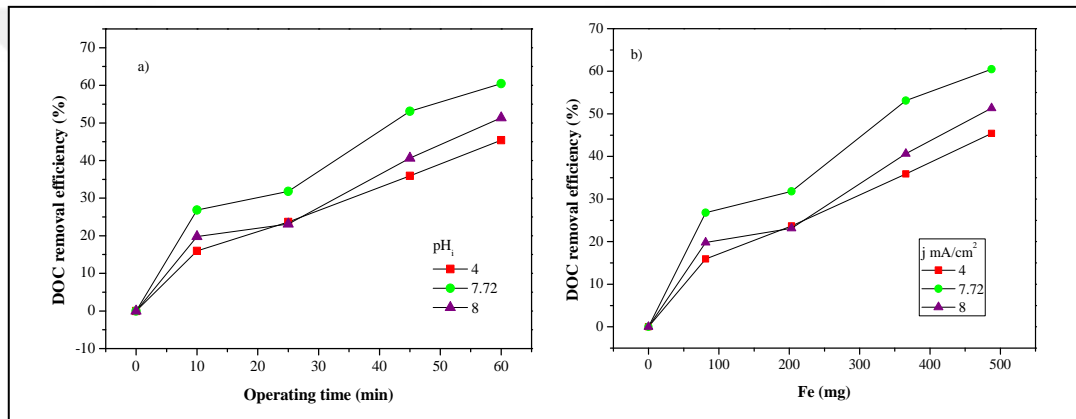
Figure 4.44: The effect of pH_i on DOC removal efficiency with a) operating time, b) the amount of coagulant generated (Fe electrode, pH_i=7.72).

Table 4.5: The effect of pH_i on removal of LTW by Fe electrodes, t_{EC}=60 min, j=6 mA/cm^2.

Electrode type	pH	q (C/L)	ELC (mg)	q_t, Removed mg NOM/C	q_t, Removed mg NOM/g Fe
Fe	4	1296	487.52	0.0023	6.1
Fe	7.72	1296	487.52	0.0031	8.2
Fe	8	1296	487.52	0.0026	6.9

Table 4.6: The effect of current density on removal of LTW by Al and Fe electrodes, t_{EC}=60 min, pH_i=7.76 for Al and pH_i=7.72 for Fe.

Electrode type	j_i mA/cm^2	q (C/L)	ELC (mg)	q_t, Removed mg NOM/C	q_t, Removed mg NOM/g Al or Fe
Al	3	648	78.58	0.0041	33.8
Al	6	1296	157.15	0.0026	21.0
Fe	3	648	243.76	0.0041	10.8
Fe	6	1296	487.52	0.0031	8.2

It can be seen in Figure 4.45, the effect of different electrodes on removal of DOC. The investigation was conducted at optimum current density 6 mA/cm^2 for Al and Fe, and 3 mA/cm^2 for hybrid, at original pH of raw water. Fe and hybrid electrodes obtained the best short term DOC reduction performance with almost 20% DOC removal at 10 min. The hybrid and Al electrodes could be achieved 52.4% and 50.2% DOC reduction at 60 min. The maximum DOC reduction was 60.5% with residual DOC concentration of 2.61 mg/L by Fe electrode.
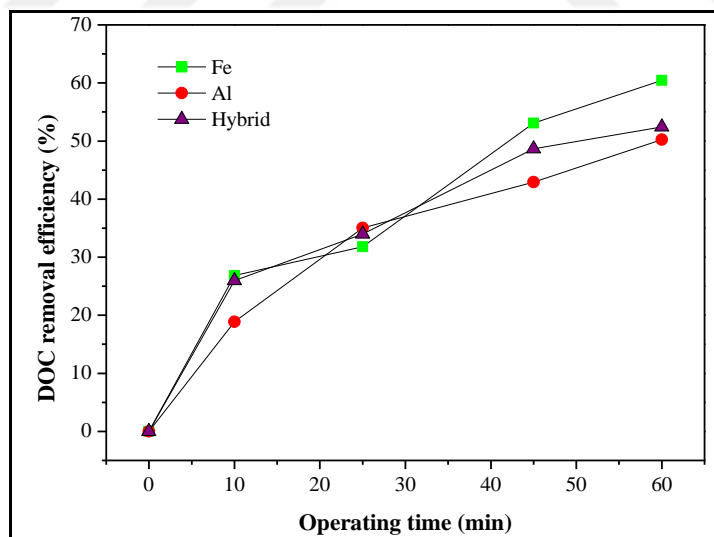
Figure 4.45: The effect of electrode types on removal efficiency of DOC during the EC process at optimum conditions.

4.2. The Investigation of Removal Mechanism of HS and Natural Organic Matter during EC Process by Zeta Potential and Floc Size Measurements

In order to understand the removal mechanism and improve the removal efficiency of NOM, the zeta potential, and floc formation in electrocoagulation process were investigated under determined optimum conditions for CHA, LSW and LTW.

4.2.1. Effect of Initial pH on Zeta Potential and Floc Size for CHA

As a result of the humic acid structure, electrostatic repulsions between negatively charged sites with the nearby compounds cause stretching of the molecule. Ghosh and Schnitzer [Ghosh and Schniter, 1980], in 1980, also reported that humic molecules show a large, flexible and linear shape, with low ionic strength and low humic concentration at high pH; and it can cause a change by reducing the pH to a small, rigid and spherocolloidal conformation, with high ionic strength and high humic concentration. For this reason, initial UV absorbance values at 254 nm are different for different initial pH 3, 4, 5, 6 and 8, as given in above for $UV_{254(i)}$ of samples.

The results show that the initial pH value of solution had a significant effect on the zeta potential and floc formation (Figure 4.46-4.49) As it is seen in Figure 4.46 and 4.47, zeta potential increased gradually during the process for all applied pH_i with Al electrodes at current density 1.2 mA/cm^2. The larger flocs and higher zeta potential values were observed at pH_i 4 rather than pH_i 5, 6 and 8. This difference may result from the lower solubility of humic acid. Humic acid was less hydrophilic at lower pH [Cheng et al., 2002]. Therefore, it was easier to make HA destabilization and precipitation. The other reason for this, aluminum species has a more positive charge at low pH when they were formed in acidic initial pH due to lack of hydrolysis and Al existed in the form of positively charged species.

At pH 5 aluminum mononuclear $AlOH^{2+,}$ $Al(OH)_2^+$ species govern the solution, as well as Al^{3+}. The pH rise to almost 5.5 conditions become favorable for aluminum hydroxide ($Al(OH)_3$) precipitation [Harif and Adin, 2007]. The maximum DOC

removal was obtained at acidic condition. At acidic pH_i, small precipitates were occurred associated with adsorption to produce charge neutralization which was verified by zeta potential. As it is seen in Figure 4.46, Zeta potential was 0 mV at time 20 min, when the pH reached the pH of 5.22. It shows that the alum-humic flocs are neutral at this point. The pH_i 4 rised to 6.3 and at current density of 1.2 mA/cm^2 (Figure 4.46) and charge reversal occurred at 25 min with +1.74 mV. At pH_i 5 was closed to -10 mV while reaching the pH value 7.8. These results showed that the stability of colloidal was destroyed. Strong coagulation-flocculation and incipient instability was occurred according to D4187-82 ASTM Zeta Potential of Colloids in Water and Wastewater at pH_i 4 and 5. While zeta potential was getting less negative (close to 0 mV) value with acidic initial pH values, the removal efficiency of DOC and UV_{254} increased (Figure 4.1, 4.2).

It could be indicated that charge neutralization was the dominated mechanism under acidic condition. When zeta potential approached the isoelectric point, a diminished electrostatic repulsive barrier took place. Zeta potential was more negative at pH_i 8 and 6 (Figure 4.47). The pH_i 6 and 8 reached the pH 7.9 and 9.7, respectively, the end of the process. The implication is that adsorption on a hydroxide precipitation is responsible for the removal at this pH [Duan and Gregory, 2003]. DOC reduction was 72.7% and 59.5%, at pH_i 6 and 8, respectively. These removal efficiencies were lower compared to DOC reduction at pH_i 4 and 5. Aluminium existed predominantly as hydroxides and easily settleable or filterable flocs were formed and therefore, residual aluminum did not have a significant effect on the zeta potential at pH_i 6 and 8 (Figure 4.47).

It can be concluded that, the removal of pollutant is due to sweeping and entrapment at higher pH. If a sufficient quantity of metal dissolved, large amounts of metal hydroxide floc would occur. This metal hydroxide floc goes towards large floc particles which is settleable. When floc particles settle, they sweep the colloidal particles. On the other hand, the increase in pH after an EC process time results in changes in the charge of humic matter and Al metal species. The charge of humic acid gets more negative while the protations reaction (Eq. 2.1; 2.2; 2.3) shift right side.

The removal mechanism goes to adsorption. It can be concluded that decrease in adsorption capacity was observed due to changes in functional groups of humic acid, as well as formed coagulant species. The ZP was observed more negative.
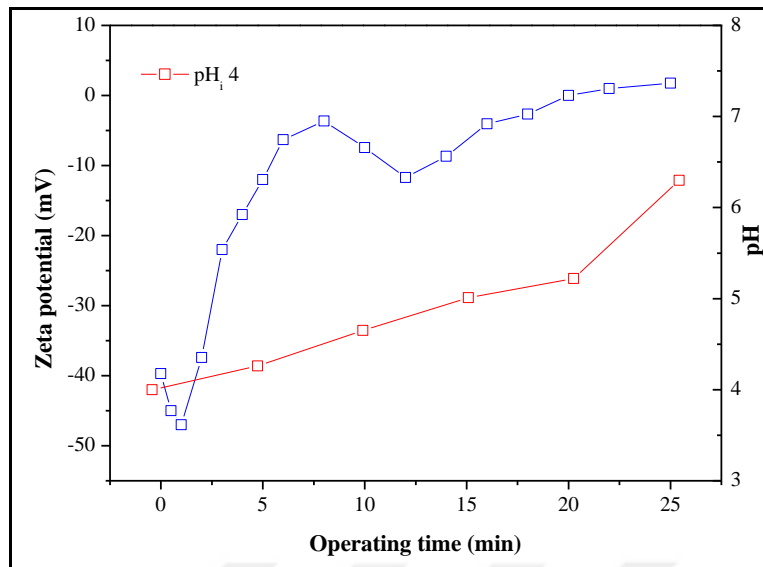
Figure 4.46: Change in zeta potential and pH_i during EC process at pH_i, j=1.2 mA/cm^2 with Al electrode.
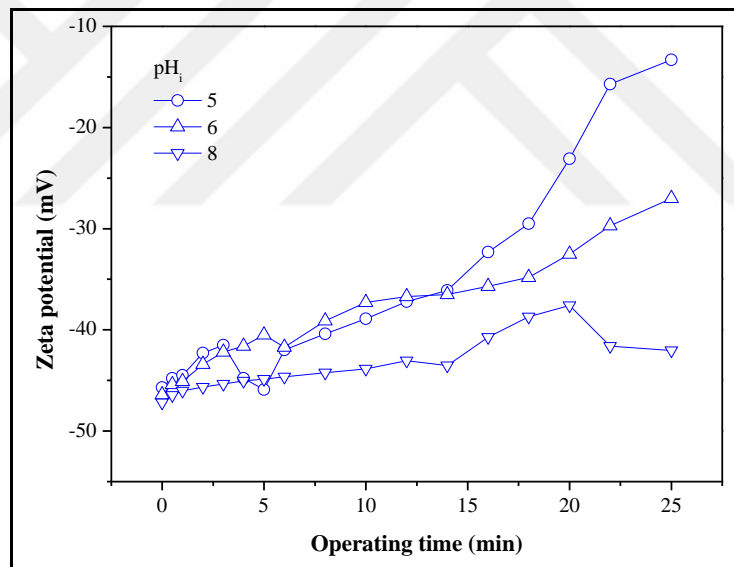
Figure 4.47: Zeta potential during EC process at different pH_i at j=1.2 mA/cm^2 with Al electrode.

Figure 4.48 shows the floc growth profiles at 1.2 mA/cm^2 and different initial pHs (4, 5, 6, 8) by Al electrode. Flocculation consists of the aggregation of coagulated particles and/or precipitate precursors in flocs. Successful inter-particle aggregation will depend on the destabilization degree attained in the coagulation phase (the extent of a repulsive force barrier existing between the particles), and on the collision rate between particles [Harif et al., 2012]. As it is seen in Figure 4.48, at

initial pH 4, floc growth rate was faster compared to pH 5, 6, and 8. At pH_i 5, 6, and 8 floc formation did not take place before almost 14 min. At these pHs, stable phase was longer compared to pH_i 4. At low pH cationic mononuclear species such as Al^{3+} and $Al(OH)_2^+$ govern the solution and at suitable pH values occur firstly $Al(OH)_3$ and subsequently $Al_n(OH)^{2+}$ polymerization [Holt et al., 2002].

It was required more operating time at high pH_i. At pH_i 4, the upward period indicating high collision efficiency at the early stages (Figure 4.48). It can be concluded that a diminished electrostatic repulsive barrier results in a rapid growth rate. Reduction of repulsive forces between particles results from change in ZP, as it is seen in Figure 4.46. When the process reached almost 7 min, zeta potential approached isoelectricpoint (IEP) and floc size reached above 4000 nm for pH_i 4. While pH was increasing, ambient conditions became favorable for $Al(OH)_3$ precipitation, approached sweep coagulation. But a major amount of humic matter have been removed by charge neutralization at initial stage, and therefore, caused an increasing in floc growth at later stage. Also transition into floc breakage can result from shear forces which limited evolution into a larger floc [Harif et al., 2012], [Slavik et al., 2012]. Operating time is important for the aggregation and aggregate breakage of colloidal. The floc size evolution does not depend on only solution chemistry but also on specific flocculation conditions (shear and time).
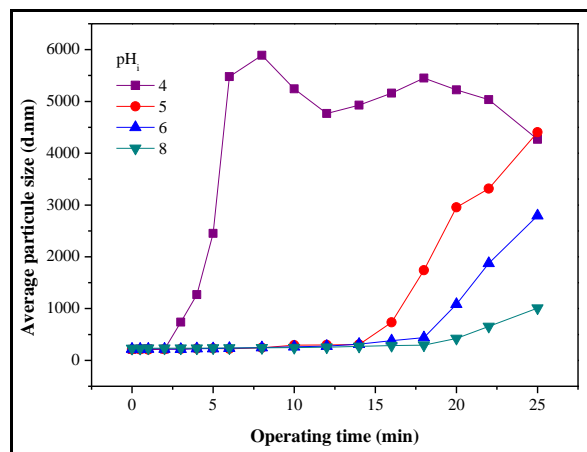
Figure 4.48: Particle size growth during the EC process at different pHi, j=1.2 mA/cm^2 with Al electrode.

Figure 4.49 shows the effect of pH on zeta potential and floc size-growth rate was observed during electrolysis with Fe electrode at 3 mA/cm^2. The zeta potential remained negative over the whole pH range, but approached zero at pH_i 3 and pH_i 4

(Figure 4.49.a). At pH_i 4 and current density of 3 mA/cm^2, zeta potential value was -4.1 mV that indicate strong coagulation-flocculation according to D4187-82 ASTM Zeta Potential of Colloids in Water and Wastewater. The maximum floc formation that was 3270 nm occurred at pH_i 4 (Figure 4.49.a). It can be concluded that the removal efficiency was max at pH_i 4 compared to the other pH values. At pH 4, positively charged monomeric iron species occur and this species provides charge neutralization on negatively charged humic substance colloids. The floc size decreased after it reached the max value at pH 4 this was because of sedimentation of occurred Fe(III)-HS particles but iron species continued to produce during the process. Also, the sheer stress can limit floc growth. At pH_i 5, the very negative zeta potential indicates that the solution was at moderate force stability according to D4187-82 ASTM Zeta Potential of Colloids in Water and Wastewater. Also high repulsive electrostatic barrier existed in solution reflected by the very negative zeta potential. The charge neutralization was not dominant coagulation mechanism. The anionic Fe complexes result in more negative ZP value.
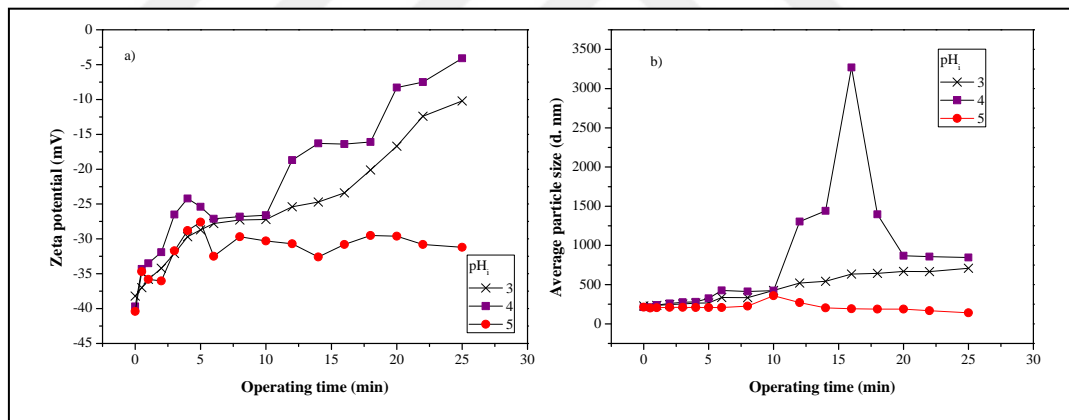
Figure 4.49: a) Zeta potential, b) particle size growth during the EC process at different pH_i, j=3 mA/cm^2 with Fe electrode.

4.2.2. Effect of Initial pH on Zeta Potential and Floc Size for Aquatic NOM

The firstly, effect of initial pH on floc size and zeta potential was investigated for Lake Saimaa Water. Figure 4.50 shows the change in zeta potential and pH_i 4, 5 and 7.3 (the original pH of water) with Al electrodes at 3 mA/cm^2, during EC process, for LSW.

The zeta potential of the water was -17.9, -18.5 and -19.5 at the initial pH 4, 5 and 7.3, respectively. As it is seen in Figure 4.50, the initial pH and changes in pH during EC process affects the zeta potential and floc growth. The final pH of solution was 7.3, 7.7 and 8.3 for pH_i 4, 5 and 7.3, respectively. The changes in the chemical conditions (pH conditions) of dispersion media can be contributed to the formation of the different aluminum and iron hydroxide polymers, changes in the charge and solubility of humic substances. The reactions (Eq. 2.1; 2.2; 2.3) mentioned above shift to the right and colloids are negatively charged with increase in pH during EC process. Functional groups of humic substances react with the positively charged metal species. When the pH is at the IEP, the particle is neutral. Under this light, rapid coagulation or flocculation occurred and reached IEP in EC process via Al electrodes for all pH values as it is seen in Figure 4.50. Also, the charge reversal was observed as 0.37 mV, 2.34 mV, and 1.23 mV, at pH 5.06, 6.24 and 8.08 for pH_i 4, 5 and 7.3, at different electrolysis time during process, respectively. At acidic condition, the rate of degradation of stability of the colloidal was fast. As it is seen in Figure 4.19.a) and 4.20, the maximum removal efficiency both DOC and UV_{254} was obtained at pH_i 4. It could be indicated that charge neutralization was the dominated mechanism under acidic condition. The effect of coagulation of the negative polymeric mononuclear Al species on removal of humic matter can negligible the through the end of the process. Because formed $Al(OH)_3$ flocs have already achieved the more positive ZP. In acidic conditions, less coagulant was required due to less negative charge of humic acid for destabilization. It can be a reason for high rate of removal.
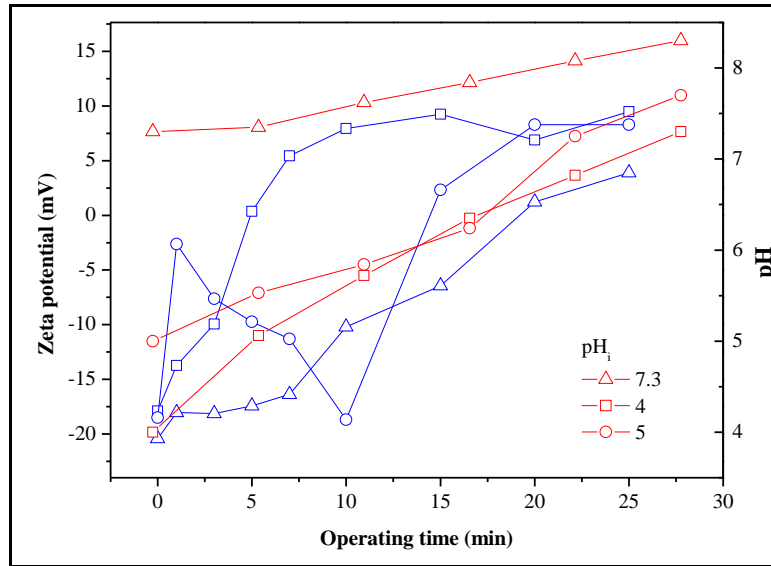
Figure 4.50: Change in zeta potential (blue line) and pH_i (red line) at different pH_i during EC process time at j=3 mA/cm^2 with Al electrode.
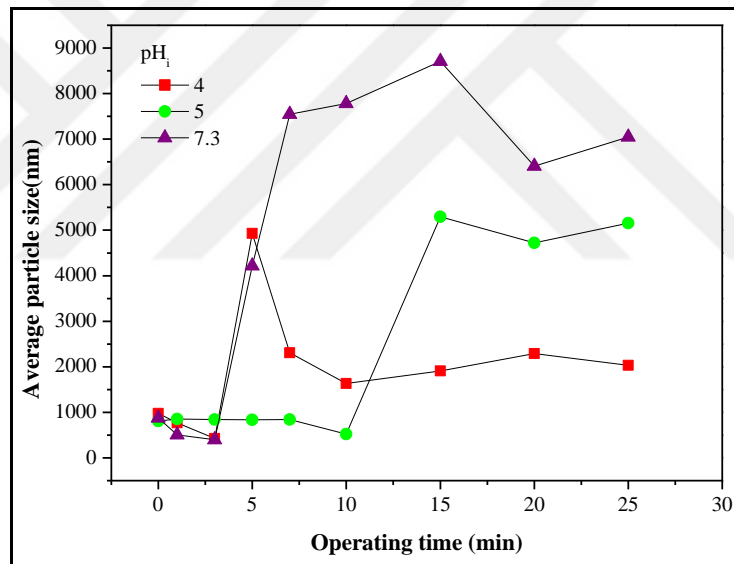
Figure 4.51: Change in growth of particle size at different pH_i during EC process time at j=3 mA/cm^2 with Al electrode.

As it is seen in Figure 4.52, the zeta potential of the water was -17.9, -18.5 and -19.3 and –16.2 at pH_i 4, 5 and 7.3, and 8, respectively.

Figure 4.52 shows, when iron electrodes used in EC process, zeta potential did not reach IEP at any pH values, at current density 3 mA/cm^2. However, rapid coagulation or flocculation occurred at pH 6.63 with zeta potential was -3.38 mV, at pH_i 4, after 25 min electrolysis time. At pH_i 5, the ZP was closed to IEP with final pH 5.83. It can be concluded that by a less negative zeta potential value shows

electrostatic repulsive barrier is enough lowered and Fe(OH)$_3$ precursor mass production in suffice at the pH$_i$ 5. The maximum DOC and UV$_{254}$ reduction was obtained pH$_i$ 4 and 5 by Fe electrode at 15 min. The final pH of solution was 7.3 and 7.5 for pH$_i$ 7.3 and 8, respectively, with Fe electrodes. At these high initial pHs, zeta potentials ranged from -10 to -20 which show incipient instability. At higher pH values, ZP results showed that charge neutralization was not the dominant coagulation mechanism for NOM removal by Fe electrode. As it is seen in Figure 4.62, at pH$_i$ 7.3 and 8, after a less increment of ZP value at initial stage, ZP dropped until almost 5 min. A small part of produced Fe^{2+} ions could react with HA but it was not enough in reducing the electrostatic barrier. The excess amount of OH$^-$ ions occur and remainder Fe^{2+} formed negatively charged Fe(OH)$_3$ species and Fe(OH)$^{4-}$ ions, which gave weak charge neutralization in alkaline conditions. At alkaline conditions, the removal efficiency of DOC was lower than acidic conditions at 15 min (Figure 4.22.a).
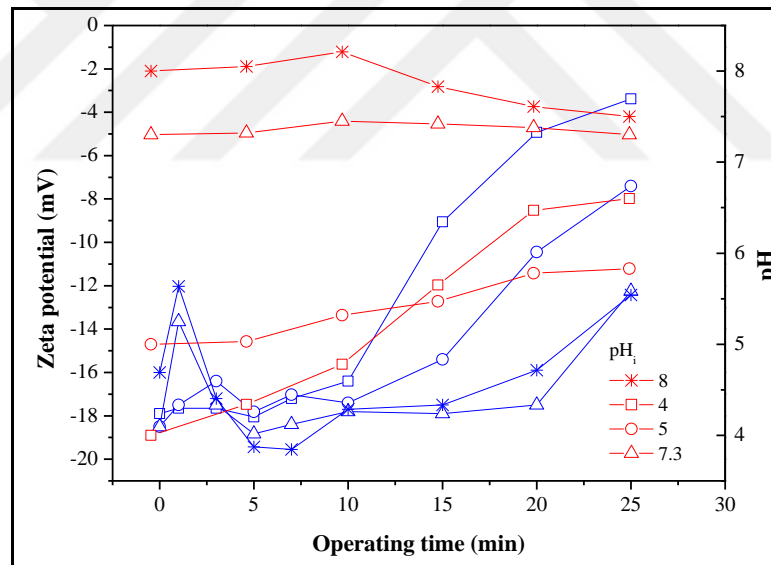
Figure 4.52: Change in zeta potential (blue line) and pH$_i$ (red line) at different pH$_i$ during EC process time at j=3 mA/cm^2 with Fe electrode.
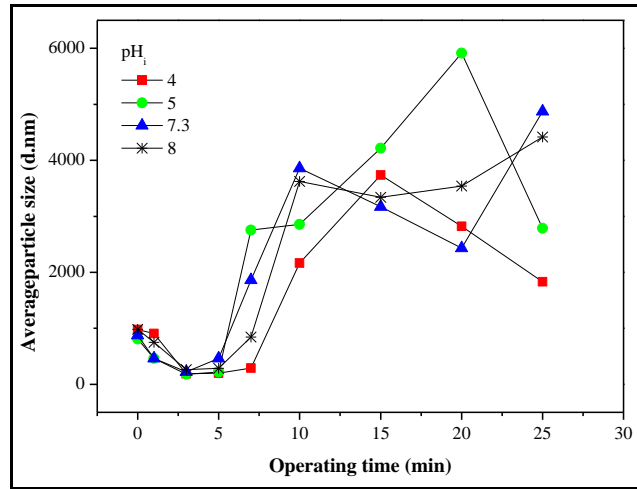
Figure 4.53: Changes in growth of particle size at different pH_i during EC process time at $j=3$ mA/cm^2 with Fe electrode.

As it is seen in Figure 4.54.a), when hybrid electrode configuration was used, different initial pH_s showed different zeta potential trend. Firstly, it can be said that rapid coagulation/flocculation observed at pH_i 4 in only 5 min while it was provided with Fe electrode after 25 min. The maximum DOC and UV_{254} reduction was obtained at pH_i 4. At further operating time, (10 min), the charge reversal was observed in hybrid system at all studied pH_i values (7.86 mV, 2.73 mV, and 0.34 mV for pH_i = 4, 7.3, 8, with pH_f= 8.2, 8.5, 8.9 respectively) which it was not observed by using Fe electrode. But the zeta potential showed more negative value with hybrid electrode as Fe electrode, after an increment in ZP, at pH_i 7.3 and 8.

a)   b)
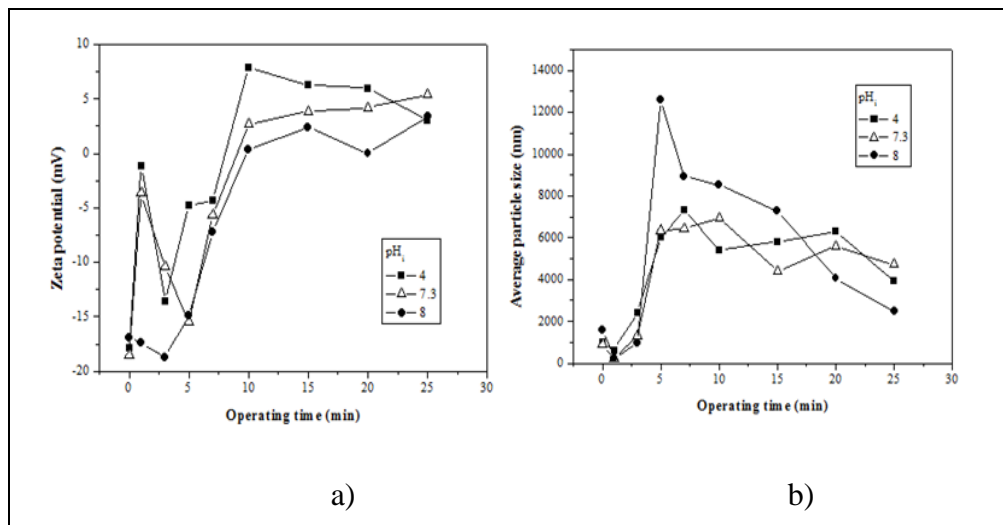
Figure 4.54: a) Change in zeta potential, b) particle size growth during EC process time at different pH at $j = 3$ mA cm^{-2} with hybrid electrode.

The floc size growth rate in the EC process for Al, Fe, and hybrid electrode was shown in Figure 4.51, 4.53, and 4.54.b), respectively. The maximum floc size was 4930 nm at the electrolysis time of 5 min when charge reversal was observed (mentioned above), at pH_i 4 by Al electrode (Figure 4.51). After this time, floc size was diminished. It can be concluded that positively charged Al species can be effective by adsorption to produce charge neutralization on negative charge of humic substance colloids at initial reaction time. Humic substances in the media decreased as the short term removal efficiency at pH_i 4 was better than other pH values and coagulation process by hydrolyzed Al (III) species would be expected to exhibit restabilization by overdosing. Under certain conditions, as the process was destabilized and aggregated, the floc size can be decreased by overdosing (restabilization) due to sedimentation of occurred Me(III)–HS particles. At pH 5 and 7.3, the floc size of colloids was larger during further operating time in contrast to pH_i 4 (Fig. 4.51). This is due to occurrence of different Al (III) species with the change of pH (see Figure 2.16). High dosages of counterions were necessary for reaching IEP and better removal of humic substance. DOC reduction slowly increased at pH 5 and 7.3 compared to at pH 4.

As it is seen in Figure 4.53, the floc size showed acceleration trend by Fe electrode during EC process. At pH_i 4 and 5 the floc size was reduced after 15 and 20 min operating time, respectively. The maximum floc size was 5915 nm at pH_i 5.

Floc size reached 12602 nm as max value in only 5 min at pH 8 for the hybrid system (Fig 4.54.b). Also, at pH 4, floc size was measured as 7324 nm at 7 min while it was 6931 nm at 10 min at its original pH. The decrease of floc size was observed also for the hybrid electrodes after reaching the max value.

The changes in pH did not directly affect growth of particle size. There was not a certain outcome about growth rate of particle size at acidic or alkaline conditions. The breakage of flocs was observed at all pH values with all electrodes.

The second studied aquatic water was LTW at optimum conditions. The Figure 4.55 shows the changes in ZP and pH_i during EC process at different pH_i by using Fe electrode. At the pH_i 4, 7.7 and 8, the ZP_i was -8.34, -8.71, -6.45, respectively, of the samples of LTW. The pH_i 4 increased until 45 min. It reached pH 7.01. The ZP was indicated that incipient instability until 10 min. At 10 min, ZP value was -5.0 and pH value 6.45. At 25 min, the ZP was observed as -4.87 at pH 6.83.

While the original pH 7.7 and pH_i 8 of sample showed slowly an increment, the ZP value was more negative compared to ZP_i. The excess amount of OH^- ions can be present in solution. The IEP was not observed at any pH during EC process at high pH values. As it is seen in section 4.1.3.2, the DOC reduction was limited even optimum conditions. At the pH_i 4, the dominate mechanism can be charge neutralization but it was not obtained effective NOM removal. At this pH_i, the formed positive mononuclear species such as $AlOH^{2+}$ were not enough for lowered electrostatic repulsive barrier. In high alkaline conditions, the adsorption capacity of the form of negatively charged $Fe(OH)_3$ flocs and $Fe(OH)_4^-$ ions has poor coagulation performance. The initial ZP of raw water was high (low negative). The adsorption to produce charge neutralization or double layer compression could not effectively destroy the low stability of colloidal. Sweep coagulation of organic matters by occurred polymeric-complex Fe species may increase removal of DOC.
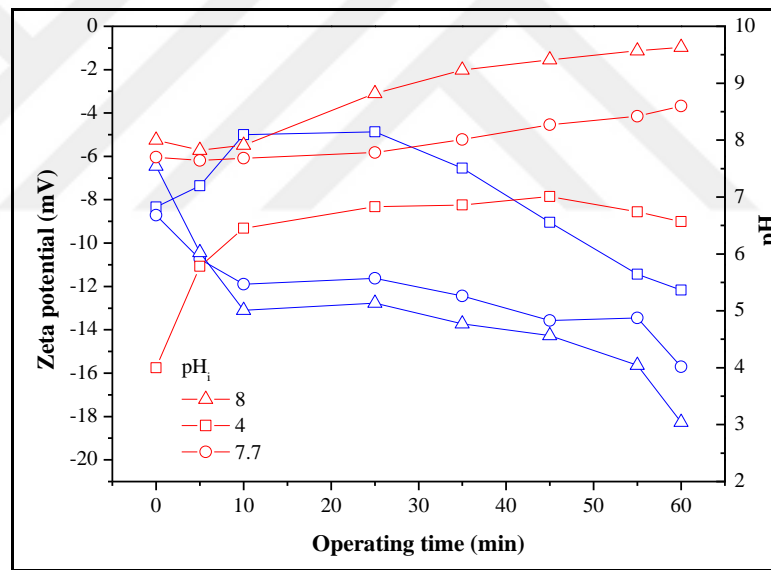
Figure 4.55: Changes in zeta potential (blue line) and pH_i (red line) at different pH_i during EC process time at j=6 mA/cm^2 with Fe electrode.

Figure 4.56 shows the highest growth rate floc formation was observed at pH_i 8. The breakage and re-growth of flocs was observed at all pH_i.
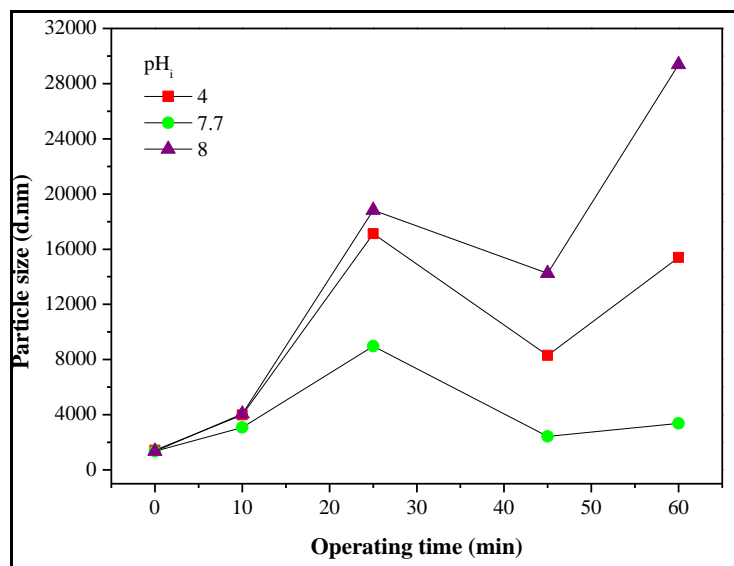
Figure 4.56: Changes in growth of particle size at different pH_i during EC process time at j=6 mA/cm^2 with Fe electrode.

4.3. The Determination of Characterization of Lake Terkos Before and After EC Process by HPSEC Method

The distribution of MW of raw samples LTW and treated water samples of LTW by EC process at different operating time were determined by HPSEC analysis. RID and DAD was used. Figure 4.57, shows the raw water had three different MW of DOC. After 25 min electrolysis time, the high MW of raw water obviously reduced. The decreasing in response of RID was observed after 45 min, while MW reduction was not so much. After 60 min electrolysis, the response of RID was not almost changed, as MW. The higher MW was $3.3*10^5$ Da in the effluent water, while the highest MW was $8.8*10^5$ Da of raw water. As it is seen Figure 4.58, the raw water had three peak that shows aromatic structure of organic matter. After the end of the process, all peaks reduced. Initial 25 min of electrolysis showed faster removal of aromatic structure.
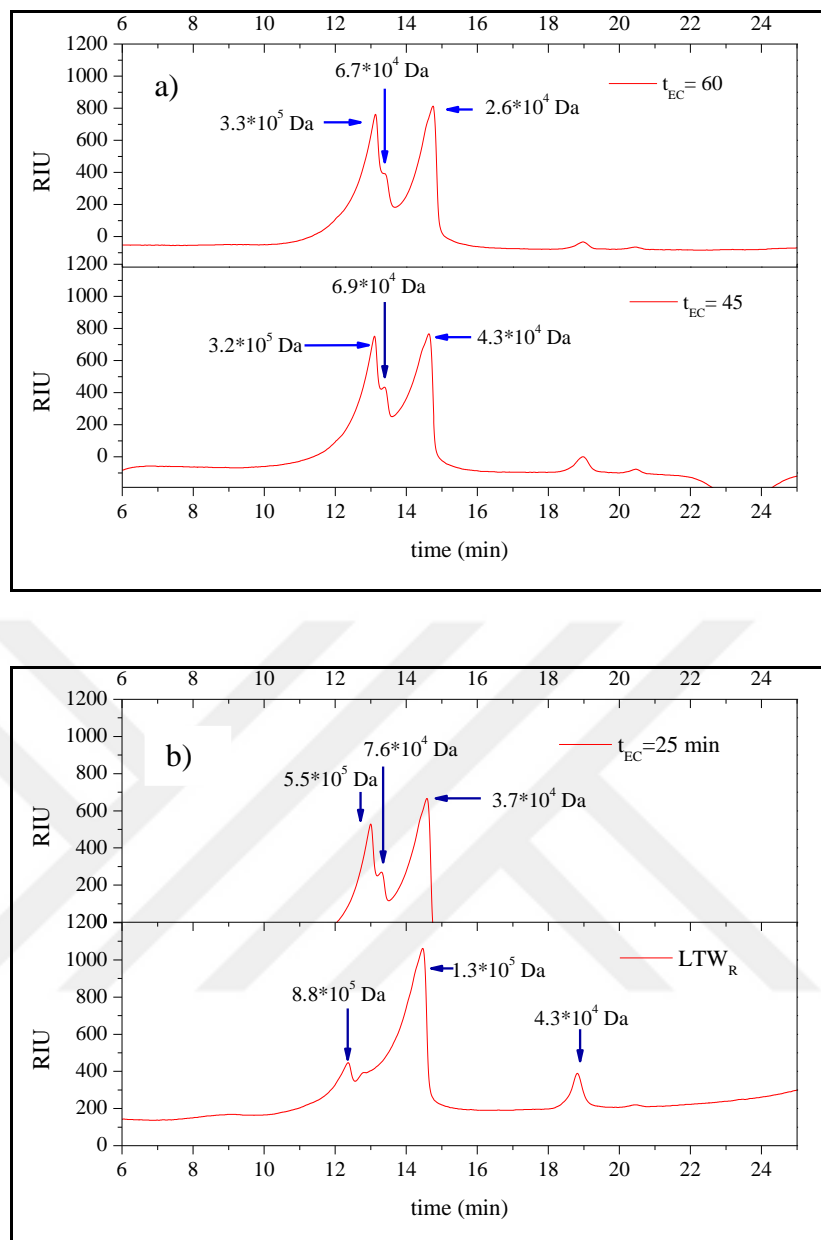
Figure 4.57: RID chromatography of NOM at different operating time in EC process.. at a) t_{EC}=60, t_{EC}=45, b) t_{EC} 25, LTW$_R$ (Fe electrode, pH = 7.72, j=6 mA/cm^2)
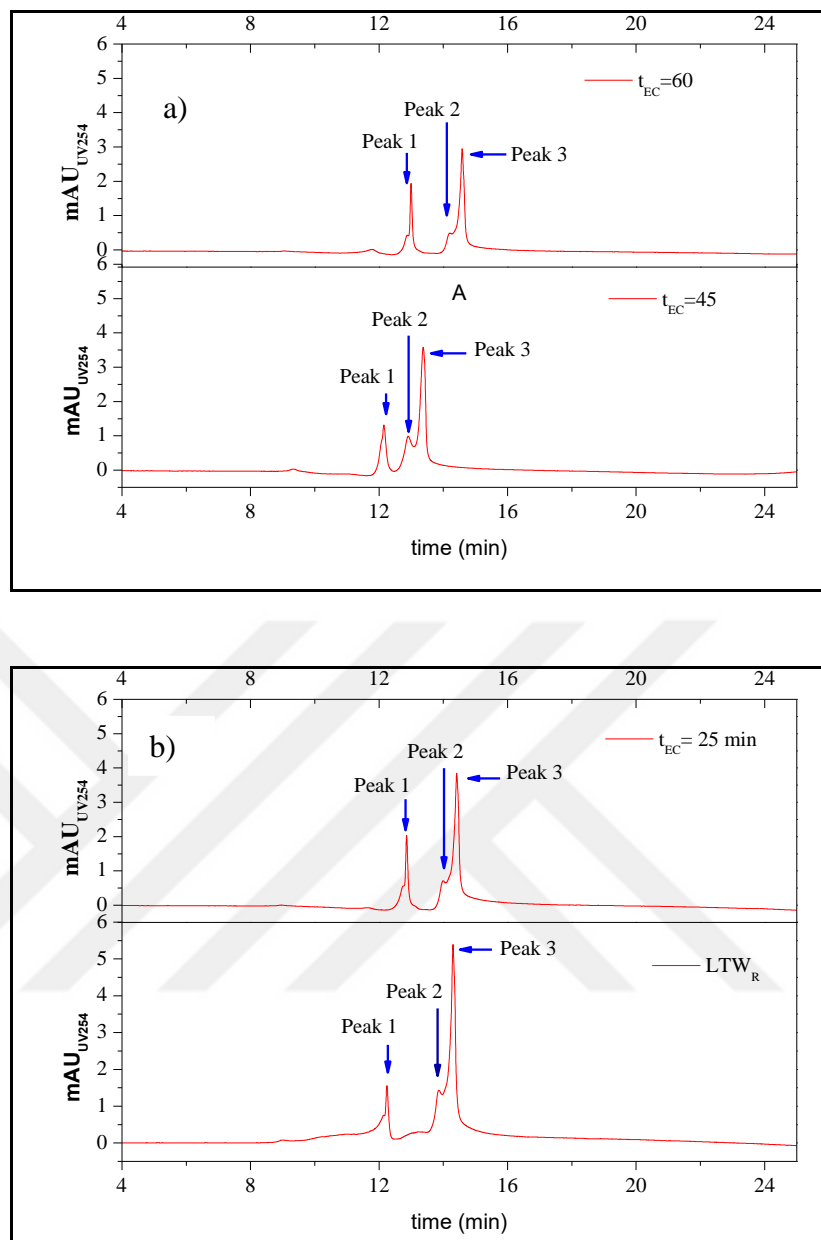
Figure 4.58: DAD (UV$_{254nm}$) chromatography of NOM at different operating time in EC process. at a) t_{EC}=60, t_{EC}=45, b) t_{EC} 25, LTW$_R$, (Fe electrode, pH = 7.72, j=6 mA/cm^2).

Figure 4.59 shows initial distribution of MW of organic matter and fraction of MW in effluent water samples. The response of RID reduced for all different MW after 25 min. A major MW reduction was not observed until 45 min electrolysis. The MW of NOM in effluent water was $1.1*10^5$ Da. The highest MW was $7.3*10^5$ Da of raw water. As it is seen in Figure 4.60, the aromatic fraction of water reduced effectively until 45 min electrolysis time. The first peak almost removed from water.
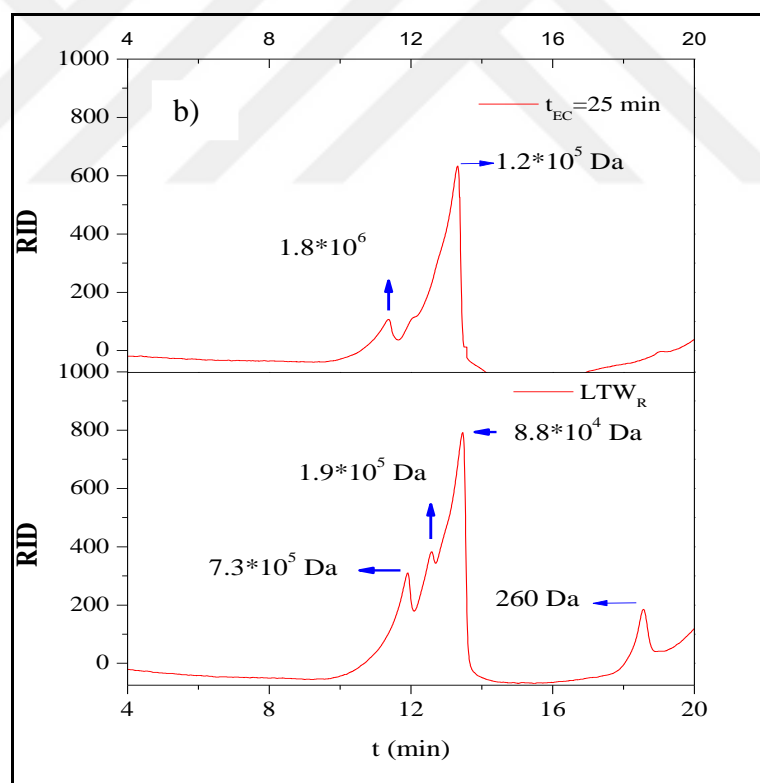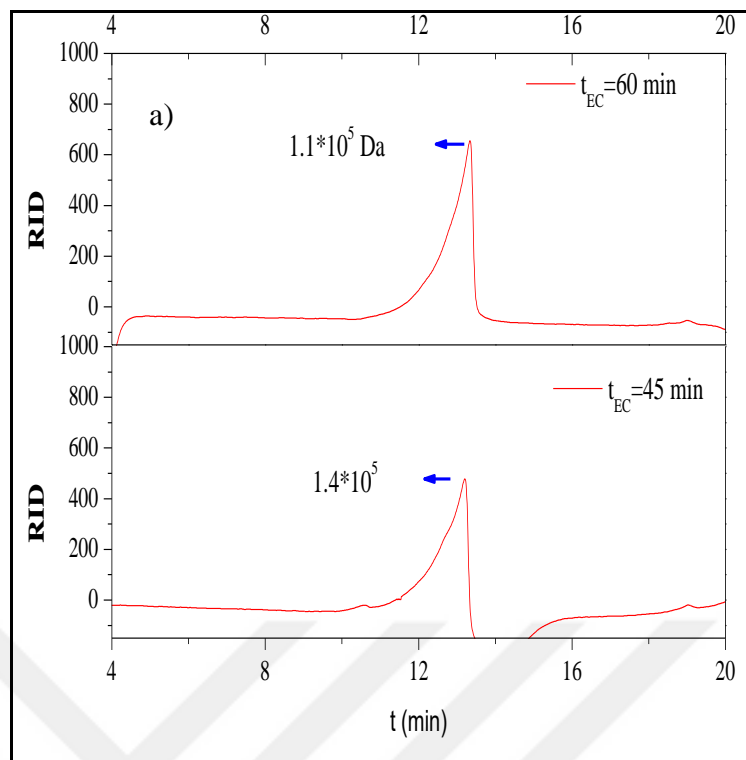
Figure 4.59: RID chromatography of NOM at different operating time in EC process. at a) t_{EC}=60, t_{EC}=45, b) t_{EC} 25, LTW$_R$ (hybrid electrode, pH = 7.72, j=3 mA/cm^2).
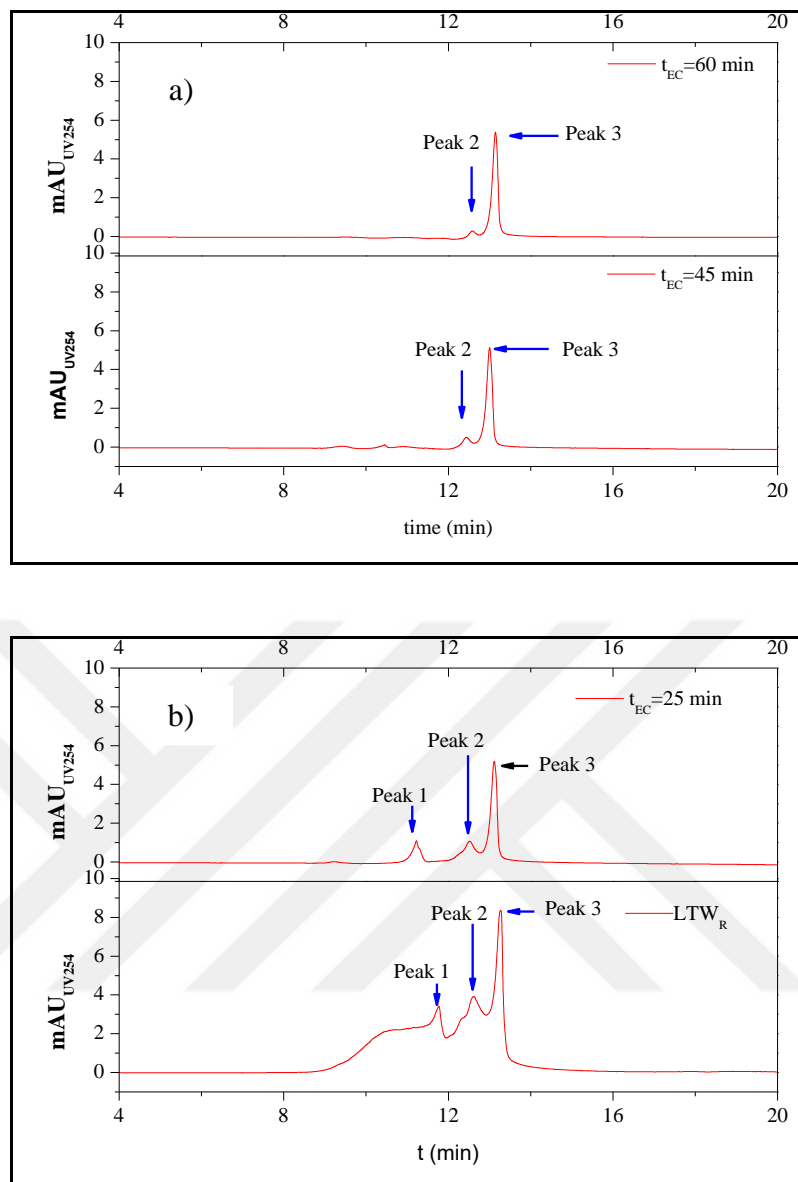
Figure 4.60: DAD (UV$_{254nm}$) chromatography of NOM at different operating time in EC process at a) t$_{EC}$=60, t$_{EC}$=45, b) t$_{EC}$ 25, LTW$_R$ (hybrid electrode, pH = 7.72, j=3 mA/cm^2).

5. CONCLUSIONS AND COMMENTS

This study represents the treatability and removal mechanisms of different humic matter sources by EC process using different anode electrodes (Table 5.1). CHA and SHA used as terrestrial humic matter, and Lake Saimaa and Terkos Water as natural organic matter in drinking water supplies.

Table 5.1: DOC and UV_{254} removal of different organic matter sources at optimum conditions by EC, t_{EC}=25 min. pH_i=4 and j=3 mA/cm^2 by Fe and 1.2 mA/cm^2 by Al; pH_i=5, j=3 mA/cm^2 by hybrid for HA ($UV_{254(i)}$= 1.1960 cm^{-1} at pH_i 5). pH_i=4 and j=3 mA/cm^2 by Fe, Al, and hybrid for SHA. pH_i=4 and j=3 mA/cm^2 by Fe, Al, and hybrid for LSW (at pH_i 4 $UV_{254(i)}$=0.3841 for LSW).

Effluent	Iron	Aluminium	Hybrid
HA			
$DOC_{treated}$ (mg/L)	2.29	2.02	4.33
DOC removal %	85.9	87.5	73.2
UV_{254} (cm^{-1})	0.026	0.017	0.0211
UV_{254} removal%	97.2	98.2	98.2
$SUVA_{treated}$ [L/(m mg)]			0.49
SHA			
$DOC_{treated}$ (mg/L)	2.90	2.52	5.85
DOC removal %	88.5	90.0	76.9
UV_{254} cm^{-1}	0.0559	0.0220	0.0121
UV_{254} removal%	96.4	98.7	99.3
$SUVA_{treated}$ [L/(m mg)]	1.93	0.87	0.21
Lake Saimaa			
$DOC_{treated}$ (mg/L)	5.97	4.29	4.66
DOC removal %	59.8	71.1	68.6
UV_{254} cm^{-1}	0.0310	0.0530	0.0348
UV_{254} removal%	91.9	86.2	90.9
$SUVA_{treated}$ [L/(m mg)]	0.52	1.24	0.75

Table 5.2: DOC and UV_{254} removal of aquatic NOMs at original pH of raw water (no pH adjustment) and at optimum conditions (t_{EC}=25 min, 3 j=mA/cm^2 by Al, Fe, and hybrid for LSW; t_{EC}=60 min; 6mA/cm^2 by Al, Fe, 3 mA/cm^2 by hybrid for LTW).

Effluent	Iron	Aluminium	Hybrid
Saimaa			
$DOC_{treated}$ (mg/L)	5.71	5.68	5.05
DOC removal %	61.6	61.7	66.0
UV_{254} cm^{-1}	0.0860	0.0771	0.0311
UV_{254} removal%	79.1	81.3	92.4
$SUVA_{treated}$ [L/(m mg)]	1.51	1.36	0.61
Terkos			
$DOC_{treated}$ (mg/L)	2.61	3.28	3.13
DOC removal %	60.5	50.2	52.4
UV_{254} cm^{-1}	0.0359	0.0342	0.0430
UV_{254} removal%	73.5	76.1	68.4
$SUVA_{treated}$ [L/(m mg)]	1.38	1.04	1.37

The results demonstrate that sufficient DOC, UV_{254} and VIS_{436} removal efficiency were obtained by EC process using Fe, Al and hybrid electrode especially humic matter removal from CHA and SHA. Lower pH values showed better removal rate of HA with both aluminum and iron electrode, but the higher current density was necessary when using iron electrode for providing efficient removal at a short time. At the end of the process, the best treatment efficiency of HA was obtained DOC removal of 87.5% ($DOC_{treated}$ 2.02 mg/L) with at pH_i 4 and at current density 1.2 mA/cm^2 by aluminum electrode for CHA. The maximum DOC removal efficiency was obtained at 15 min and 20 min with 89.2% and 79.5% for Fe and hybrid electrode, respectively. The removal efficiency of DOC was reduced and/or a stabile phase was observed in DOC reduction after a certain EC operating time.

The removal efficiency of natural aquatic NOMs was lower than CHA and SHA for all studied electrode. The LTW and LSW have different character, as initial DOC concentration and NOM structure. The LTW that has lowest initial DOC concertation and SUVA value was most resistant to treatment by EC process with DOC reduction 60.5%, 52.4%, 50.2% for Fe, hybrid and Al, respectively. The optimum current density was 6 mA/cm^2 for Fe, Al and current density 3 mA/cm^2 for hybrid electrode. The best color efficiency was obtained hybrid electrode with

76.4%. The Fe electrodes were most effective for NOM removal with $DOC_{treated}$ 2.61 mg/L.

The organic matter from LSW was removed 66.0%, 61.7%, 61.6%, and by hybrid, Al and Fe electrode, respectively, at the original pH of raw water, the end of the process. It is important that the effective treatment efficiency was obtained no pH adjustment. At pH_i 4, the removal efficiency was 71.1% ($DOC_{treated}$ 4.29 mg/L) with Al electrode. At pH_i 4, the removal efficiency was 68.6% ($DOC_{treated}$ 4.66 mg/L) with hybrid electrode. The best UV_{254} and color removal reduction was obtained by hybrid electrodes. The most effective removal of DOC was obtained by hybrid anodes, at original pH of LSW.

The results show that the initial pH and changes in pH during EC process effects the zeta potential and floc growth. When the ZP reached IEP, the removal of DOC and UV_{254} was increased for all humic matter sources. At high pH_i values, the ZP was more negative and the removal of humic matter was not so successful. According to zeta potential and particle size growth rate, it can be concluded that the removal mechanism of humic matter is based on dominantly charge neutralization and compression of double layer at lower initial pH value. The adsorption capacity of formed metal flocs is not so effective at alkaline conditions. The floc size evolution does not depend on only solution chemistry but also on specific flocculation conditions (shear and time).

When removal of CHA was studied, zeta potential values during the process indicated that rapid coagulation or flocculation occurred when Al and hybrid electrodes were used at pH 5.22. At pH_i 6 and 8, the ZP was more negative and floc formation did not observed until a certain time for Al. In case of use of Fe electrode, the zeta potential remained negative over the whole pH range and incipient instability was observed. The maximum floc size was observed when charged neutralization was occurred at pH_i 4. Afterwards, breakage of the flocs was observed.

At the treatment of LSW, rapid coagulation or flocculation occurred and ZP reached IEP in EC process via Al electrodes for all pH values for LSW at almost pH 5.06. The high pH values, negatively charged Fe species, which gave weak charge neutralization. The charge reversal was observed in hybrid system at all studied pH_i values with increasing in pH_i. The maximum floc size was observd when charge reversal was occured at pH_i 4 by Al electrode. After this time, floc size was

diminished. There was not a certain outcome effect of pH on growth rate of particle size. The breakage of flocs was observed at all pH values with all electrodes.

When LTW was treated, The ZP was indicated that incipient instability until 10 min by EC process using Fe electrode at almost pH 6.5. While the original pH 7.7 and pH_i 8 of sample, the ZP value was more negative compared to ZP_i. The adsorption to produce charge neutralization or double layer compression could not effectively destroy the low stability of colloidal.

The SUVA value of Lake Saimaa and Lake Terkos was higher than 2, meaning that the natural organic matter consisted mixture of hydrophobic and hydrophilic fraction, and had both low and high molecular weight (MW). SUVA values decreased to less than 2 L/ (m mg) for all electrode types in NOM source waters. HA and SHA had SUVA value higher than 4 that indicate dominant fraction of organic matter is hydrophobic moieties. Treated waters for all electrode types showed SUVA below 2 indicating the EC process is effective on removing high MW fractions of the NOM. Also, it is concluded that major part of hydrophobic fraction of dissolved organic carbon was removed. However, little fraction of hydrophilic moieties of NOM was removed from the bulk solution. Especially UV_{254} removal efficiency of aquatic NOM was higher than DOC removal, such as hybrid-SHA combination. Removal efficiency of UV_{254} was more than removal of DOM which is a proof that the aromatic removal was successful but lower molecular weight NOM was still in solution. The higher effluent SUVA value was observed using iron electrode used were likely due to the high UV_{254} of iron, rather than a difference at removal efficiency of hydrophobic or hydrophilic fraction of NOM in the treated solution. The hybrid electrodes reduce this effect of Fe electrode.

It can be concluded that the electrolysis time limits removal efficiency of humic matter. The color removal efficiency of aluminum and hybrid electrodes under optimum conditions was better than iron electrodes. The results indicate that DOC and color removal efficiency depends on initial pH of solution. The results show hybrid electrodes is effective for humic matter removal. This innovative design can be improved in further studies. The current density should be optimized.

Acidic conditions are optimum for humic matter removal by EC process. The humic matter removal efficiency can be increased at acidic conditions. At alkaline conditions, sweep-entrapment flocculation mechanisim would be increase with adding various polyelectrolyte. But, the formed sludge amount should be considered.

In the literature, the studies about the removal mechanism of organic matter by EC process and analysis of fraction of organic matter during treatment very limited. The HPSEC results show EC process successfully removes the hydrophobic fraction of organic matter. The low MW fraction of DOC could be reduced. The HPSEC results support the outcomes of SUVA.

It is known that the hydrophobic colloids are responsible for water coloration. The removal of hydrophobic fraction shows EC process remove color. Also, the formation of DBPs can decrease due to removal of hydrophobic moiety by EC process. At optimum conditions that obtained in this study, after EC treatment conventional disinfection process can applied. Afterwards, the effluent water of EC process and disinfection process can analyzed in terms of DBPs. The formation potential of DBPs could be verified by toxicity analysis.

REFERENCES

Adhoum N., Monser L., (2004), "Decolourization and removal of phenolic compounds from olive mill wastewater by electrocoagulation", Chemical Engineering and Processing: Process Intensification, 43(10), 1281-1287.

Aiken G., Cotsaris E., (1995), "Soil and Hydrology: their effect of NOM", J. AWWA, 87 (1), 36-45.

Akbal F., Camcı S., (2011), "Copper, chromium and nickel removal from metal plating wastewater by Electrocoagulation", Desalination, 269(1), 214-222.

Akşiyan F., Bekbölet M., Eroskay O., (1990), "Investigation of Chemical Physical and Ecological Balance of the Terkos Lake and Environmental", 88, Bosphorus University, Institute of Environmental Sciences.

Allpike B. P., Heitz A., Joll C. A., Kagi R. I., (2007), "A new organic carbon detector for size exclusion chromatography", Journal of Chromatogrography A., 1157, 472–476.

Ang W. L., Mohammad A. W., Teow Y. H., Benamor A., Hilal N., (2015), "Hybrid chitosan/$FeCl_3$ coagulation–membrane processes: Performance evaluation and membrane fouling study in removing natural organic matter", Separation and Purification Technology, 152, 23-31.

Anglada A., Urtiaga A., Ortiz I., (2009), "Contributions of electrochemical oxidation to wastewater treatment: fundamentals and review of applications", Journal of Chemical Technology and Biotechnology, 84(12), 1747-1755.

Asselin M., Drogui P., Benmoussa H., Blais J. F., (2008), "Effectiveness of electrocoagulation process in removing organic compounds from slaughterhouse wastewater using monopolar and bipolar electrolytic cells", Chemosphere, 72(11), 1727-1733.

Attour A., Touati M., Tlili M., Amor M. B., Lapicque F., Leclerc J. P., (2014), "Influence of operating parameters on phosphate removal from water by electrocoagulation using aluminum electrodes", Separation and Purification Technology, 123, 124-129.

Awang Z. B., Bashir M. J. K., Kutty S. R. M., Isa M. H., (2011), "Post-Treatment of Slaughterhouse Wastewater using Electrochemical Oxidation", Research Journal of Chemistry and Environment, 15(2), 229-237.

Bagga A., Chellam S., Clifford D. A., (2008), "Evaluation of iron chemical coagulation and electrocoagulation pretreatment for surface water microfiltration", Journal of Membrane Science, 309(1), 82-93.

Bayar S., Yıldız Y. Ş., Yılmaz A. E., İrdemez Ş., (2011), "The effect of stirring speed and current density on removal efficiency of poultry slaughterhouse wastewater by electrocoagulation method", Desalination, 280(1), 103-107.

Baker A., Tipping E., Thacker S. A., Gondar D., (2008), "Relating dissolved organic matter fluorescence and functional properties", Chemosphere, 73(11), 1765-1772.

Baki T., (1997), "Terkos Lake Water Quality Assessment", Master Thesis, Yıldız Technical University.

Baykal B. B., Tanik A., Gonenc I. E., (2000), "Water quality in drinking water reservoirs of a megacity", Istanbul. Environmental Management, 26(6), 607-614.

Bayramoglu M., Kobya M., Eyvaz M., Senturk E., (2006), "Technical and economic analysis of electrocoagulation for the treatment of poultry slaughterhouse wastewater", Separation and Purification Technology, 51(3), 404-408.

Belkacem M., Khodir M., Abdelkrim S., (2008), "Treatment characteristics of textile wastewater and removal of heavy metals using the electroflotation technique", Desalination, 228, 245-254.

Bellar T. A., Lichtenberg J. J., Kroner R. C., (1974), "The occurrence of organohalides in chlorinated drinking waters", Journal American Water Works Association, 703-706.

Bolto B., and Gregory J., (2007), "Organic polyelectrolytes in water treatment", Water Research., 41, 2301–2324.

Bond T., Goslan E. H., Parsons S. A., Jefferson B., (2010), "Disinfection by-product formation of natural organic matter surrogates and treatment by coagulation, MIEX® and nanofiltration", Water Research, 44(5), 1645-1653.

Budd G. C., Hess A. F., Shorney-Darby H., Neemann J. J., Spencer C. M., Bellamy J. D., Hargette P. H., (2004), "Coagulation applications for new treatment goals", Journal American Water Works Association, 102-113.

Buffle J., Greter F. L., Haerdi W., (1977), "Measurement of complexation properties of humic and fulvic acids in natural waters with lead and copper ion-selective electrodes", Analytical Chemistry, 49(2), 216-222.

Bukhari A. A., (2008), "Investigation of the electro-coagulation treatment process for the removal of total suspended solids and turbidity from municipal wastewater", Bioresource Technology, 99(5), 914–921.

Can O. T., Bayramoglu M., (2014), "A Comparative Study on the Structure–Performance Relationships of Chemically and Electrochemically Coagulated Al (OH)$_3$ Flocs", Industrial & Engineering Chemistry Research, 53(9), 3528-3538.

Can O. T., Kobya M., Demirbas E., Bayramoglu M,. (2006), "Treatment of the textile wastewater by combined electrocoagulation", Chemosphere, 62(2), 181-187.

Can O.T., Bayramoglu M., Kobya M., (2003), "Decolorization of reactive dye solutions by electrocoagulation using aluminium electrodes", Industrial Engineering Chemical Research, 42, 3391-3396.

Canizares P., Martinez F., Lobato J., Rodrigo M.A., (2006), "Electrochemically assisted coagulation of wastes polluted with Eriochrome Black T", Industrial Engineering Chemistry Research, 45 3474-3480.

Casqueira R.G., Torem M.L., Kohler H.M., (2006), "The removal of zinc from liquid streams by electroflotation", Minerals Engineering 19 (2006) 1388–1392.

Cathalifaud G., Ayele J., Mazet M., (1998), "Aluminium effect upon adsorption of natural fulvic acids onto PAC", Water Research, 32(8), 2325-2334.

Chen G., (2004), "Electrochemical technologies in wastewater treatment", Separation and Purification Technology, 38(1), 11-41.

Chen G., Chen X., Yue P.L., (2000), "Electrocoagulatıon and electroflotatıon of restaurant wastewater", Journal of Environmental Engineering, 126 (9) 858-863.

Chen X., Chen G., Yue P. L., (2000), "Separation of pollutants from restaurant wastewater by Electrocoagulation", Separation and Purification Technology, 19(1), 65-76.

Cheng W. P., (2002), "Comparison of hydrolysis/coagulation behavior of polymeric and monomeric iron coagulants in humic acid solution", Chemosphere, 47, 963-969.

Cheng W. P., Chi F. H., (2002), "A study of coagulation mechanisms of polyferric sulphate reacting with humic acid using a flourescence-quenching method", Water Research, 36, 4583-4591.

Chin Y. P., Aiken G., O'Loughlin E., (1994), "Molecular weight, polydispersity, and spectroscopic properties of aquatic humic substances", Environmental Science and Technology, 28(11), 1853-1858.

Chow C. W. K., Fabris R., Drikas M., (2004), "A rapid fractionation technique to characterise natural organic matter for the optimisation of water treatment processes", Aqua, 53, 85-92.

Chow C. W. K., Kuntke P., Fabris R., Drikas M., (2009a), "Organic characterization tools for distribution system management", Water Science Technology, 9 (1), 1–8,

Chow C. W. K., von Leeuwen J.A., Fabris R., Drikas M., (2009b), "Optimised coagulation using aluminium sulfate for the removal of dissolved organic carbon", Desalination, 245, 120–134.

Cornelissen A., Burnett M. G., McCall R. D., Goddard D. T., (1997), "The structure of hydrous flocs prepared by batch and continuous flow water treatment systems and obtained by optical, electron and atomic force microscopy", Water Science and Technology, 36(4), 41-48.

Coskun T., İlhan F., Demir N. M., Debik E., Kurt U., (2012), "Optimization of energy costs in the pretreatment of olive mill wastewaters by Electrocoagulation", Environmental Technology, 33(7), 801-807.

Croue J.P., Debroux J.F., Amy G.L., Aiken G.R., Leenher J.A., (1999), "Natural Organic matter: structural characteristic and reactive properties, In: P.C. Singer (Ed.) Formation and Control of Disinfection By-Products in Drinking Water, American Water Works Association.

Daneshvar N., Oladegaragoze A., Djafarzadeh N., (2006), "Decolorization of basic dye solutions by electrocoagulation: An investigation of the effect of operational parameters", Journal Hazardous. Material, 129 116-122.

Dennett K. E., Amirtharajah A., Moran T. F., Gould, J. P., (1996), "Coagulation: Its effect on organic matter", Journal of American Water Works, Association, 88(4), 129-142.

Derenne S., Tu T. T. N., (2014), "Characterizing the molecular structure of organic matter from natural environments: an analytical challenge", Comptes Rendus Geoscience, 346(3), 53-63.

Duan, J., Gregory J., (2003), "Coagulation by hydrolysing metal salts", Advances in Colloid and Interface Science, (100), 475-502.

Dubrawski K. L., Fauvel M., Mohseni M., (2013), "Metal type and natural organic matter source for direct filtration electrocoagulation of drinking water", Journal of Hazardous Materials, 244, 135-141.

Dubrawski K. L., Mohseni M., (2013), "In-situ identification of iron electrocoagulation speciation and application for natural organic matter (NOM) removal", Water Research, 47(14), 5371-5380.

Edzwald J. K., Becker W. C., Wattier K. L., (1985), "Surrogate parameters for monitoring organic matter and THM precursors", Journal American Water Works Association, 122-132.

Edzwald J. K., (1993), "Coagulation in drinking water treatment: Particles, organics and coagulants", Water Science and Technology, 27(11), 21-35.

Eikebrokk B., (1999), "Coagulation-direct filtration of soft, low alkalinity humic waters", Water Science and Technology, 40(9), 55-62.

Elimelech M., Gregory J., Jia X., (1998), "Particle deposition and aggregation: measurement, modelling and simulation", Colloid and surface engineering series, 2nd Ed., Butterworth-Heinemann, Oxford.

Emamjomeh M. M., Sivakumar M., (2006), "An empirical model for defluoridation by batch monopolar electrocoagulation/flotation (ECF) process", Journal of Hazardous Materials B131 (2006) 118–125.

ElBishlawi H., Jaffe P. R., (2015), "Characterization of dissolved organic matter from a restored urban marsh and its role in the mobilization of trace metals", Chemosphere, 127, 144-151.

El-Naas M. H., Al-Zuhair S., Al-Lobaney A., Makhlouf S., (2009), "Assessment of electrocoagulation for the treatment of petroleum refinery wastewater", Journal of Environmental Management, 91(1), 180-185.

Espinoza L. A. T., ter Haseborg E., Weber M., Frimmel F. H., (2009), "Investigation of the photocatalytic degradation of brown water natural organic matter by size exclusion chromatography", Applied Catalysis B: Environmental, 87(1), 56-62.

Fabris R., Chow C.W.K., Drikas M., Eikebrokk B., (2008), "Comparison of NOM character in selected Australian and Norwegian drinking waters", Water Research, 42, 4188–4196.

Feng C., Suzuki K., Zhao S., Sugiura N., Shimada S., Maekawa T., (2004), "Water disinfection by electrochemical treatment", Bioresource Technology, 94(1), 21-25.

Feng Q. Y., Li X. D., Cheng Y. J., Lei M. E. N. G., Meng Q. J., (2007), "Removal of humic acid from groundwater by electrocoagulation", Journal of China University of Mining and Technology, 17(4), 513-520.

Fukui Y., Yuu S., (1985), "Removal of colloidal particles in electroflotation", AIChE Journal, 31 (2), 201–208.

Glembotskii V.A., Mamokov A.A., Romanov A.M., Nenno V.E., (1975), 11th International Mineral Processing Congress, Cagliari, 561-164.

Gaffney J. S., Marley N. A., Clark S. B., (1996a), "Humic and fulvic acids and organic colloidal materials in the environment, In: ., J. S. Gaffney, N.A. Marley, and S. B. Clark, "Humic and Fulvic Acids: Isolation, Structure, and environmental Role", Editors, ACS Symposium Series 651, American Chemical Society.

Gaffney J. S., Marley N. A., Clark S. B., (1996b), "Humic and fulvic acids: isolation, structure, and environmental role", Proceedings of a symposium at the 210th American Chemical Society's National Meeting Series.

Ghernaout D., Ghernaout B., Saiba A., Boucherit A., Kellil A., (2009), "Removal of humic acids by continuous electromagnetic treatment followed by electrocoagulation in batch using aluminium electrodes", Desalination, 239(1), 295-308.

Gamble D.S., Schnitzer M., (1974), "The chemistry of fulvic acid and its reaction with metal ions, Trace Metals and Metal-Organic Interactions", Ann Arbor Science, Ann Arbor, Editors, Singer.

Gengec E., Kobya M., Demirbas E., Akyol A., Oktor K., (2012), "Optimization of baker's yeast wastewater using response surface methodology by electrocoagulation", Desalination, 286, 200-209.

Ghernaout D., Naceur M. W., Ghernaout B., (2011), "A review of electrocoagulation as a promising coagulation process for improved organic and inorganic matters removal by electrophoresis and electroflotation", Desalination and Water Treatment, 28(1-3), 287-320.

Ghosh K., Schnitzer M., (1980), "Macromolecular structures of humic substances", Soil Science, 129(5), 266-276.

Ghosh D., Medhi C. R., & Purkait M. K., (2008), "Treatment of fluoride containing drinking water by electrocoagulation using monopolar and bipolar electrode connections", Chemosphere, 73(9), 1393-1400.

García-García P., Arroyo-López F. N., Rodríguez-Gómez F., (2014), "Partial purification of iron solutions from ripe table olive processing using ozone and electro-coagulation", Separation and Purification Technology, 133, 227-235.

Gibbs R. J., (1983), "Effect of natural organic coatings on the coagulation of particles", Environmental Science and Technology, 17(4), 237-240.

Gomes J. A., Daida P., Kesmez M., Weir, M., Moreno, H., Parga J. R., Cocke, D. L., (2007), "Arsenic removal by electrocoagulation using combined Al–Fe electrode system and characterization of products", Journal of Hazardous Materials, 139(2), 220-231.

Gotsi M., Kalogerakis N., Psillakis E., Samaras P., Mantzavinos D., (2005), "Electrochemical oxidation of olive oil mill wastewaters", Water Research, 39(17), 4177-4187.

Gregor J. E., Nokes C. J., Fenton E., (1997), "Optimising natural organic matter removal from low turbidity waters by controlled pH adjustment of aluminium coagulation", Water Research, 31(12), 2949-2958.

Gregory J. in: C.A. Finch (Ed.), (1996), "Polymer adsorption and flocculation", Industrial Water Soluble Polymers., Royal Society of Chemistry, Cambridge.

Han M.Y., Kim M.K., Ahn H.J., (2006), "Effects of surface charge, micro-bubble size and particle size on removal efficiency of electro-flotation", Water Science and Technology, 53 (7), 127–132.

Harif T., Adin A., (2007), "Characteristics of aggregates formed by electroflocculation of a colloidal suspension", Water Research, 41(13), 2951-2961.

Hay M. B., Myneni S. C., (2007), "Structural environments of carboxyl groups in natural organic molecules from terrestrial systems", Part 1: Infrared spectroscopy, Geochimica et Cosmochimica Acta, 71(14), 3518-3532.

Her N., Amy G., Chung J., Yoon J., Yoon Y., (2008), "Characterizing dissolved organic matter and evaluating associated nanofiltration membrane fouling", Chemosphere, 70(3), 495-502.

Heidmann I., Calmano W., (2008), "Removal of Zn (II), Cu (II), Ni (II), Ag (I) and Cr (VI) present in aqueous solutions by aluminium electrocoagulation", Journal of Hazardous Materials, 152(3), 934-941.

Herzsprung P., von Tümpling W., Hertkorn N., Harir M., Büttner O., Bravidor J., ... & Schmitt-Kopplin P., (2012), "Variations of DOM quality in inflows of a drinking water reservoir: linking of van Krevelen diagrams with EEMF spectra by rank correlation", Environmental Science and Technology, 46(10), 5511-5518.

Holt P. K., Barton G. W., Mitchell C. A., (2005), "The future for electrocoagulation as a localised water treatment technology", Chemosphere, 59(3), 355-367.

Holt P.K., Barton G.W., Wark M., Mitchell C.A., (2002), "A quantitative comparison between chemical dosing and electrocoagulation", Colloid Surface A. 211 (2–3), 233–248.

Holt P. K., Barton G. W., Mitchell C. A., (2004), "Deciphering the science behind electrocoagulation remove suspended clay particles from water", Water Science and Technology, 50(12), 177-184.

Hongve D., Baann J., Becher G., Lømo S., (1996), "Characterization of humic substances by means of high-performance size exclusion chromatography", Environment International, 22(5), 489-494.

Hosny A.Y., (1996), "Separating oil from oil–water emulsions by electroflotation technique", Separation Technology 6, 9–17.

Huber S. A., Balz A., Abert M., Pronk W., (2011), "Characterisation of aquatic humic and non-humic matter with size-exclusion chromatography–organic carbon detection–organic nitrogen detection (LC-OCD-OND)", Water Research, 45(2), 879-885.

Huber S. A., Frimmel F. H., (1991), "Flow injection analysis for organic and inorganic carbon in the low-ppb range", Analytical Chemistry, 63(19), 2122-2130.

Irdemez S., Demircioğlu N., Yildiz Y.S., (2006), "The effects of pH on phosphate removal from wastewater by electrocoagulation with iron plate electrodes", Journal Hazardous Material, 137, 1231–1235.

Jacangelo J. G., DeMarco J., Owen D. M., Randtke SJ., (1995), "Selected processes for removing NOM: an overview", Journal of American Water Works Association 87(1), 64-77.

Janpoor F., Torabian A., Khatibikamal V., (2011), "Treatment of laundry wastewater by Electrocoagulation", Journal of Chemical Technology and Biotechnology, 86(8), 1113-1120.

Jenke, D. R., Diebold, F. E., (1984), "Electroprecipitation treatment of acid-mine wastewater", Water Research, 18(7), 855–859.

Jiang J-Q., Graham N. J. D., (1998), "Observations of the comparative hydrolysis/precipitation behavior of polyferric sulphate and ferric sulphate", Water Research 32(3), 930-935.

Kabdaşlı I., Vardar B., Arslan-Alaton I., Tünay O., (2009), "Effect of dye auxiliaries on color and COD removal from simulated reactive dyebath effluent by electrocoagulation", Chemical Engineering Journal, 148(1), 89-96.

Kamali M., Khodaparast Z., (2015), "Review on recent developments on pulp and paper mill wastewater treatment", Ecotoxicology and Environmental Safety,114, 326-342.

Karels A. E., Niemi A., (2002), "Fish community responses to pulp and paper mill effluents at the southern Lake Saimaa, Finland", Environmental Pollution, 116(2), 309-317.

Katal R., Pahlavanzadeh H., (2011), "Influence of different combinations of aluminum and iron electrode on electrocoagulation efficiency: Application to the treatment of paper mill wastewater", Desalination, 265(1), 199-205.

Katsumata H., Sada M., Kaneco S., Suzuki T., Ohta K., Yobiko Y., (2008), "Humic acid degradation in aqueous solution by the photo-Fenton process", Chemical Engineering Journal, 137(2), 225-230.

Kawasaki N., Matsushige K., Komatsu K., Kohzu A., Nara F. W., Ogishi F., Yahata M., Mikami H., Goto T., Imai, A., (2011), "Fast and precise method for HPLC–size exclusion chromatography with UV and TOC (NDIR) detection: Importance of multiple detectors to evaluate the characteristics of dissolved organic matter", Water Research, 45(18), 6240-6248.

Kent F. C., Montreuil K. R., Stoddart A. K., Reed V. A., Gagnon G. A., (2014), "Combined use of resin fractionation and high performance size exclusion chromatography for characterization of natural organic matter", Journal of Environmental Science and Health, Part A, 49(14), 1615-1622.

Khandegar V., Saroha A. K., (2013), "Electrocoagulation for the treatment of textile industry effluent–A review", Journal of Environmental Management, 128, 949-963.

Kovatchva V.K., Parlapanski M.D., (1999), "Sono-electrocoagulation of iron hydroxides", Colloids Surface, 149 603–608.

Ketkar D. R., Mallikarjunan R., Venkatachalam S., (1991), "Electroflotation of quartz fines", International Journal of Mineral Processing, 31(1), 127-138.

Burns S.E., Yiacoumi S., Tsouris C., (1997), "Microbubble generation for environmental and industrial separations", Separation and Purification Technology, (11) 221–232.

Kim H. C., Yu M. J., (2007), "Characterization of aquatic humic substances to DBPs formation in advanced treatment processes for conventionally treated water", Journal of Hazardous Materials, 143(1), 486-493.

Kim, K. S., Oh, B. S., Kang, J. W., Chung, D. M., Cho, W. H., & Choi, Y. K. (2005). "Effect of ozone and GAC process for the treatment of micropollutants and DBPs control in drinking water: pilot scale evaluation", Ozone: Science and Engineering, 27(1), 69-79.

Kobya M., Senturk E., Bayramoglu M., (2006), "Treatment of poultry slaughterhouse wastewaters by Electrocoagulation", Journal of Hazardous Materials, 133(1), 172-176.

Kobya M., Gebologlu U., Ulu F., Oncel S., Demirbas, E., (2011a), "Removal of arsenic from drinking water by the electrocoagulation using Fe and Al electrodes", Electrochimica Acta, 56(14), 5060-5070.

Kobya M., Ulu F., Gebologlu U., Demirbas E., Oncel M.S., (2011b), "Treatment of potable water containing low concentration of arsenic with electrocoagulation: Different connection modes and Fe–Al electrodes", Separation and Purification Technology, 77(3), 283-293.

Kobya M., Oncel M.S., Demirbas E., Şık E., Akyol A., Ince M., (2014), "The application of electrocoagulation process for treatment of the red mud dam wastewater from Bayer's process", Journal of Environmental Chemical Engineering, 2(1), 2211-2220.

Kobya M., Demirbas E., Sahin O., (2012), "Effect of operational parameters on the removal of phenol from aqueous solutions by electrocoagulation using Fe and Al electrodes", Desalination and Water Treatment, 46(1-3), 366-374.

Kobya M., Ozyonar F., Demirbas E., Sik E., Oncel M. S., (2015), "Arsenic removal from groundwater of Sivas-Şarkişla Plain, Turkey by electrocoagulation process: Comparing with iron plate and ball electrodes", Journal of Environmental Chemical Engineering, 3(2), 1096-1106.

Korbahti B. K., Tanyolaç A., (2003), "Continuous electrochemical treatment of phenolic wastewater in a tubular reactor", Water Research, 37(7), 1505-1514.

Korshin G., Chow C. W., Fabris R., Drikas M., (2009), "Absorbance spectroscopy-based examination of effects of coagulation on the reactivity of fractions of natural organic matter with varying apparent molecular weights", Water Research, 43(6), 1541-1548.

Kuokkanen V., Kuokkanen T., Rämö J., Lassi U., (2015), "Electrocoagulation treatment of peat bog drainage water containing humic substances", Water Research, 79, 79-87.

Kuokkanen V., Kuokkanen T., Ramo J., Lassi U., (2013), "Recent applications of electrocoagulation in treatment of water and wastewater-A review", Green and Sustainable Chemistry, 3, 89-121.

Kurt S., (2015), "The Geographıcal Analysis of the Changes Occurrıng in Terkos Lake (Istanbul) and Its Surroundings", The Journal of Academic Social Science Studies, 34, 333-344.

Labanowski J., Pallier V., Feuillade-Cathalifaud G., (2010), "Study of organic matter during coagulation and electrocoagulation processes: Application to a stabilized landfill leachate", Journal of Hazardous Materials, 179(1), 166-172.

Liao A. A., Spitzer M., Motheo A. J., Bertazzoli R., (2008), "Electrocombustion of humic acid and removal of algae from aqueous solutions", Journal of Applied Electrochemistry, 38(5), 721-727.

Lin S.H., Shyu C.T., Sun M.C., (1998), "Saline wastewater treatment by electrochemical method", Water Research, 32, 1059–1067.

Lin S. H., Chang C. C., (2000), "Treatment of landfill leachate by combined electro-Fenton oxidation and sequencing batch reactor method", Water Research, 34(17), 4243-4249.

Linares-Hernández I., Barrera-Díaz C., Roa-Morales G., Bilyeu B., Ureña-Núñez F., (2009), "Influence of the anodic material on electrocoagulation performance", Chemical Engineering Journal, 148(1), 97-105.

Liu H., Liu R., Tian C., Jiang H., Liu X., Zhang R., Qu J., (2012), "Removal of natural organic matter for controlling disinfection by-products formation by enhanced coagulation: a case study", Separation and Purification Technology, 84, 41-45.

Liu S., Lim M., Fabris R., Chow C., Chiang K., Drikas M., Amal R., (2008), "Removal of humic acid using TiO 2 photocatalytic process–fractionation and molecular weight characterisation studies", Chemosphere,72(2), 263-271.

Liu H., Zhao X., Qu J., (2010), "Electrocoagulation in Water Treatment, in: Comninellis C., Chen G., (Eds.)", Electrochemistry for the Environment, Springer, New York, 245–262.

Llerena C., Ho J.C.K., Piron D.L., (1996), "Effect of pH on electroflotation of sphalerite", Chemical Engineering Communications, 155, 217–228.

Mahvi A. H., Malakootian M., Heidari M. R., (2011), "Comparison of polyaluminum silicate chloride and electrocoagulation process, in natural organic matter removal from surface water in Ghochan, Iran", Journal of Water Chemistry and Technology, 33(6), 377-385.

Maktav D., Erbek F. S., Kabdasli S., (2002), "Monitoring coastal erosion at the Black Sea coasts in Turkey using satellite data: a case study at the Lake Terkos, north-west Istanbul", International Journal of Remote Sensing, 23(19), 4115-4124.

Malcolm R. L., (1991), "Factors to be considered in the isolation and characterization of aquatic humic substances", In: B. Allard, H. Boren and A. Grimvall, Editors, "Humic Substances in the Aquatic and Terrestrial Environment Book", Spring.

Mao R., Wang Y., Zhang B., Xu W., Dong M., Gao B., (2013), "Impact of enhanced coagulation ways on flocs properties and membrane fouling: Increasing dosage and applying new composite coagulant", Desalination, 314, 161-168.

Matilainen A., Gjessing E. T., Lahtinen T., Hed L., Bhatnagar A., Sillanpää M., (2011), "An overview of the methods used in the characterisation of natural organic matter (NOM) in relation to drinking water treatment", Chemosphere, 83(11), 1431-1442.

Matilainen A., Vepsäläinen M., and Sillanpää M., (2010b), "Natural organic matter removal by coagulation during drinking water treatment: A review." Advances in Colloid and Interface Science, 159(2), 189-197.

Matilainen A., Iivari P., Sallanko, J., Heiska E., Tuhkanen T., (2006), "The role of ozonation and activated carbon filtration in the natural organic matter removal from drinking water", Environmental Technology, 27(10), 1171-1180.

Matilainen A., Sillanpää M., (2010a), "Removal of natural organic matter from drinking water by advanced oxidation processes", Chemosphere, 80(4), 351-365.

Matis K. A. Peleka E. N., (2010), "Alternative flotation techniques for wastewater treatment: Focus on electroflotation", Separation Science and Technology, 45(16), 2465–2474.

Matteson M. J., Dobson R. L., Glenn R. W., Kukunoor N. S., Waits W. H., Clayfield E. J., (1995), "Electrocoagulation and separation of aqueous suspensions of ultrafine particles". Colloids and Surfaces A: Physicochemical and Engineering Aspects, 104(1), 101-109.

Mollah M. Y. A., Schennach R., Parga J. R., Cocke D. L., (2001), "Electrocoagulation (EC)—science and applications", Journal of Hazardous Materials, 84(1), 29-41.

Mollah M. Y., Morkovsky P., Gomes J. A., Kesmez M., Parga J., Cocke D. L., (2004), "Fundamentals, present and future perspectives of electrocoagulation", Journal of Hazardous Materials, 114(1), 199-210.

Moreno C, H. A., Cocke D. L., Gomes J. A., Morkovsky P., Parga J. R., Peterson E., & Garcia C., (2009), "Electrochemical reactions for electrocoagulation using iron electrodes", Industrial and Engineering Chemistry Research, 48(4), 2275-2282.

Mori S., Barth H. G., (2013), "Size exclusion chromatography", Springer Berlin Heidelberg, Germany.

Moussas P. A., Zouboulis A. I., (2012), "Synthesis, characterization and coagulation behavior of a composite coagulation reagent by the combination of polyferric sulfate (PFS) and cationic polyelectrolyte", Separation and Purification Technology, 96, 263-273.

Mouedhen G., Feki M., Wery M. D. P., Ayedi H. F., (2008), "Behavior of aluminum electrodes in electrocoagulation process", Journal of hazardous materials, 150(1), 124-135.

Meas Y., Ramirez J. A., Villalon M. A., Chapman T. W., (2010), "Industrial wastewaters treated by electrocoagulation", Electrochimica Acta, 55(27), 8165-8171.

McGhee T.J., (1991), "Water Supply and Sewerage", 6th Edition., McGraw-Hill,

Mameri N., Yeddou A. R., Lounici H., Belhocine D., Grib H., Bariou B., (1998), "Defluoridation of septentrional Sahara water of North Africa by electrocoagulation process using bipolar aluminium electrodes", Water Research, 32(5), 1604-1612.

Miwa D. W., Malpass G. R. P., Machado S. A. S., Motheo, A. J., (2006), "Electrochemical degradation of carbaryl on oxide electrodes", Water Research, 40(17), 3281-3289.

Minor E. C., Swenson M. M., Mattson B. M., Oyler A. R., (2014), "Structural characterization of dissolved organic matter: a review of current techniques for isolation and analysis", Environmental Science: Processes Impacts, 16(9), 2064-2079.

Motheo A. J., Pinhedo L., (2000), "Electrochemical degradation of humic acid", Science of the Total Environment, 256(1), 67-76.

Mulholland P. J., (1990), Group report "What are the temporal and spatial variations of organic acids at the ecosystem level?", In: Organic Acids in Aquatic Ecosystems, Perdue E. M., Gjessing E. T. Editors, 315-329, John Wiley & Sons.

Murugananthan M., Latha S. S., Raju G. B., Yoshihara S., (2010), "Anodic oxidation of ketoprofen—an anti-inflammatory drug using boron doped diamond and platinum electrodes", Journal of Hazardous Materials, 180(1), 753-758.

Naumczyk J., Szpyrkowicz L., Zilio-Grandi F., (1996), "Electrochemical treatment of textile wastewater", Water Science and Technology, 34(11), 17-24.

Nerger B. A., Peiris R. H., Moresoli C., (2015), "Fluorescence analysis of NOM degradation by photocatalytic oxidation and its potential to mitigate membrane fouling in drinking water treatment", Chemosphere, 136, 140-144.

Niu X., Li X., Zhao J., Ren Y., Yang, Y., (2011), "Preparation and coagulation efficiency of polyaluminium ferric silicate chloride composite coagulant from

wastewater of high-purity graphite production", Journal of Environmental Sciences, 23(7), 1122-1128.

Nobili M., Gjessing E., Sequi P., (1989), "Sizes and shapes of humic substances by gel chromatography", Humic substances II, John Wiley & Sons.

O'Melia C.R., In: Physicochemical processes for water quality control, Webber W.J., Jr. (Ed.), Wiley-Interscience.

Parga J. R., Cocke D. L., Valverde V., Gomes J. A., Kesmez M., Moreno H., Mencer D., (2005), "Characterization of electrocoagulation for removal of chromium and arsenic", Chemical Engineering & Technology, 28(5), 605-612.

Philippe A., Schaumann G. E., (2014), "Interactions of dissolved organic matter with natural and engineered inorganic colloids: a review", Environmental Science and Technology, 48(16), 8946-8962.

Owen D. M., Amy G. L., Chowdhury Z. K., Paod, R., McCoy G., Viscosil K., (1995), "NOM: characterization and treatability: Natural organic matter", Journal-American Water Works Association, 87(1), 46-63.

Oxenford J. L., Amy G. L., (1996), "Disinfection by-products: current practices and future directions". In: R. A. Minear, G. L. Amy, Editors, "Disinfection by-products in Water Treatment: The Chemistry of Their Formation and Control Book", Lewis Publishers.

Ozyonar F., Karagozoglu B., (2014), "Investigation of technical and economic analysis of electrocoagulation process for the treatment of great and small cattle slaughterhouse wastewater", Desalination and Water Treatment,52(1-3), 74-87.

Panizza M., Cerisola G., (2004), "Electrochemical Oxidation as a Final Treatment of Synthetic Tannery Wastewater", Environmental Science and Technology, 38, 54705475.

Penru Y., Simon F. X., Guastalli A. R., Esplugas S., Llorens, J., & Baig, S. (2013). "Characterization of natural organic matter from Mediterranean coastal seawater", Journal of Water Supply: Research & Technology- AQUA, 62(1), 42-51.

Peralta-Hernandez J.M., Mendez-Tovar M., Guerra-Sanchez R., Martıınez-Huitle C. A., Nava J.L., (2012), "A brief review on environmental application of boron doped diamond electrodes as a new way for electrochemical incineration of synthetic dyes", International Journal of Electrochemistry.

Pernitsky D. J., Edzwald J. K., (2003), "Solubility of polyaluminium coagulants", Journal of Water Supply: Research and Technology-AQUA, 52(6), 395-406.

Picard T., Cathalifaund G., Mazet M., Vandensteendam C., (2000), "Cathodic dissolution in the electrocoagulation process using aluminum electrodes", Journal of Environmental Monitoring., 2, 77-80.

Pletcher D., Walsh F.C., (1990), "Industrial Electrochemistry", second ed., Chapman and Hall.

Rajeshwar K. I. J. G., Ibanez J. G., Swain G. M., (1994), "Electrochemistry and the environment", Journal of Applied Electrochemistry, 24(11), 1077-1091.

Raju G. B., Khangaonkar P. R., (1984), "Electroflotation of chalcopyrite fines with sodium diethyldithiocarbamate as collector", International Journal of Mineral Processing, 13(3), 211-221.

Rebhun M., Lurie M., (1993), "Control of organic matter by coagulation and floc separation", Atmosphere, 638, 02.

Reynolds T. D., (1977), "Unit operations and processes in environmental engineering", Brooks.

Rizzo L., Di Gennaro A., Gallo M., Belgiorno V., (2008), "Coagulation/chlorination of surface water: A comparison between chitosan and metal salts", Separation and Purification Technology, 62(1), 79-85.

Rodríguez F. J., Schlenger P., García-Valverde M., (2014), "A comprehensive structural evaluation of humic substances using several fluorescence techniques before and after ozonation. Part I: Structural characterization of humic substances", Science of the Total Environment, 476, 718-730.

Romanov A.M., (1998), "Electroflotation in Waste Water Treatment: Results and Perspectives", In: Mineral Processing and the Environment, Gallios, G.P.; Matis, K.A., eds.; Kluwer: Dordrecht, 335-360.

Romero J.A. P., Junior F.S.S.C., Figueiredo R.T., Silva D.P., (2013), Cavalcanti E.B., "Treatment of biodiesel wastewater by combined electroflotation and electrooxidation processes", Separation Science and Technology, 48, 2073-2079.

Sarathy S. R., Mohseni M., (2007), "The impact of UV/H2O2 advanced oxidation on molecular size distribution of chromophoric natural organic matter", Environmental Science & Technology, 41(24), 8315-8320.

Sasson M. B., Calmano W., & Adin A., (2009), "Iron-oxidation processes in an electroflocculation (electrocoagulation) cell", Journal of Hazardous Materials, 171(1), 704-709.

Sawyer C. N., McCarty P. L., Parkin G. F., (2002), 5th Edition, "Chemistry for Environmental Engineering and Science", McGraw-Hill.

Schnitzer M., Kahn S. U., (1972), "Humic substances in the environment", Marcel Dekker, New York, U.S.A.

Scott K., (1995), "Electrochemical Processes for Clean Technology", UK. The Royal Society of Chemistry.

Shammas N.K., "Coagulation and flocculation (ch. 4)", (2005), From: Handbook of environmental engineering, Vol. 3: Physicochemical treatment processes, L.K. Wang, Y.-T. Hung and N.K. Shammas (Eds.), The Humana Press Inc., Totowa, New Jersey, USA.

Sharp E. L., Jarvis P., Parsons S. A., Jefferson B., (2006a), "Impact of fractional character on the coagulation of NOM", Colloids and Surfaces A: Physicochemical and Engineering Aspects, 286(1), 104-111.

Sharp E. L., Parsons S. A., Jefferson B., (2006b), "Seasonal variations in natural organic matter and its impact on coagulation in water treatment", Science of the Total Environment, 363(1), 183-194.

Sharp E. L., Parsons S. A., Jefferson, B. (2006c), "The impact of seasonal variations in DOC arising from a moorland peat catchment on coagulation with iron and aluminium salts", Environmental Pollution, 140(3), 436-443.

Shafaei A., Rezaie M., Nikazar M., (2011), "Evaluation of Mn^{2+} and Co^{2+} removal by electrocoagulation: a case study", Chemical Engineering and Processing: Process Intensification, 50(11), 1115-1121.

Shen F., Chen X., Gao P., Chen G., (2003), "Electrochemical removal of fluoride ions from industrial wastewater", Chemical Engineering Science 58 (3–6), 987–993.

Shi B., Li G., Wang D., Feng C., Tang H., (2007), "Removal of direct dyes by coagulation: The performance of preformed polymeric aluminum species", Journal of Hazardous Materials, 143(1), 567-574.

Shirshova L. T., Ghabbour E. A., Davies G., (2006), "Spectroscopic characterization of humic acid fractions isolated from soil using different extraction procedures", Geoderma, 133(3), 204-216.

Singer P. C., Bilyk, K., (2002), "Enhanced coagulation using a magnetic ion exchange resin", Water Research, 36(16), 4009-4022.

Slavik I., Müller S., Mokosch R., Azongbilla J. A., Uhl W., (2012), "Impact of shear stress and pH changes on floc size and removal of dissolved organic matter (DOM)", Water Research, 46(19), 6543-6553.

Smith E., Kamal Y., (2009), "Optimizing treatment for reduction of disinfection by-product (DBP) formation", Water Science Technology Water Supply (9)191–198

Soh Y.C., Roddick F., Leeuwen J.v., (2008), "The impact of alum coagulation on the character, biodegradability and disinfection by-product formation potential of reservoir natural organic matter (NOM) fractions", Water Science and Technology, 58(6), 1173.

Staaks C., Fabris R., Lowe T., Chow C. W., van Leeuwen J. A., Drikas, M., (2011), "Coagulation assessment and optimisation with a photometric dispersion analyser

and organic characterisation for natural organic matter removal performance", Chemical Engineering Journal, 168(2), 629-634.

Stevenson J. (EDs.), (1982), "Humus Chemistry: Genesis, composition, reactions", John Wiley and Sons, New York, Inc., U.S.A.

Suffet I. H., MacCarthy P., (1989), "Aquatic humic substances and their influenc on the fate and treatment of pollutants", In: H., Suffet, P. MacCarthy, Editors, "Aquatic humic substances, Influence on fate and treatment of pollutants, Advances in Chemical Series Book, The American Chemical Society.

Thaveemaitree Y., Polprasert C., Seung-Hwan L., (2003), "Application of electrochemical process for landfill leachate treatment with emphasis on heavy metal and organic removal", Environmental Technology, 24(9), 1135-1145.

Thurman E. M., (1985), "Organic Geochemistry of Natural Waters" Kluwer Academic, Martinus Nijhaff/Dr W. Junk Publisher, Springer

Toor R., Mohseni M., (2007), "UV-H_2O_2 based AOP and its integration with biological activated carbon treatment for DBP reduction in drinking water", Chemosphere, 66(11), 2087-2095.

Uduman N., Bourniquel V., Danquah M. K., Hoadley A. F., (2011), "A parametric study of electrocoagulation as a recovery process of marine microalgae for biodiesel production", Chemical Engineering Journal, 174(1), 249-257.

USEPA, 1998, "Natural primary drinking water regulations: disinfectants and disinfection by-products", final rule. Fed. Reg. 63, 69389-69476.

Uyak V., Ozdemir K., Toroz I., (2008), "Seasonal variations of disinfection by-product precursors profile and their removal through surface water treatment plants", Science of the Total Environment, 390(2), 417-424.

Uyak V., Toroz I., (2007), "Disinfection by-product precursors reduction by various coagulation techniques in Istanbul water supplies", Journal of hazardous materials, 141(1), 320-328.

Uyguner C. S., Bekbolet M., Selcuk H., (2007), "A comparative approach to the application of a physico-chemical and advanced oxidation combined system to natural water samples", Separation Science and Technology, 42(7), 1405-1419.

Uyguner C. S., Bekbolet M., (2005), "A comparative study on the photocatalytic degradation of humic substances of various origins", Desalination, 176(1), 167-176.

Ulu F., Barışçı S., Kobya M., Sillanpää M., (2015), "An evaluation on different origins of natural organic matters using various anodes by electrocoagulation", Chemosphere, 125, 108-114.

Ulu F., Barışçı S., Kobya M., Särkkä H., Sillanpää M., (2014), "Removal of humic substances by electrocoagulation (EC) process and characterization of floc size

growth mechanism under optimum conditions", Separation and Purification Technology, 133, 246-253.

Velten S., Knappe D. R., Traber J., Kaiser H. P., von Gunten U., Boller M., Meylan, S., (2011), "Characterization of natural organic matter adsorption in granular activated carbon adsorbers", Water Research, 45(13), 3951-3959.

Vepsäläinen M., Pulliainen, M., Sillanpää, M., (2012), "Effect of electrochemical cell structure on natural organic matter (NOM) removal from surface water through electrocoagulation (EC)", Separation and Purification Technology, 99, 20-27.

Vik E. A., Carlson D. A., Eikum A. S., Gjessing E. T., (1984), "Electrocoagulation of potable water", Water Research, 18(11), 1355-1360.

Vlyssides A., Barampouti E.M., Mai S., Arapoglou D., Kotronarou A., (2004), "Degradation of Methylparathion in Electrochemical Oxidation", Environmental Science and Technology, 38, 6125-6131.

Vuorio E., Vahala R., Rintala J., Laukkanen R., (1998), "The evaluation of drinking water treatment performed with HPSEC", Environment International, 24(5), 617-623.

Wang B., Kong W., Ma H., (2007), "Electrochemical treatment of paper mill wastewater using three-dimensional electrodes with $Ti/Co/SnO_2-Sb_2O_5$ anode", Journal of Hazardous Materials, 146(1), 295-301.

Walter J., Weber JR., (1972), "Physicochemical Processes for Water Quality Control", Wiley Interscience.

Web 1, (2015), https://en.wikipedia.org/wiki/Saimaa, (Erişim tarihi: 10/12/2015).

Web 2, (2015), http://www.saimaageoparkproject.fi/en/geopark-tells-the-story-of-saimaa/, (Erişim Tarihi: 10/12/2015).

Wei Q., Feng C., Wang D., Shi B., Zhang L., Tang H., (2008), "Seasonal variations of chemical and physical characteristics of dissolved organic matter and trihalomethane precursors in a reservoir: a case stud", Journal Hazardous Materials, 150, 257–264.

Wu F. C., Evans R. D., Dillon P. J., Cai, Y. R., (2007), "Rapid quantification of humic and fulvic acids by HPLC in natural waters", Applied Geochemistry, 22(8), 1598-1605.

Xie J., Wang D., van Leeuwen J., Zhao Y., Xing L., Chow C. W., (2012), "pH modeling for maximum dissolved organic matter removal by enhanced coagulation", Journal of Environmental Sciences, 24(2), 276-283.

Yan M., Wang D., Qu J., Ni J., Chow C. W., (2008), "Enhanced coagulation for high alkalinity and micro-polluted water: the third way through coagulant optimization", Water Research, 42(8), 2278-2286.

Yildiz Y. Ş., Koparal A. S., İrdemez Ş., Keskinler B., (2007), "Electrocoagulation of synthetically prepared waters containing high concentration of NOM using iron cast electrodes", Journal of Hazardous Materials, 139(2), 373-380.

Yu M.J., Koo J.S., Myung G.N., Cho Y.K., Cho Y.M., (2005) "Evaluation of bipolar electrocoagulation applied to biofiltration for phosphorus removal", Water Science Technology, 51, 231–239.

Yu J., Wang D., Yan M., Ye C., Yang M., Ge X., (2007), "Optimized coagulation of high alkalinity, low temperature and particle water: pH adjustment and polyelectrolytes as coagulant aids", Environmental monitoring and assessment, 131(1-3), 377-386.

Zhang P., Wu Z., Zhang G., Zeng G., Zhang H., Li J., Dong J., (2008), "Coagulation characteristics of polyaluminum chlorides PAC-Al 30 on humic acid removal from water", Separation and Purification Technology, 63(3), 642-647.

Zhao Z. Y., Gu D. J., Li H. B., Li X. Y., Leung K. M. Y., (2009), "Disinfection characteristics of the dissolved organic fractions at several stages of a conventional drinking water treatment plant in South China", Journal Hazardous Materials, 172, 1093–1099.

Zhou Q., Cabaniss S. E., Maurice P. A., (2000), "Considerations in the use of high-pressure size exclusion chromatography (HPSEC) for determining molecular weights of aquatic humic substances", Water Research, 34(14), 3505-3514.

Zhu X., Ni J., Lai P., (2009), "Advanced treatment of biologically pretreated coking wastewater by electrochemical oxidation using boron-doped diamond electrodes", Water Research, 43(17), 4347-4355.

Zodi S., Louvet J. N., Michon C., Potier O., Pons M. N., Lapicque F., Leclerc J. P., (2011), "Electrocoagulation as a tertiary treatment for paper mill wastewater: Removal of non-biodegradable organic pollution and arsenic", Separation and purification Technology, 81(1), 62-68.

Zouboulis A. I., Tzoupanos N. D., (2009), "Polyaluminium silicate chloride—A systematic study for the preparation and application of an efficient coagulant for water or wastewater treatment", Journal of Hazardous Materials, 162(2), 1379-1389.

BIOGRAPHY

Feride ULU KAÇ was born in 1986 in Kars. She studied Environmental Engineering in Sakarya University between the years of 2004-2008. She started Master of Science degree in Gebze Institute of Technology (GIT), Graduate Schol of Natural and Applied Science, Department of Environmental Engineering in 2008 and finished in 2010. At the same year, she started doctoral degree in Gebze Technical University (GTU), Graduate Schol of Natural and Applied Science, Department of Environmental Engineering. She has been working as a researcher in GIT since 2012.

APPENDICES

Appendix A: Articles Published During the Thesis Study

Ulu F., Barışçı S., Kobya M., Sarkka H., Sillanpaa M., (2014), "Removal of humic substances by electrocoagulation (EC) process and characterization of floc size growth mechanism under optimum Conditions", Separation and Purification Technology 133, 246–253.

Ulu F., Barışçı S., Kobya M., Sillanpaa M., (2015), "An evaluation on different origins of natural organic matters using various anodes by electrocoagulation", Chemosphere 125, 108-114.